TECHNICAL

REPORT

THREE-DIMENSIONAL POLLUTANT GRADIENT STUDY - 1972-1973 PROGRAM

MRI 74 FR-1262

Submitted to

California Air Resources Board

Agreement Nos. ARB-631 and
ARB 2-1245

Date November 1974

By: D. L. Blumenthal, T. B. Smith, W. H. White, S. L. Marsh,
D. S. Ensor, Meteorology Research, Inc., Altadena, California
R. B. Husar, Washington University, St. Louis, Missouri
P. S. McMurry, S. L. Heisler, California Institute of Technology, Pasadena, California
P. Owens, U. S. Naval Weapons Center, China Lake, California

METEOROLOGY RESEARCH, INC.
Box 637, 464 West Woodbury Road
Altadena, California 91001
Telephone (213) 791-1901
A Subsidiary of Cohu, Inc.

Abstract

A 3-D Air Pollutant Gradient Study has been sponsored by the California Air Resources Board. Two years of data on the 3-D distribution and transport of aerosols and gaseous pollutants in the South Coast (Los Angeles), San Joaquin Valley, and San Francisco Bay air basins have been obtained and analyzed. Two hundred forty sampling flights on 59 different days were made by two aircraft in conjunction with ground-level sampling. Extensive meteorological data were obtained along with the b_{scat}, condensation nuclei, O_3, NO_x, CO, turbulence, temperature, and humidity data obtained by the aircraft.

The data present a detailed picture of the mixing layer structure and ventilation processes in the Los Angeles Basin and point out the modifications to the normal mixing and ventilation processes which lead to episode conditions. The air pollution problem in Los Angeles and other air basins is shown to be a regional problem exemplified by the accumulation of pollutants in a stagnant air mass and subsequent transport to downwind areas. Various statistical and other analyses were performed on the data which demonstrated the changes in the aerosol and gaseous pollutants as they aged and indicated certain factors contributing to aerosol formation and growth.

Other special studies were performed which documented in some detail the structure of a few point source plumes and demonstrated the possible buoyant effect of roadways. A 24-hour sampling program in the eastern Los Angeles Basin documented the overnight stability of ozone at high concentrations in aged polluted air.

TABLE OF CONTENTS

TABLE OF CONTENTS (Continued)

TABLE OF CONTENTS (Continued)

TABLE OF CONTENTS (Continued)

TABLE OF CONTENTS (Continued)

LIST OF FIGURES

LIST OF FIGURES (Cont'd)

LIST OF FIGURES (Cont'd)

LIST OF FIGURES (Cont'd)

LIST OF FIGURES (Cont'd)

LIST OF FIGURES (Cont'd)

LIST OF FIGURES (Cont'd)

LIST OF FIGURES (Cont'd)

LIST OF FIGURES (Cont'd)

LIST OF FIGURES (Cont'd)

LIST OF FIGURES (Cont'd)

LIST OF TABLES

LIST OF TABLES (Cont'd)

I. INTRODUCTION

A. General

The California Air Resources Board has funded a series of research programs to study the aerosol formation and transport processes in three major air basins of California. One of these programs is the Aerosol Gradient Study performed during 1972 and 1973 by Meteorology Research, Inc. in cooperation with the U. S. Naval Weapons Center at China Lake, California. The Gradient Study is a program to measure the three dimensional distribution of aerosols and other pollutants using light aircraft as instrument platforms. A description of the study, along with its findings, is presented in this report.

The remainder of this introduction presents the rationale for the program, a review of previous work, and a short description of the program. Detailed descriptions of the experimental plan and results and several discussions of topics of particular interest are presented in succeeding chapters.

The discussions presented in this volume are based on data from several days selected for special analysis. These data are presented only in summary in this volume. A complete collection of the data from the study is presented in the 1972 and 1973 data volumes.

B. Why Three-Dimensional Sampling

To date, most air pollution sampling has taken place at fixed locations at ground level. Some scientists have tried to use the data obtained from this ground-level sampling to define the transport of pollution while others have studied the temporal variations in pollutants to try to determine the chemical and physical processes which affect smog. Much has been learned from these studies, but the technique of sampling only at ground level precludes a more complete understanding of many aspects of the transport and mixing of pollution.

The atmosphere is three-dimensional, and likewise, air pollution is a three-dimensional problem. Meteorologists have long recognized the importance of the vertical dimension in the transport of air pollution, but many scientists involved in pollution research are unfamiliar with meteorology. Although the term "temperature inversion" is familiar to most pollution researchers, and it is well known that pollutants are sometimes trapped under the inversion, the assumption that the air under the inversion is uniform and that measurements made at ground level are characteristic of all the air in the polluted layer is often questionable.

There are many mechanisms at work in the atmosphere which can cause variations in pollutant concentration with altitude. Most air contaminants are directly or indirectly the products of combustion and are thus associated with a mass of warm air which is buoyant with respect to the surrounding

atmosphere. At least initially, until it cools or is mixed with the surrounding air by diffusion or turbulence, this warm air will tend to rise, lowering the concentration of pollutants near the ground level. If the atmosphere is unstable below a raised temperature inversion, the polluted air mass will tend to rise until it reaches the stable inversion layer, causing higher concentrations of pollutants in the vicinity of the inversion than near the ground. On the other hand, if the air is stable and if turbulent mixing is minimal, pollutants can remain concentrated within a few hundred feet of the ground and may not even rise to the level of the inversion, if one exists.

In the Los Angeles area, the sea breeze is an important factor in creating strong vertical variations in pollutant concentrations. The marine air can either undercut old polluted air with clean air, leaving a polluted layer aloft, or it can create a temperature inversion by undercutting warm air with cool air, thereby trapping pollutants released near the ground.

The importance of vertical data should be apparent from these examples. Smog transport and dis tribution are three dimensional phenomena. To thoroughly understand the physics and transport of smog, the vertical dimension must be taken into account. Sampling networks, atmospheric models, and pollutant transport models should be based on a three-dimensional atmosphere. Without knowledge of the three-dimensional pollutant distribution along with properly interpreted meteorological data, understanding of air pollution processes will be greatly limited.

Atmospheric models should be updated to include the mechanisms which can cause vertical variations in pollutant concentration, and three-dimensional measurements of pollutant concentrations on representative days should be used to validate the models. Present models recognize the role of turbulent diffusion in mixing pollutants vertically, but without inclusion of other mechanisms, estimates of residence times and eventual disposition of pollutants will be in error. Particulates which are concentrated in a layer at 3000 feet will take longer to precipitate out of the atmosphere and might travel farther than if the same particulates were evenly distributed between the ground and the 3000-foot level. High concentrations of pollutants at a single level might also affect reaction rates.

The California Air Resources Board has recognized the importance of understanding the three-dimensional distribution of pollutants in funding this program. We believe that the results of this mapping program can provide guidance for a more organized approach to ground-level sampling and can lead to better validation of pollution models and a more thorough understanding of the pollutant transport processes. The simultaneous mapping of gaseous as well as aerosol pollutant concentrations should also contribute significantly to the understanding of air chemistry, particularly as it relates to photochemical aerosol formation.

C. Previous Work on Airborne Sampling and the Distribution of Pollutants

In recent years as fast response instruments have become available, greater use has been made of aircraft instrumented specifically to study air pollution. Blumenthal and Ensor (1972) summarized the important considerations in choosing between fixed-wing aircraft, helicopters, and various lighter-than-air vehicles. Adams and Koppe (1969) described in detail the instrumenting of a Cessna 336 with an integrating nephelometer and instruments to measure CO_2, CO, hydrocarbons, SO_2, temperature, humidity, and position parameters, all of which were recorded on a 1/2-inch tape data logger. Adams and Koppe also reported experiments demonstrating the suitability of light fixed-wing aircraft for air pollution studies and showed that propwash and exhaust contamination did not affect the measurements. The air pollution studies using aircraft include plume tracking, vertical soundings, and mapping of air pollutant concentrations.

McCaldin and Johnson (1969) used a Cessna 172 equipped with a Bausch and Lomb 40-1 particle counter to track and measure the aerosol concentration downwind of the source. Stephens and McCaldin (1972) reported the use of a Cessna 182 equipped with a Bausch and Lomb dust counter and various SO_2 measuring instruments to measure the downwind properties of smoke plumes emitted from various large coal-fired power plants. Brown, et al. (1972) reported the mapping of plumes of oil fogs using a light scattering photometer as a sensor in a light aircraft.

McCaldin and Sholtes (1971) compared radiosonde observations of mixing depths to aircraft measurements of mixing depths using aerosol concentration measured with a dust counter, turbulence measured with an inertial sensor, and temperature. They found that the mixing depth as determined by the temperature of the atmosphere was often different from the depth of the aerosol trapped near the earth's surface. Ahlquist and Charlson (1968) reported both soundings and aerosol concentrations over Seattle measured with an integrating nephelometer. Bach and Hagedorn (1971) presented an extensive contour map of the aerosol concentrations over the city of Cincinnati. Kocmond and Mack (1971) discussed the effects of urban pollution sources on the distribution of condensation nuclei downwind of Buffalo. Stampfer (1972) reported the results of aircraft soundings over Missouri in which he measured particle concentration and size distribution with an optical counter as well as temperature and humidity. Stampfer also provides a good review of other airborne sampling work not mentioned here.

Some limited airborne sampling has also been carried out in the air basins covered by this study. As early as 1955, Neiburger, et al. (1955) presented data from oxidant and NO_2 concentration soundings in the Los Angeles area taken using a blimp. Blumenthal and Smith (1972) reported aerosol soundings with the integrating nephelometer, a condensation nuclei monitor, and an

ozone monitor along with measurements of temperature, humidity, and turbulence for the Los Angeles Basin, San Joaquin Valley, and San Francisco Bay Area. Scott Research Laboratories, Inc. studied atmospheric air pollutant reactions in the Los Angeles Basin using an aircraft equipped with a number of instruments, including an oxidant and an NO_x monitor with provision for grab samples for subsequent hydrocarbon analysis. Gloria, et al. (1974) have reported data describing atmospheric pollutant reactions and transport in various air basins in California. The ozone transport in the mountain valleys near Fresno, California, was measured by Miller, et al. (1972) with a Beechcraft 36 equipped with oxidant, temperature and humidity sensors. Edinger et al. (1972) and Edinger (1973) have also presented data on the vertical distribution of oxidants in the Los Angeles Basin and have shown the existence of polluted layers aloft. Miller and Ahrens (1970) have used a light aircraft to study the spatial and temporal distribution of ozone in the San Francisco Bay area.

Extensive ground level pollution concentration data have been obtained by various air pollution agencies which show the horizontal distribution of pollutants. A description of the seasonal variations in ground-level concentrations in Los Angeles as measured by the LAAPCD is presented by Mosher et al. (1970). Behar (1972) has developed a computer technique to draw pollutant contours using Los Angeles APCD data and to demonstrate the ground-level movement of pollutants throughout the day.

Additional airborne programs have been started in recent years, but as yet, few published results are available from these studies. Among them are Metromex and RAPS (Regional Air Pollution Study) being conducted in the St. Louis area and the LARPP (Los Angeles Reactive Pollutant Program) conducted in Los Angeles in 1973.

D. The Aerosol Gradient Study

The primary objective of this study has been to gain an understanding of the three-dimensional distribution of aerosols in the Los Angeles (South Coast), San Joaquin Valley, and San Francisco air basins under meteorological conditions representative of persistent air pollution problems. However, to measure the distribution at a fixed time and to understand how it came about are two different things. An understanding of the dynamics of aerosol distribution and transport requires not only the measurement of aerosol distribution but also the understanding of the chemical constituents and processes from which much of the aerosol is formed in the atmosphere and of the relevant meteorological parameters and effects.

Thus, in addition to the aerosol measurements, simultaneous measurements have been made of key gaseous pollutants and several meteorological parameters, and extensive ground-level meteorological data have been obtained for all sampling days. To further enhance the usefulness of

of the data, the sampling program has also coordinated and cooperated with the ARB's Aerosol Characterization (ACHEX) and Particulate Tracer Studies.

The study utilized two instrumented light aircraft (a Cessna 205 and a Cessna 310) and a mobile van. Observational systems were identical in each aircraft and included instruments to measure the following parameters:

Air Quality	Meteorological
Light Scattering (b_{scat})	Temperature
Condensation Nuclei	Humidity
CO	Turbulence
NO_x	Pressure (altitude)
O_3	

The van measured the above parameters (except for turbulence and pressure) and also recorded wind speed and direction.

All data processing was computerized, enabling data to be processed and checked between sampling missions; thus, the sampling program was continually updated, taking into account data from previous flights. In addition to the data taken by the vehicles, extensive meteorological and pollution data were collected from the FAA, NOAA, local air pollution control agencies, and MRI Mechanical Weather Stations so that the pollution data from any sampling mission could be interpreted in light of a firm understanding of the meteorology.

On any sampling day, both aircraft and the van operated in the same air basin. By flying two separate routes, an entire basin could be covered in a few hours. The routes consisted of a series of spirals (or soundings) from the top of the polluted layer to ground level over about eight points per flight. The soundings provided a series of snapshots of the vertical distribution of pollutants and other parameters over fixed points on the ground. Each route was flown two or three times per day, giving a picture of both the spatial and temporal variations of pollutant concentrations. The van was stationed at a fixed point and ran continuously for 24 to 48 hours whenever the aircraft were sampling. The van data provided information on the changes of pollutant concentrations and meteorological variables as a function of time and facilitated the interpretation of aircraft data when changes took place during a particular flight.

The program was started during the summer of 1972 and continued through the summer and fall of 1973. Although the program was originally set up to study all three air basins, most of the 1972 studies and virtually all of the 1973 program were concentrated in the South Coast (L.A.) Air Basin.

II. SUMMARY OF RESULTS, CONCLUSIONS, AND RECOMMENDATIONS

A. Summary of Results

The 3-D Gradient Study sampling has been successfully completed, and an unprecedented data base on the three-dimensional distribution of pollutants in several air basins has been obtained. The data have been reviewed and analyzed in a qualitative and sometimes quantitative manner, and plans for more detailed analyses have been made. The potential uses of the data, however, are much more numerous than those presently planned, and it is hoped that maximum use will be made of the data from this program in future studies of both the meteorology and air pollution of Southern California. Several of the results of the program are summarized below.

1. Over the two year period, a total of 241 sampling flights were made on 59 different days. In general, excellent meteorological, O_3, b_{scat}, and condensation nuclei data were obtained. During the 1973 program, high quality NO_x data were also obtained, but the 1972 NO_x data must be used with caution. The CO data for the entire program are usable and valuable, but due regard must be given to the zero drift problems encountered (see Chapter III). The aircraft data taken at low altitudes were found to be in good agreement with ground level data obtained by local control agencies. All aircraft instruments were calibrated in accordance with the procedures used by the California Air Resources Board.

2. Extensive meteorological data were obtained during the program. It was found that the temperature at 850 mb (5000 ft msl) can be used as an excellent indicator of the strength of the semi-permanent low level temperature inversion over the south coast basin. As such, the 850 mb temperature is a good indicator of the pollution potential on any given day. Temperatures greater than about 20°C at 850 mb during the summer months generally indicate a strong inversion and high pollution potential.

   The 3-D data also provided detailed information on the structure of the mixing layer and the ventilation processes in the south coast basin. In general, during the morning hours the mixing layer height

above sea level was relatively constant over most of the basin, with slightly greater heights over areas of elevated terrain. By afternoon, however, surface heating in inland areas and along the mountain slopes usually became a dominant factor, and mixing layer heights increased dramatically inland. Late in the afternoon, mixing layers often varied from 500 ft deep at the coast to 4000 ft deep in the inland valleys.

The heating of the slopes and inland valleys provided a major mechanism for ventilation of the basin. Flow up the mountain slopes due to heating was important in carrying pollutants aloft to layers above the surface mixing layer where they could be carried off by the winds aloft. Breaks in the inversion caused by intense surface heating in the inland areas also served the same purpose.

The deepening of the mixing layer during the day in the inland areas was also a major mechanism for reducing concentrations in those areas. The data showed that the total budget of pollutants within the mixing layer (integrated vertically) often remained constant as the air mass was transported eastward with the sea breeze. The ground-level concentrations, however, were reduced because, as the mixing layer deepened, clean air was entrained from aloft, thus decreasing the average concentration near the surface.

Smog episodes tend to occur during periods of strong subsidence. Under these conditions, the mechanisms mentioned above were modified. First, the ventilation to upper layers was restricted due to the subsidence inversion. Second, any pollutants carried aloft remained in layers and were not carried off, due to the light winds aloft. Third, if the mixing layer deepened at all in inland areas, dirty layers aloft rather than clean air were entrained, thus not reducing, and possibly increasing, surface concentrations. Finally, under these conditions, the sea breeze was often weak and late in starting, allowing more pollutants to accumulate in a limited air mass.

3. The 3-D Gradient Study has revealed complex and varied patterns of pollutant formation and transport in the Los Angeles Basin. Nevertheless, certain phenomena are so characteristic on smoggy days that they survive extensive averaging of the data. Morning and afternoon "grand average" vertical profiles for Hawthorne, El Monte, Ontario, and Riverside were prepared using all the 1973 soundings at these locations. The averages of the meteorological parameters show the erosion of the nighttime radiation inversion during the day and show the increased temperatures and mixing due to surface heating in the inland areas. The semi-permanent subsidence inversion is also seen at a higher level over the whole basin.

The average contaminant profiles illustrate the photochemical aging of the pollutants as they move away from source areas. Characteristics were compared at Hawthorne (source area near coast) and Riverside (receptor area several hours transport time inland). The afternoon contaminant mixes within the mixing layer at Hawthorne and Riverside reflect the different ages of the air mass at the two locations, with significantly more NO_x and CN at Hawthorne and significantly more O_3 and b_{scat} at Riverside. Direct emissions account for most NO_x and CN, which decay in the atmosphere. High values of these parameters are thus generally indices of fresh emissions. Ozone, and a large fraction of the light scattering aerosol, are not emitted directly, but are produced in the atmosphere. High values of these parameters are generally indices of pollutant aging. Concentrations of pollutants characteristic of an aged air mass are also seen in the averages in layers aloft which are separated from the surface mixing layer. In addition, the morning profiles indicate scavenging of ozone by primary emissions in source areas within the mixing layer. These profiles actually show a deficit of ozone within the mixing layer with higher values aloft.

4. Several specific episodes were examined in detail in the course of the data analysis. Of these, the data for the episode occurring from July 24 to 26, 1973, were the most complete and were analyzed in the most detail. This episode occurred during a period of strong subsidence with pollutants trapped below a 3000 ft msl inversion which covered most of the basin. Near the coast, a marine inversion was also present beneath the subsidence inversion with the effect that pollutants were generally trapped within a layer about 1000 to 1500 ft thick throughout the basin. The normal deeper mixing and ventilation up the mountain slopes which generally occurs in the northern and eastern portions of the basin was severely limited by the subsidence.

Analysis of the pollutant and meteorological data for the 25th indicated that pollutant transport in the basin can occur in a pulsing fashion. During the night and morning hours, pollutants accumulated for several hours in the stagnant air over the strong source areas in the vicinity of Los Angeles. As the sea breeze started up, this heavily polluted air mass was transported northeastward and replaced by air with a much shorter residence time over land. As the air was transported downwind of the strong source areas, scavenging of ozone by fresh NO emissions became less important, and photochemical production of ozone became a dominant factor. Trajectory analyses show that by about 1600 PDT, the air over Upland was just ahead of the sea breeze "front" and had been over strong source areas longer than any other air in the basin. Upland at 1600 recorded the highest ozone concentrations in the basin for the day (0.63 ppm).

Examination of the ratios of the various pollutants at different locations on the 25th generally showed photochemically younger air in the coastal and western areas and well aged air in the eastern basin in the afternoon and in the layers aloft (between the marine and subsidence inversions) all day. Ozone concentrations in excess of 0.5 ppm were observed in layers aloft separated from the surface mixing layer even near the coast.

An analysis of the ozone flux below the subsidence inversion from the western to the eastern portion of the basin on the afternoon of the 25th showed that roughly 185 ± 60 metric tons/hr were being transported eastward across a line between Pomona and Corona. This is enough to account for an average of about 0.25 ppm of ozone over the whole eastern basin.

At the end of this episode, a 24-hour sampling program was performed in the eastern basin. Ozone was seen to remain stable all night in layers aloft, isolated from surface emissions, at concentrations in excess of 0.12 ppm. Within the surface mixing layer during the night, however, ozone was almost totally scavenged by fresh NO emissions.

5. Analysis of two sampling days in the San Joaquin Valley indicates that the meteorology of the valley is complex and poorly understood. Mixing layer heights were influenced by heating of the mountain slopes, surface wind convergence zones, and the afternoon intrusion of sea breeze air in the northwest section of the valley. Pollutant concentrations were sufficiently low on the sampling days so that no pronounced pattern was apparent.

   In the San Francisco area, mixing layer heights are characteristically lower during the day over the water surfaces of the bay and higher over the surrounding heated ground surfaces. Pollutants were traced from the metropolitan area eastward over Livermore and southeastward past San Jose.

6. Several special analyses of the data have been performed during the program. An analysis of the data along a trajectory was performed to determine how well the Eulerian data obtained could be used to study the evolution of contaminants in a moving air mass. This Lagrangian interpretation was of help in understanding the phenomenon of pollutant aging and transport. Pollutant concentrations were integrated vertically through the mixing layer to examine the total pollution budget along a trajectory. Although there was considerable scatter in the data,

certain trends were apparent. Loadings increased during the passage over the heavily urbanized western Los Angeles Basin as the air mass accumulated primary emissions and reaction products. The observed rate at which the CO loading increased during this period was comparable with the calculated rate at which CO was emitted (e.g., Roth et al., 1974). Later, as the air mass crossed the eastern basin, loadings decreased due to meteorological factors such as dilution and spreading.

7. A statistical analysis of the correlation between various pollutants in layers aloft was also performed. These layers were separated from fresh surface emissions and were photochemically well aged. Within the elevated pollutant layer on one typical vertical profile, ozone concentrations were relatively high and condensation nuclei counts were relatively low. The ratio $[O_3]/b_{scat}$, which was less than 0.03 ppm x 10^4 m in the surface mixed layer, was about 0.1 ppm x 10^4 m in the elevated pollutant layer. Similarly, the ratio b_{scat}/CN, which was less than 0.7×10^{-14} m^2 in the surface mixed layer, was about 1.5×10^{-14} m^2 in the elevated layer. These differences are similar to those observed when the surface mixed layers at Hawthorne and Riverside are compared as mentioned previously.

All variables studied in the layers aloft were somewhat correlated and, in general, the regression equations for well correlated variables did not depend strongly upon location. The independence of location shown by elevated pollutant layers contrasts with the dependence on location of surface mixed layer pollutant characteristics and suggests that the elevated layers reflected larger scale phenomena.

The contaminant indices which correlated most closely above the surface mixed layer were ozone concentration and b_{scat}, which had correlation coefficients greater than 0.9 in one quarter of the profiles. The regression coefficients for ozone and b_{scat} were also quite consistent from one profile to the next, indicating that both the ozone and b_{scat} are of similar origin, i.e., both photochemical products.

8. Another of the special analyses performed was a study of ozone concentrations in California. The results indicated that the ozone background level in clean air in California is between 0.03 and 0.05 ppm (roughly one-half the federal ambient air standard). Ozone was found to be stable in the absence of other pollutants to scavenge it and to be transported long distances over non-source areas. In one study, ozone concentrations of 0.12 ppm were found to exist undiminished in layers aloft overnight and, in another, background levels of ozone were seen aloft even in the rain. In the absence of photochemistry (on cloudy days or at night) ozone was found to be scavenged within the surface mixing layer in source areas.

9. Observations of the spatial distribution of b_{scat} in the Los Angeles Basin show that large patches of light scattering aerosol (0.1 to 1 μm) are often generated rapidly in the morning and then transported across the basin during the day. The patches appear in source areas, but not always in the same areas. There is apparently an optimum set of conditions under which prolific aerosol growth occurs. The patches are especially apparent in isopleth maps of b_{scat} integrated through the mixing layer (optical depth) where one looks at the total aerosol budget in the mixing layer rather than just the surface concentration.

It is suggested that these patches of low visibility are indicative of the growth of secondary aerosols, presumably by photochemical action. This is supported by the rapid increase in b_{scat} values in spite of general decreases in the primary constituent concentrations as indicated by CO concentrations. The localized nature of the patches may be due to local concentrations of major sources or local morning meteorological conditions which are unusually favorable for aerosol growth. Meteorological factors which might be conducive to the formation of these local patches are light winds, shallow mixing layers, and high humidities.

Observations of the spatial distribution of condensation nuclei (less than 0.1 μm) indicate that condensation nuclei are generated in areas with strong combustion sources, but are quickly scavenged from the atmosphere (by coagulation) in the presence of larger particles (characterized by high b_{scat}). As a consequence, a photochemically aged air mass is characterized by high b_{scat} values and low CN values.

10. A statistical data analysis was performed with the 1972 data in which the relationship between b_{scat}, CO, and relative humidity (RH) was investigated. The following observations were made.

For various constant values of CO concentration, the b_{scat} increased strongly with increasing RH. Qualitatively, the observed increase of b_{scat} with RH is consistent with earlier humidification studies of other investigators. In this case, however, the b_{scat} increases by approximately a factor of three with a humidity increase from 37 to 80 percent, which is considerably more than the increase observed by humidifying ambient air. The light scattering coefficient also increases consistently with increasing CO concentration (i. e., with auto-exhaust concentration in the air). In fact, for the above data, the increase of b_{scat} is almost linear with CO. This latter statement, if it can be substantiated by further data analysis, is of significance for developing effective control strategies for visible particulates.

11. In addition to the standard basin-wide sampling programs, three special field programs were undertaken. One was a study of the plumes from the Moss Landing and Ormond Beach power plants, the second was a special flight devoted to looking at horizontal gradients in the Upland area, and the third was a flight made for the purpose of obtaining samples for electron microscopy.

The Ormond Beach sampling was done under strong summer subsidence conditions. The buoyant plume partially penetrated into a very stable layer above

the surface mixing layer, contributing to high pollutant concentrations in the layer aloft. The ozone concentration in the upper layer was greater than 0.4 ppm, and more than 80 percent of the NO from the power plant was found to be converted to NO_2 within a distance of about 2 miles (or about 20 minutes travel time).

The Moss Landing plume was sampled in clean air during neutral winter conditions with a moderate cloud cover. The NO/NO_x ratio was difficult to determine in this case, but the conversion rate appeared to be quite slow. Crude measurements of the SO_2 to sulfate conversion rate for the Moss Landing plume indicated that between 0.3 and 3 percent of the SO_2 was converted to sulfate per hour.

Plume height, dispersion rates, pollutant concentrations, and reaction rates were found to be highly depend upon ambient meteorological conditions and pollutant concentrations, but it was shown that even invisible plumes could easily be identified, mapped, and analyzed using a light aircraft as a sampling platform.

12. A special flight was conducted in the Upland area to examine the horizontal gradients in pollutant concentrations. The concentration variations within the mixing layer were not large, but flights just above the average mixing layer height showed great variations. The peaks measured above the layer appeared to be associated with main roadways which were parallel to the wind. The roads were apparently acting as heat sources which lifted the mixing layer in their immediate vicinity. It is reasonable to expect that the main cause of the buoyant air was the heating of the roadway surface by solar radiation rather than the heat contributed by the cars. In either case, if this conclusion is backed up by further experiment, it suggests that roadways must be considered to have buoyant plumes and that this fact must be accounted for in modeling the effects of highways.

13. Several aerosol samples were collected by an impactor at 2100 ft msl in the mixing layer over the Pasadena area. These samples were later analyzed by electron microscopy and compared to those obtained at the surface. The micrograph of the surface-collected aerosol shows both solid particles and liquid droplet residues with many of each, indicating a mixture of both primary (fresh) and secondary (aged) aerosol.

Nearly all the particles appearing in the 2100 ft micrograph, however, are liquid droplets. Without exception, each of the droplet residues contains a nucleus of high electron opacity. These nuclei, most of which have diameters of about 0.02 microns and resemble poppy seeds in the electron micrographs, are similar in appearance to particles present in large numbers in automobile exhaust. The above observations strongly suggest that the aerosol at 2100 ft grew by heterogeneous nucleation on solid primary aerosol particles. It has previously been hypothesized (Husar and Whitby, 1973) that this is the primary mechanism of photochemical aerosol production in the Los Angeles Basin.

Many of the larger droplet residues in the 2100 ft micrograph contain numerous nuclei. This is due in part to superposition of droplets on the impactor stage. It appears also to be due in part to coagulation in the atmosphere of droplets with both other droplets and with primary nuclei.

B. Conclusions

1. Meteorology

a. In general, the summer mixing layer in the L. A. Basin starts out relatively shallow in the night and morning hours. During the day, the layer deepens in the inland areas due to surface heating and the inversion often breaks near heated slopes or in inland valleys, allowing the escape of pollutants. The basic summer flow patterns in the three basins are controlled by local thermal, rather than

synoptic, effects. These wind fields have distinct diurnal patterns. During episode conditions, the mixing layer structure and ventilation processes are modified.

b. The mixing layer structure and the basin ventilation rates are the keys to pollutant accumulation and thus to prediction in the three air basins studied. In source areas, the rate of accumulation and the ultimate total concentrations depend upon wind speed, mixing depth, and the length of the characteristic night and morning stagnation period. During episode conditions, the onset of the sea breeze is often delayed, lengthening the stagnation period, and the mixing depth is restricted by subsidence.

c. In the Los Angeles Basin, the pollutants accumulated in source areas in the stagnant morning air are transported downwind to areas of lesser source strength (receptor areas) with the onset of the sea breeze. The ultimate concentrations in the downwind areas depend on the mixing layer structure. If the mixing layer deepens, entrains clean air, and ventilates pollutants upward, concentrations will be lowered. If the mixing depth and thus the ventilation is limited by subsidence, the products of photochemical reactions will be confined to a shallow layer, and ozone and other secondary pollutant concentrations will be high.

d. The primary mechanisms for escape of pollutants from the Los Angeles Basin are horizontal transport out of the passes surrounding the basin and vertical transport to elevations above the mixing layer where pollutants can be carried off by winds aloft. During most episode conditions, the vertical transport is limited by subsidence, and in some cases the transport out of the passes is limited as well.

e. Upper winds are an important part of the ventilation process for the L. A. Basin. Flow up heated slopes and transport up through breaks in the inversion can create stratified layers aloft, often with very high pollutant concentrations. If these layers are not carried off by the upper winds, they can remain to be re-entrained within the surface mixing layer as the inversion is eroded on subsequent days. When this dirty air, rather than clean air, is entrained, surface concentrations are not reduced and may even be increased, contributing to episode conditions.

f. Buoyant point source plumes, especially those near the coast, can become trapped in stable layers above the surface mixing layer, contributing to high pollutant concentrations aloft. These upper layers can be transported to inland areas and be re-entrained as the surface mixing layer deepens.

g. Preliminary interpretation of some of the data obtained in this study indicates that roadways can be significant buoyant heat sources which can actually modify the height of the mixing layer. This fact should be accounted for in modeling highway plumes.

h. The "Upland anomaly" of high ozone concentrations was found to be real and a result of the transport patterns in the basin. Upland is sited such that it often receives an air mass containing pollutants accumulated during the night and morning hours over strong source areas. This air mass, which has often been over source areas longer than any air in the basin, reaches Upland in a well aged state. The source strength in the Upland area is low and ozone is not well scavenged. Under these conditions, other areas of the basin receive air which is less polluted to start with or which has been diluted with clean air from aloft.

i. Detailed three-dimensional chemical and aerosol data are invaluable in interpreting meteorology, especially where standard meteorological variables are ambiguous.

2. Chemistry

a. The ratios of various pollutants are useful to determine the photochemical age of an air mass and thus to help understand the meteorological and transport phenomena taking place. Direct emissions account for most NO_x and CN, which decay in the atmosphere. High values of these parameters are thus generally indices of fresh emissions. Ozone, and a large fraction of the light scattering aerosol, are not emitted directly, but are produced in the atmosphere. High values of these parameters are generally indices of pollutant aging.

b. A statistical analysis of aged air masses above the surface mixed layer showed that the contaminant indices which correlated most closely were ozone concentration and b_{scat}. These parameters had correlation coefficients greater than 0.9 in one quarter of the profiles. The regression coefficients for ozone and b_{scat} were also quite consistent from one profile to the next, indicating that both ozone and b_{scat} are of similar origin, i.e., both photochemical products.

c. The data from Los Angeles indicate that there is apparently an optimum set of conditions under which prolific aerosol growth occurs. It is suggested that the rapidly forming patches of low visibility are indicative of the growth of secondary aerosols, presumably by photochemical action. The localized nature of the patches may be due to local concentrations of major sources or local morning meteorological conditions favorable for aerosol growth. A single factor which appears to have an unusually large effect is relative humidity.

d. The SO_2 to sulfate conversion rate was crudely measured during clean winter conditions in the Moss Landing power plant plume while the plant was burning low sulfur oil. The conversion rate was found to be between 0.3 and 3 percent per hour.

e. The NO to NO_2 conversion rate was also measured in a crude fashion in both the Ormond Beach and Moss Landing power plant plumes. At Ormond Beach, under strong summer subsidence conditions with the plume being emitted into a background of 0.4 ppm ozone, roughly 80 percent of the NO was converted to NO_2 in about 20 minutes. The conversion rate at Moss Landing under clean winter conditions with cloud cover was on the order of 1/10 to 1/2 that at Ormond Beach.

f. Ozone was found to be stable in the absence of other pollutants to scavenge it and to be transported long distances over non-source areas. Concentrations higher than 0.12 ppm were seen to remain undiminished in layers aloft all night. In the absence of photochemistry (on cloudy days or at night), ozone was found to be scavenged within the surface mixing layer in source areas. The background ozone level in clean areas was found to vary from 0.03 to 0.05 ppm.

g. In general, comparatively low NO_x values were found in aged air masses with high values of b_{scat}. There is some evidence to indicate that a significant portion of the NO_x ends up in aerosol form as the pollutants react and age.

3. General

a. Perhaps the most important conclusion of this study is that air pollution is a regional problem. Afternoon concentrations in the eastern part of the south coast basin are

dependent upon emissions earlier in the day in the western basin. The same is probably true of the afternoon concentrations in the Santa Clara and Livermore valleys in the San Francisco Bay area. To be effective, air pollution control must be on a regional basis.

b. Ground-level data are unable to provide total pollutant budgets. To truly define pollutant fluxes and understand transport phenomena, three-dimensional data are needed. Ground-level ozone measurements in source areas are not true indicators of total pollution and should not be the primary criteria for judging trends in air quality. Ozone concentrations of greater than 0.5 ppm have been observed aloft over coastal areas with low surface ozone concentrations.

c. Lagrangian analysis techniques are useful to establish emission rates for area sources and to obtain an understanding of transport phenomena. Lagrangian-type analyses can be performed using Eulerian data.

d. The complex of point sources in the Fontana area was found to generate a dense elevated layer of aerosol, NO_x, and even CO over a large portion of the eastern L. A. Basin during the night and morning hours. This elevated layer was entrained within the surface mixing layer as the nighttime radiation inversion was eroded during the day.

e. Light instrumented aircraft were found to be useful tools for defining and mapping both point source plumes and the three-dimensional distribution of pollutants in an air basin. The techniques developed during this program provide a relatively inexpensive method of studying emission distribution and transport, as well as chemistry.

C. Recommendations

1. The regional nature of the air pollution problem in the three major air basins studied should be recognized and control strategies developed on this premise.

2. The meteorology of the L. A. Basin has a distinct diurnal pattern. It may be possible to regulate some emissions on a time-dependent basis with greater emissions allowed during periods of greater ventilation. If possible, emissions in the strong source areas in the vicinity of Los Angeles and the south bay should be minimized during the late night and morning hours.

3. The aerosol and visibility problem in the L. A. Basin appears to be largely the result of secondary aerosol formation. The aerosol and ozone concentrations correlate well in aged air masses, and it is probable that a solution to the ozone problem will also alleviate the aerosol problem. Control of ozone and aerosol in the light scattering size range should be approached as a joint problem on a coordinated basis.

4. Layers aloft appear to play an important role in the pollution patterns in the basin. Pollutants ventilated aloft can either be removed from the basin by upper winds or can remain and be re-entrained on subsequent days, contributing to surface concentrations. More data are needed to better understand the role these layers play. It is recommended that continuous monitoring stations be established at a few locations along the slopes of the mountains to provide data on the upslope ventilation processes and to determine whether these layers are causing high ground-level concentrations at high elevations. These stations should be located at roughly the 1500 ft level in the coastal mountains (Santa Monica) and slope upward to roughly 4000 ft in the inland mountains (San Gabriel).

5. Point source plumes contribute significantly to high concentrations in layers aloft and probably to ground-level concentrations in inland areas. More study of the interaction of these plumes with the coastal meteorological environment is needed in order to properly regulate the construction of new sources. The ARB has already funded further study in this area.

6. There is increasing interest in the role which humidity may play in both aerosol and gaseous chemistry as well as its effect on visibility. Both humidity and visibility are poorly measured within the L. A. Basin and a much denser network of observations is recommended.

7. Upper air temperatures and winds are key parameters in controlling the ventilation rate of the L. A. Basin. Further study of the relationship between the winds and temperatures above the mixing layer and surface concentrations is recommended. The upper air temperature is already used as a tool for pollution prediction, but more attention should be paid to the use of winds aloft, especially in multi-day episodes.

III DESCRIPTION OF EXPERIMENTAL PLAN

A. Aircraft and Van Instrumentation

The aircraft instrumentation is divided into four basic groups of sensors: aerosol sensors, gas monitors, meteorological sensors, and position sensors. The van instrumentation is similar except for the position sensors.

Blumenthal and Ensor (1972) described in detail the criteria for selection of instrumentation for airborne sampling, the most important instrumental requirements being low weight, power, and bulk, and a fast time response. The specific instruments selected for use in the aircraft are listed in Table III-1.

The aerosol sensors selected for this study are the MRI Integrating Nephelometer and the Environment One Condensation Nuclei Monitor. These instruments were found to be the aerosol samplers best suited to the aircraft environment which requires ruggedness and fast time response. These and all other instruments are discussed in detail in Appendix A of this report.

The gases monitored are CO, O_3, and NO-NO_x. CO was chosen because it is a fairly non-reactive compound which can be used as a tracer for automobile exhaust. O_3 and NO_x are both indicators of the photochemical processes taking place, and NO_x is also an indicator of both automobile and stack emissions. The specific gas monitors used are all at the state-of-the-art and most of them were among the first few off the production line. REM chemiluminescent O_3 and NO-NO_x monitors were selected for use in the aircraft as was an Andros CO monitor. This instrumentation remained essentially unchanged throughout both the 1972 and 1973 programs with the exception of minor modifications to the REM NO/NO_x monitor which are also detailed in Appendix A.

The meteorological parameters measured in the aircraft are temperature, relative humidity, and turbulence. These are measured with sensors incorporated in the MRI Airborne Instrument Package. This package also includes a Validyne P-24 15 psi absolute pressure sensor to monitor altitude and a pressure transducer to record the indicated airspeed.

The position instrumentation in the aircraft uses the standard aircraft VOR and DME systems interfaced to a Metrodata M/8 package to convert the signals to an analog output.

TABLE III-1

AIRCRAFT INSTRUMENTATION

	Instrument	Power Required	Ranges Available	Time Response (90%, for Usual Ranges)
1.	MRI Integrating Nephelometer	70 W	10 *, 40, 100 x 10^{-4} m^{-1}	1 sec
2.	Environment One Condensation Nuclei Monitor (Rich 100)	70 W	1, 3, 10, 30, 100*, 300* 10K x 10^3 CN/CC	5 sec
3.	REM 612 Ozone Monitor	60 W	50*, 200 pphm	5 sec
4.	REM 642 NO-NO_x Monitor	350 W	0.5*, 2*, 10 ppm	5 sec
5.	Andros 7000 CO Monitor	125 W	20, 50*, 100, 200 ppm	5 sec**
6.	Theta Sensor LS-400 SO_2 Monitor ≠	7 W	1*, 10*, ppm	20 sec
7.	MRI Airborne Instrument Package	25 W		
	Temperature		-5 to +45°C	5 sec
	Humidity		0 to 100%	30 sec
	Turbulence		0 to 10 $cm^{2/3}$ sec^{-1}	3 sec (to 60%)
	Altitude		0 to 10,000 ft	1 sec
	Indicated Air Speed		50 to 150 mph	≤ 1 sec
8.	Metrodata M/8 VOR Analog Converter (uses aircraft radio)	10 W		1 sec
9.	Metrodata 620 Data Logger (20 channels)	35 W		48 channels/sec

≠ Used occasionally. * Usual range(s). ** Fast time response by special order.

The aircraft selected for the project are a single engine Cessna 205 and a twin engine Cessna 310. Both aircraft can carry over 600 lbs of equipment plus pilot and observer. The Cessna 205 sampling system is described in detail in Appendix A of this report; the 310 system is essentially the same except that the instruments are positioned differently in the aircraft.

Data from all the instruments are recorded on a 1/4 inch tape cassette by a Metrodata 620 digital data logger. Twenty channels of information are recorded at the rate of 48 channels per second; an internal digital clock supplies the time in hours, minutes, and seconds to two tape channels.

All 110 V instruments are powered by a 1 kw, 110 V inverter run off the aircraft power system which has been modified to include a 24 V, 100 A alternator.

The air quality instrumentation employed in the ground-based van is identical to that of the aircraft with the exception of the CO monitor. A Bendix UNOR 5 CO monitor is used in the van instead of an Andros 7000. All instruments selected for use in the van are listed in Table III-2. The van is also equipped with sensors for temperature, dew point, and wind speed and direction, along with a Metrodata 620 data logger which records all data. This instrumentation and the van sampling system is discussed in detail in Appendix A.

B. Instrument Calibration and Limitations

All instruments were first calibrated in 1972 prior to installation in the aircraft and van. The ozone and CO instruments were calibrated and a bottle of CO span gas was certified at the State of California Air and Industrial Hygiene Laboratory in Berkeley, California. The NO_x instruments were calibrated at the factory by REM. The condensation nuclei instruments were also factory calibrated and the Integrating Nephelometers were calibrated absolutely with freon by MRI. A detailed discussion of all calibrations is included in Appendix B of this report.

During the 1972 program, the O_3 and NO_x instruments were recalibrated by AIHL personnel prior to the intensive sampling in the Los Angeles area and again by REM after the end of the sampling and after any maintenance performed. The nephelometers were periodically checked with freon and were adjusted using a mechanical calibrator before each flight. The condensation nuclei monitors were not recalibrated, but differed by less than 30 percent when checked at

TABLE III-2

VAN INSTRUMENTATION

	Instrument	Usual Range Used
1.	MRI Integrating Nephelometer (Model 1550 B)	0-10 (10^{-4}) m^{-1}
2.	Environment I Condensation Nuclei Monitor (Rich 100)	0-10^5 cn/cc
3.	REM 612 Ozone Monitor	0-0.5 ppm
4.	REM 642 NO-NO_x Monitor	0-0.5 ppm
5.	Bendix UNOR 5 CO Monitor	0-50 ppm
6.	MRI 1072 Wind Speed and Direction	0-50 mph, 0-540°
7.	Temperature Sensor	-5 to +45 °C
8.	Cambridge Systems Model 880 Dew Point	-40 to +50 °C
9.	Metrodata 620 Data Logger	

the end of the 1972 sampling period. CO instruments were calibrated on a regular basis with the span bottle mentioned above.

Several instruments were factory reconditioned, and all instruments were again calibrated by factory or AIHL personnel, before sampling commenced for the 1973 program. Calibrations of the O_3, NO_x, and CO instruments were then done on a monthly basis for the remainder of the program. Dates of additional calibrations included 14 August and 17-19 September 1973.

Since the span calibrations of the instruments generally varied less than the errors inherent in the measurement and calibration techniques, the data have not been adjusted on a routine basis to take into account variations in instrument calibration.

One of the problems in a field sampling program of this type is lack of control over the instrument environment. Changes in temperature and altitude, for example, affect the instrument readings. In examining and using the data from this program, these limitations must be recognized. An attempt has been made to compensate for some of the errors, such as altitude variations or zero offsets, by using a data cleaning computer program to be described later in this chapter.

The easiest variation to correct for is altitude. Table III-3 presents a summary of the effects of altitude on the output of our instruments. The term R_t/R_i for each instrument represents the ratio of the true concentration or reading to the indicated concentration. R_t/R_i is indicated for each instrument for the 5000 foot level on a standard day. Except for the condensation nuclei data, the variations with altitude are not large over the altitude range of this experiment, but corrections are nevertheless included in the data presented as "clean" data in this volume and in the data volumes.

The aircraft data have not been corrected for differences in instrument time response. The aircraft instrument time responses are listed in Table II-1. The time response figures include both delay times in getting the sample to the sensor and the electronic, or sensor, time response.

Since the aircraft generally climb and descend at approximately 500 feet per minute, most of the data will be accurate to within 100 feet. The major exceptions are the NO_x and humidity data. The NO_x monitor has a delay time of about five seconds and an electronic time response of 10 seconds. Thus, the NO_x data will often be out of

TABLE III-3

ALTITUDE CORRECTIONS

Instrument	Correction Factor	Correction at 5000'
O_3 (1)	$\frac{R_t\ (ppm)}{R_i\ (ppm)} = \sqrt{\frac{\rho_o}{\rho}}$	1.08
CO (2)	$\frac{R_t\ (ppm)}{R_i\ (ppm)} = \frac{\rho}{\rho_o}$	1.16
NO (3)	$\frac{R_t\ (ppm)}{R_i\ (ppm)} = 1$	1.0
CN	$\frac{R_t\ (CN/CC)}{R_i\ (CN/CC)}$ - As shown on chart in instrument manual	1.35
b_{scat}	$\frac{R_t\ (M^{-1})}{R_i\ (M^{-1})} = 1$	1.0

R_t = True Value
R_i = Indicated Value
ρ_o = Air Density at Calibration Point
ρ = Air Density at Point of Measurement

(1) - The ozone monitors measure number of O_3 molecules and are flow sensitive. The correction factor assumes indicated flow on flowmeter remains constant.

(2) - The CO monitor measures absolute amount of CO regardless of density of air; thus, density correction is necessary to get ppm.

(3) - The NO_x monitor is sensitive to mass flow, but this is held constant by using a critical orifice.

phase with the other data by about 50 feet and will be smoothed over about 125 feet. The RH data at a given altitude often represent the variations over the last 250 feet.

Every effort was made to keep the aircraft instrumentation working properly. As a result, the van was periodically neglected or robbed of an instrument to replace a malfunctioning aircraft instrument. This procedure resulted in the van data, especially the gaseous data, being sometimes questionable. In general, however, the CN, O_3, meteorological, and b_{scat} data are accurate. Since the van was used only as a reference to detect changes in conditions during a flight, this loss of data was not serious.

Other limitations and idiosyncracies of the various instruments are discussed in detail in Appendix B of this report. Because of these limitations, the data presented in this volume and the data volumes can by no means be considered perfect. They are, however, very interesting and useful if their limitations are taken into account.

C. Flight Plans and Routes

The various sampling routes followed during the 1972 and 1973 programs are listed in Tables III-4 through III-8 and shown in Figs. III-1 through III-4. Sampling along the San Joaquin Valley and the San Francisco Basin routes was limited to the 1972 program as was the 1972 desert route which was sampled on only one occasion. The desert-mountain route, however, was sampled only during the 1973 program. These routes were those usually used, but they were occasionally modified under certain circumstances. For example, the San Joaquin Valley route was adjusted during the 1972 program to include Hunter-Liggett (HUN) when the Aerosol Characterization Study trailer was located there.

The routes in the Los Angeles Basin were each flown three times a day, weather and equipment permitting. During the 1972 program, the Northern and Riverside routes were generally flown on the first sampling day of the week and the Southern and Riverside routes flown on the next day. During the 1973 program, route selection was governed by the goal of the sampling mission, as well as by existing meteorological conditions. Routes in the San Joaquin Valley and the San Francisco Basin were flown twice a day and three times per day, respectively. In both cases, the entire basin was covered in a single day. As often as possible, sampling days coincided with the Aerosol Characterization Study intensive study days.

TABLE III-4

SAMPLING POINTS FOR THE LOS ANGELES BASIN

Northern Route

Station	Abbreviation	Elevation
El Monte Airport	(ELM)	291 ft msl
*Cal Tech	(PAS)	864
*Los Angeles Railroad Yard	(LARR)	270
Burbank Airport	(BUR)	775
Van Nuys Airport	(VNY)	800
Santa Monica Airport	(SMO)	175
Hawthorne Airport	(HHR)	64
Shepherd Airport	(SHE)	218

Southern Route

Corona Airport	(COR)	535
Fullerton Airport	(FUL)	93
Hawthorne Airport	(HHR)	64
Torrance Airport	(TOA)	95
Long Beach Airport	(LGB)	56
Meadowlark Airport	(MEA)	30
El Toro Marine Corps Air Station	(NZJ)	380

Riverside Route

Brackett Airport	(BRA)	1000
Corona Airport	(COR)	535
Riverside Airport	(RAL)	790
Redlands Airport	(RED)	1574
Rialto Airport	(RIA)	1434
Ontario Airport	(ONT)	952
Cable Airport	(CAB)	1450

*Non-airports

TABLE III-5

SAMPLING POINTS FOR THE SAN JOAQUIN VALLEY

Station	Abbreviation	Elevation
North Route		
Fresno Air Terminal	(FAT)	331 ft msl
Eagle Airport	(EAG)	167
Merced Airport	(MER_2)	155
Weins Airport	(WEIN)	270
Modesto Airport	(MOD)	96
Tracy Airport	(TRA)	207
Stockton Airport	(SCK_1)	27
South Route		
Fresno Air Terminal	(FAT)	331
Alta Airport	(ALTA)	360
Hanford Airport	(HAN)	245
Avenal Airport	(AVN)	790
Lost Hills Airport	(LH)	285
Taft Airport	(TAFT)	875
Bakersfield Airport	(BFL)	378
Delano Airport	(DEL)	316
Portervile Airport	(POR)	444

TABLE III-6

SAMPLING POINTS FOR THE SAN FRANCISCO BAY

Station	Abbreviation	Elevation (ft)
West Route		
Crissy Army Air Field	(CRI)	8 ft msl
San Francisco Int'l Airport	(SFO)	11
Half Moon Bay Airport	(HMB)	64
San Carlos Airport	(CAR)	6
Palo Alto Airport	(PAL)	5
*Southwest San Jose	(SJC)	60
San Jose Airport	(SJC)	62
East Route		
Alameda Naval Air Station	(NGZ)	15
*West Berkeley - over Bay	(BER)	0
*Southeast San Pablo Bay	(PAB)	0
Concord (Buchanan)	(CCR)	22
Hayward Airport	(HAY)	47
Livermore Airport	(LIV)	448
Fremont Airport	(FRE)	15
Reid Hillview Airport	(REID)	134

*Non-airports

TABLE III-7

SAMPLING POINTS FOR THE 1972 DESERT ROUTE

Station	Abbreviation	Elevation (ft)
China Lake	(CHL)	2300
Agua Dulce	(ADU)	2680
Hesperia	(HES)	3390
Goldstone	(GOL)	3500

(This route not illustrated.)

TABLE III-8

SAMPLING POINTS FOR THE 1973 DESERT-MOUNTAIN ROUTE

Station	Abbreviation	Elevation (ft)
Cable Airport	(CAB)	1450
Hesperia	(HES)	3390
Lake Arrowhead	(ARR)	5114
Big Bear Lake	(BBR)	6750
Banning	(BN)	2219
Hemet	(HEM)	1512
Thermal	(TRM)	-117
Palm Springs	(PSP)	448

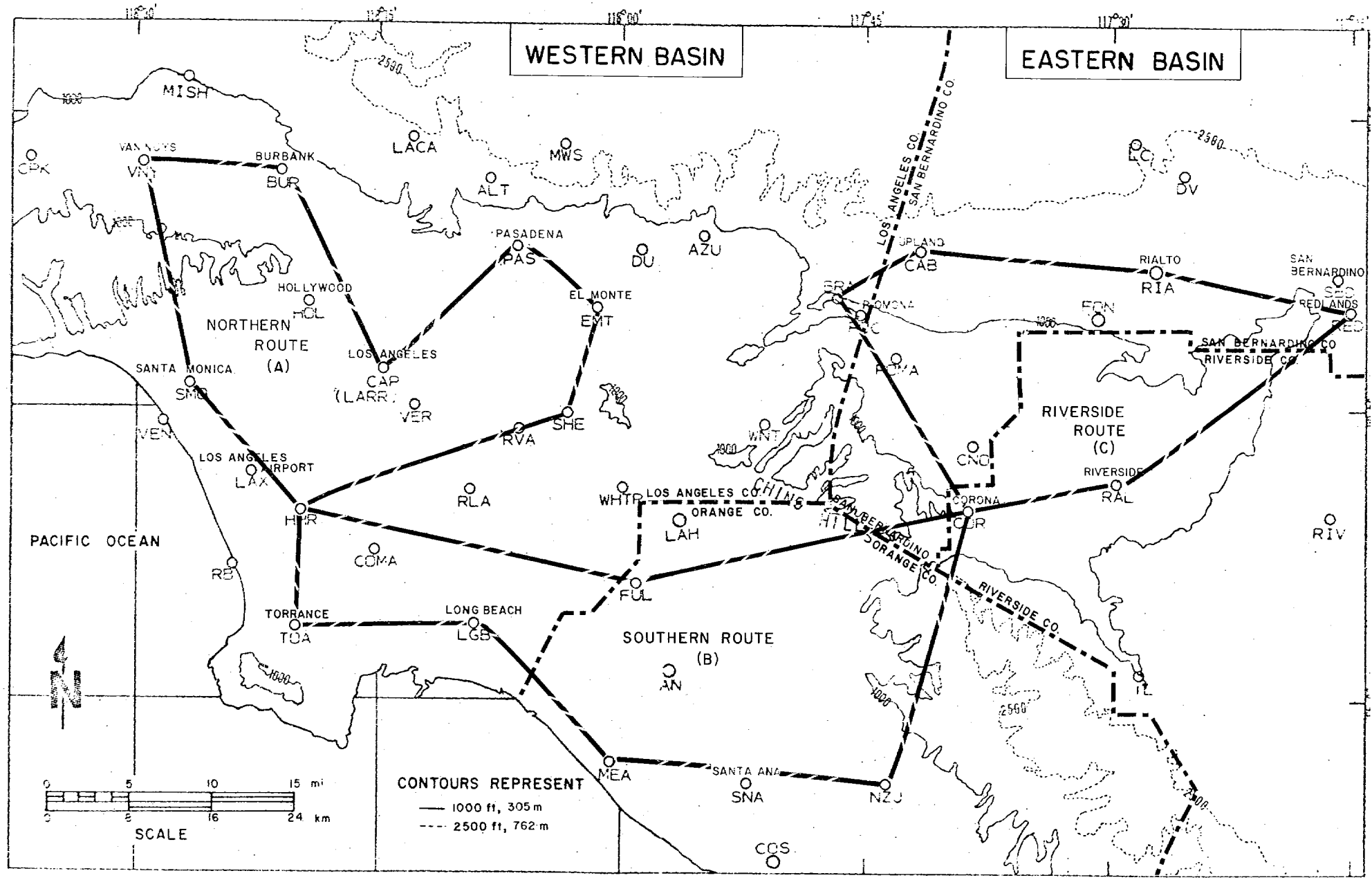

Fig. III-1. SAMPLING ROUTES IN THE LOS ANGELES BASIN

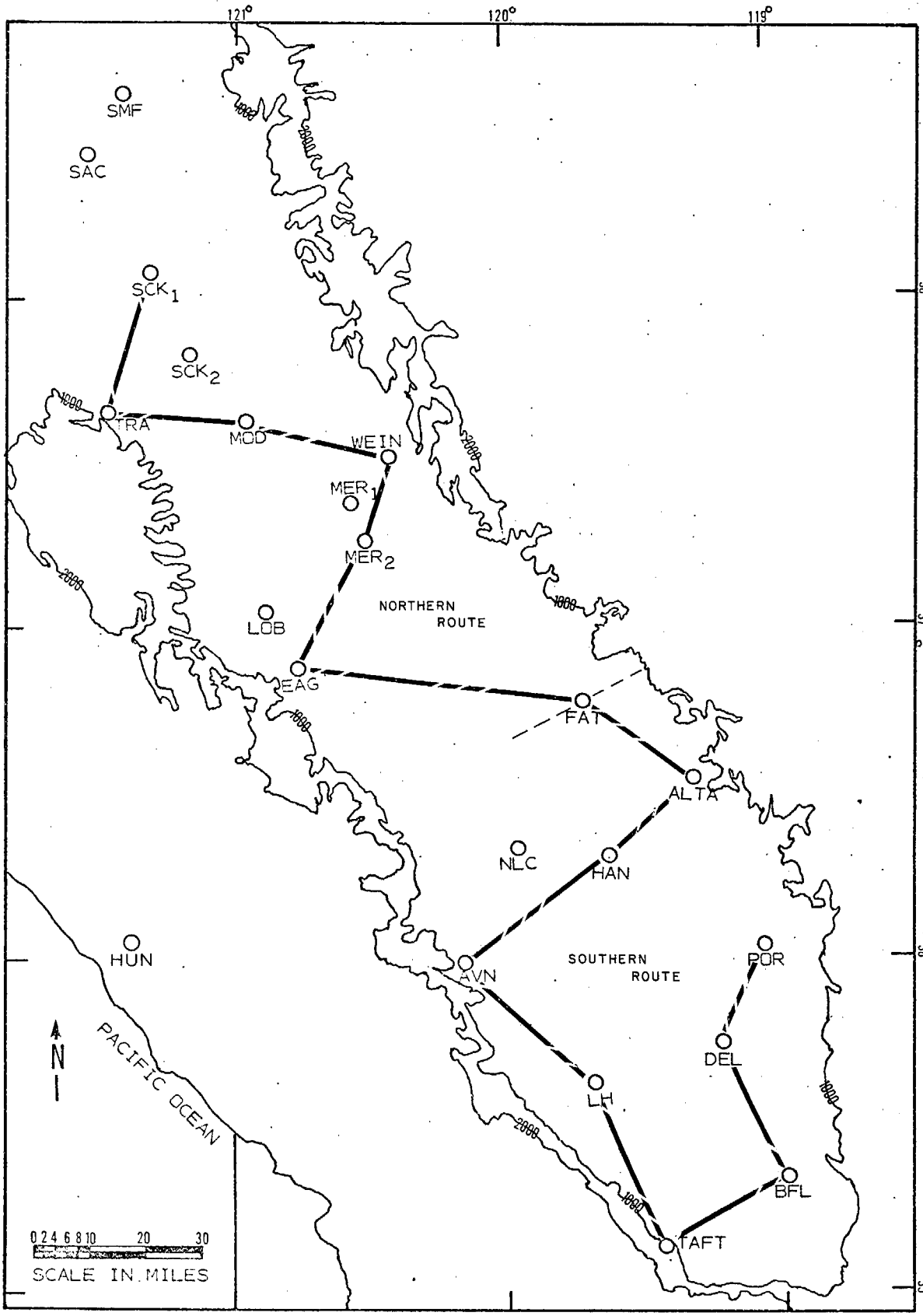

Fig. III-2. SAMPLING ROUTES IN THE SAN JOAQUIN VALLEY

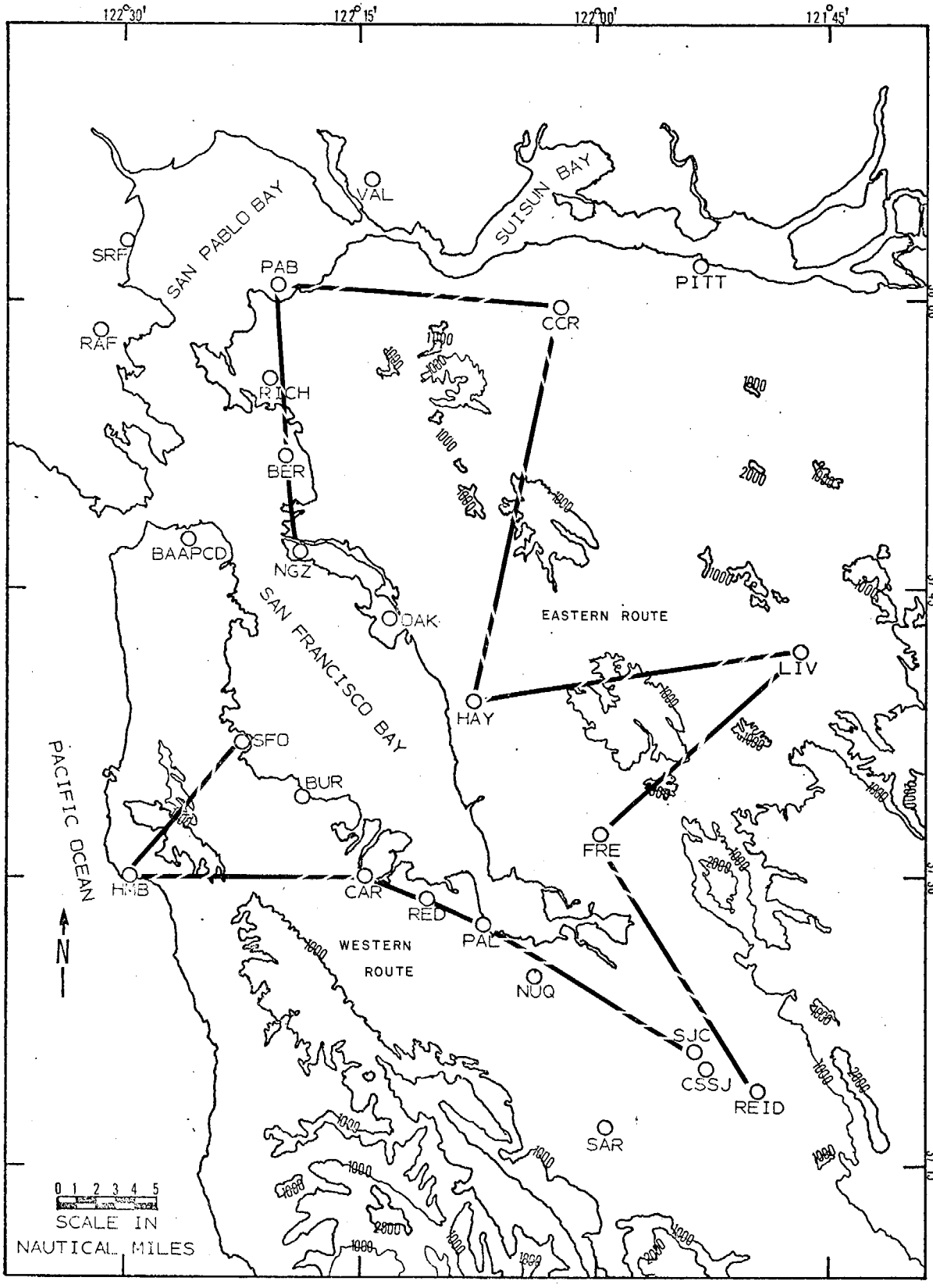

Fig. III-3. SAMPLING ROUTES IN THE SAN FRANCISCO BASIN

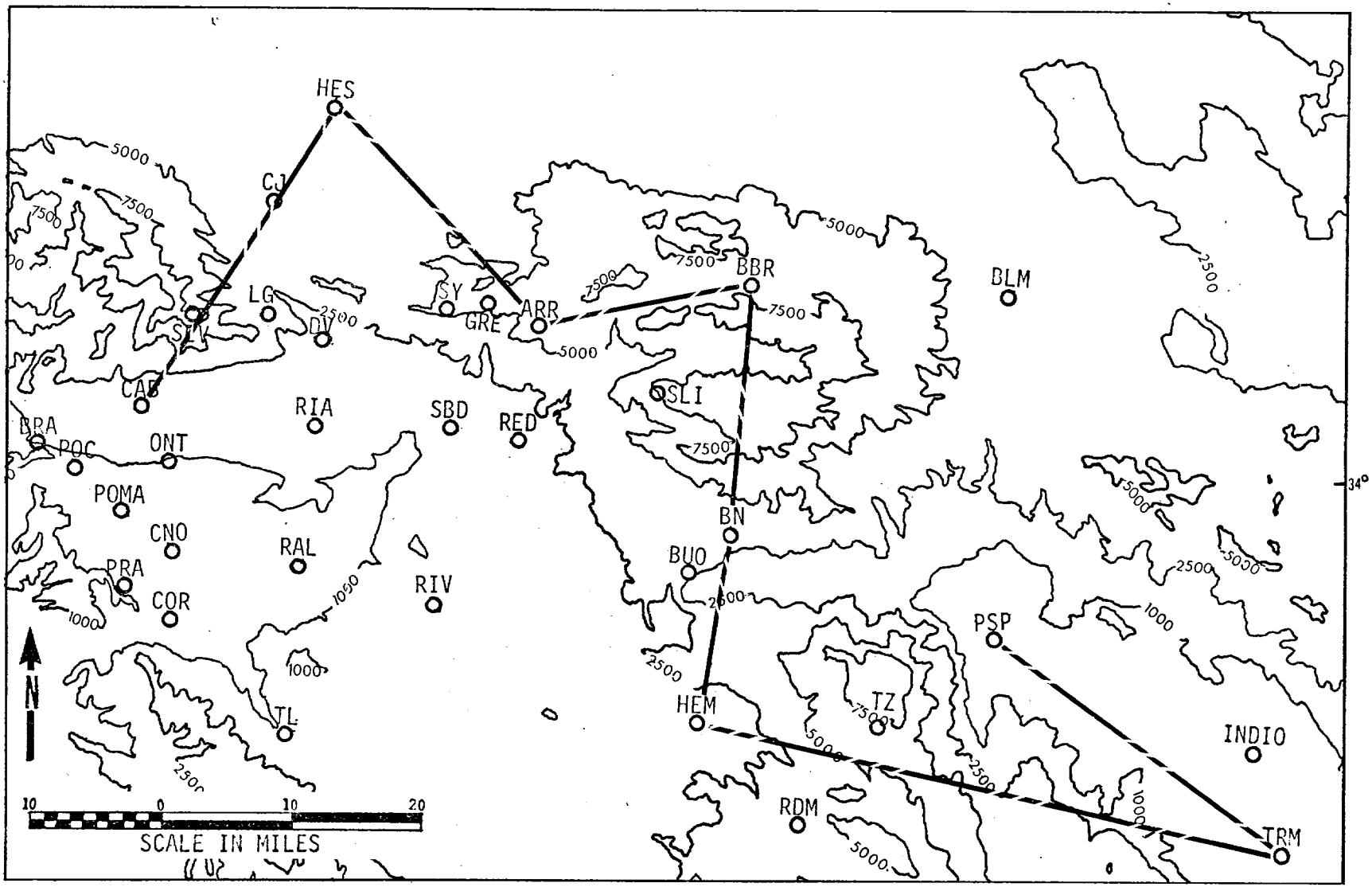

Fig. III-4. SAMPLING POINTS FOR THE 1973 MOUNTAIN-DESERT ROUTE

Specialized sampling routes and times were established when necessary to accommodate special studies. These included:

1. November 2, 1972, when the three-dimensional structure of pollutants was examined during the evening hours (2100-2300 PST).

2. July 26-27, 1973, when the Riverside route was sampled continuously throughout a 24 hour period.

3. October 4, 1973, when sampling was carried out at various levels on an east-west and a north-south tract in the vicinity of Upland, California.

A typical sampling mission starts the evening before the flights. Both planes and the van arrive on site and are checked out during the afternoon. The van system starts operation at about 6:00 p.m. and is run continuously for the one or two days of the experiment. A briefing session is also held to acquaint everyone with the details of the mission.

The aircraft are parked and connected to ground power when they arrive on site. The next morning, the aircraft systems are warmed up and checked using ground power for approximately one hour before flight time. An extensive checklist is used to insure that all systems are set and operating properly. The first flight starts at about 8:00 a.m., weather permitting, and most flights last about two hours with San Joaquin Valley flights being about three hours. At the end of each flight, the aircraft are connected to ground power and the instruments are left running. The checklist is used before each succeeding flight of the day.

A typical flight consists of a sawtooth pattern with about 8 to 10 sampling points. The aircraft departs from an airport, climbs to the next sampling point, and then spirals down as close as possible to the point. When the traverse point is at an airport, the aircraft descends to within 10 feet of the ground; elsewhere, it descends to between 50 to 500 feet above the ground.

The tops of the spirals are determined by the meteorological conditions. On clear days, the aircraft climbs to at least 3000 feet or to the top of the haze as defined by the nephelometer if below 6000 feet. If the tops are above 6000 feet, the pilot climbs to the top of the haze layer at least once during the flight and all other traverses are made from 5500 feet.

When there is a cloud ceiling, the top of the traverse is as close as possible to the ceiling. When a point is fogged in completely, it is skipped or the pilot descends down to the top of the fog. Occasionally, a few flights are made on instruments with either a climb or descent through a fog or cloud deck. Other unusual situations are dealt with at the discretion of the pilot.

At the end of the sampling day, the aircraft are returned to their base airport in the basin being studied where they are inspected and readied for additional flights if planned for the next day. The aircraft and ground crews then meet to discuss the day's activities and plan for the next day. One member of the MRI crew is responsible for writing a summary of the day and for collecting all data logger tapes and data sheets.

In addition to the data logger tapes, both aircraft are equipped with voice tape recorders which are used for recording comments during the flights. All data sheets, data logger tapes, and audio tapes are the responsibility of one person. This person must check all tapes and sheets for errors and comments and then use them in making up his summary. At the completion of the mission, this same person returns the data to MRI and sees that they are filed correctly. When the data tapes are processed, he also checks over the outputs to detect errors and answers questions that people responsible for data interpretation may have about the flight.

D. Processing of Airborne and Ground Data

1. Objectives

The objectives of the data processing function were to support the field programs with fast turn-around paper copy of the data in order to aid project control, to transfer the data logger 1/4 inch tape cartridges to industry-compatible 1/2 inch magnetic tape for data storage, and to edit the data to a verified form. Since these operations are input/output limited, a mini-computer was the logical choice for the system. A computer dedicated to this project was essential for control of the tapes at all times. This permitted the fast turn-around and reduced the chance of the loss of irreplaceable data through human error. Also, some tapes recorded in a field environment may have imperfections caused by dust, voltage sags, and vibration, no matter how sound the basic recorder. A small computer with operator interaction may be used to salvage such data.

2. Computer and Related Hardware

MRI's existing mini-computer system was upgraded for this study and the needed peripherals added. The resulting system included a PDP-8I general purpose digital computer (Digital Equipment Corporation) with additional core memory for this project, an ASR-33 teletype for communicating with the computer, two disk memory units each with a capacity of 32,000 words, two PERTEC 7-channel digital tape drives (one each of 7 inch and 12 inch reel diameter capacity), a Metrodata DL 622A tape cartridge reader with interface for the PDP-8, a Metrodata GR-109 off-line tape rewinder, and a Potter Instrument Company LP3000 line printer. When integrated into an operational system, this equipment provided an adequate data processing capability.

3. Data Processing Procedures

The 1972 and 1973 data processing procedures were similar in concept, but differed in detail. The 1973 procedures were a refinement of those initiated during the 1972 study. Program revisions were motivated principally by an effort to cut costs, although accommodation of new instruments and channel assignments was also necessary.

The data acquisition and processing procedures started with the checkout of 1/4 inch data logger tape cartridges from the MRI computer center to the field personnel for the flight sequence. After sampling, these were returned, along with data sheets and audio cassettes containing comments recorded during each flight to aid in the reduction of the data. The actual processing commenced with the rewinding of the cartridges and assignment of a volume number to each sampling day. The cartridges for one day were then dumped onto a single industry-compatible 1/2 inch magnetic tape (a volume) and an engineering unit produced. After a quality control check to ensure that the data were successfully dumped, spirals and/or traverses were identified on the printouts and the corresponding data transferred from the raw dump tape to separate smaller tapes, one each for spirals and traverses per volume. The data on these two tapes were then printed out, resulting in preliminary plots of vertical spirals and horizontal traverses. Offsets, altitude corrections, and instrument malfunctions were then determined after examining the preliminary plots, the original raw data, and the observer's data sheets. These corrections were applied to the data along with density and pressure altitude corrections. New spiral and traverse tapes were then produced along with printouts of

vertical spirals and horizontal traverses (Figs. III-5 and III-6) with scales and comments added. These finalized data are included in the data volume to this report.

E. Collection and Processing of Meteorological Data

In addition to the aircraft and van data, extensive meteorological data were necessary for an adequate understanding of the sampling days. For each sampling day, surface wind data were obtained for as many locations as possible, along with visibilities when available. These data were plotted and analyzed to give 24 hourly streamline maps for each sampling day.

These wind data were collected from a number of sources. The National Weather Service teletype circuits provided hourly meteorological observations for stations throughout the Los Angeles, San Francisco, and San Joaquin Valley air basins (Table III-9). Other major sources of surface wind data included the Los Angeles County and Bay Area Air Pollution Control Districts. Hourly wind data were obtained on a monthly basis from these organizations for the days under investigation. A list of stations in each air basin is given in Table III-10. In addition, four other stations were obtained sporadically at 0600 and 1300 PST from the NWS Micrometeorological File:

Temescal (TL)
Duarte (DU)
De Vore (DV)
Lytle Creek (LC)

Other meteorological information gathered for each sampling day included:

1. Station and general area forecasts from the National Weather Service.

2. Copy of the Daily Weather maps from the National Weather Service including surface and 500 mb charts valid at 1200 GMT (0400 PST).

3. Hourly pibal data from pibals taken by MRI personnel (1973 program only).

4. LAX and EMT radiosondes taken at about 0600 and 1200 PST.

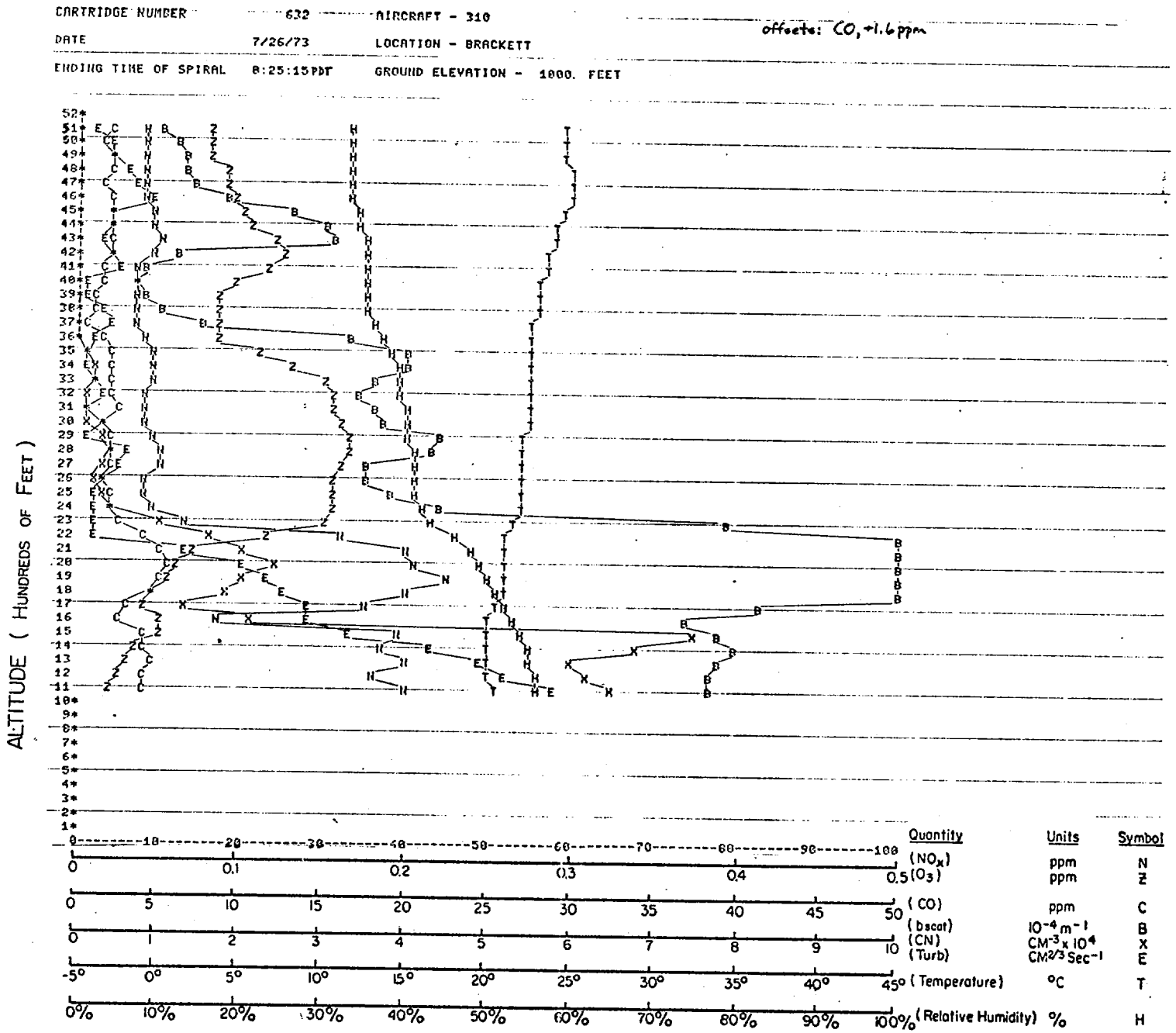

Fig. III-5. EXAMPLE OF CLEANED OUTPUT FROM PLOT PROGRAM

DATE: 1/10/74 10:10:31
CARTRIDGE NUMBER: 814
DESCRIPTION: MOSS LANDING, 1.0 mile DOWNWIND, 1400'

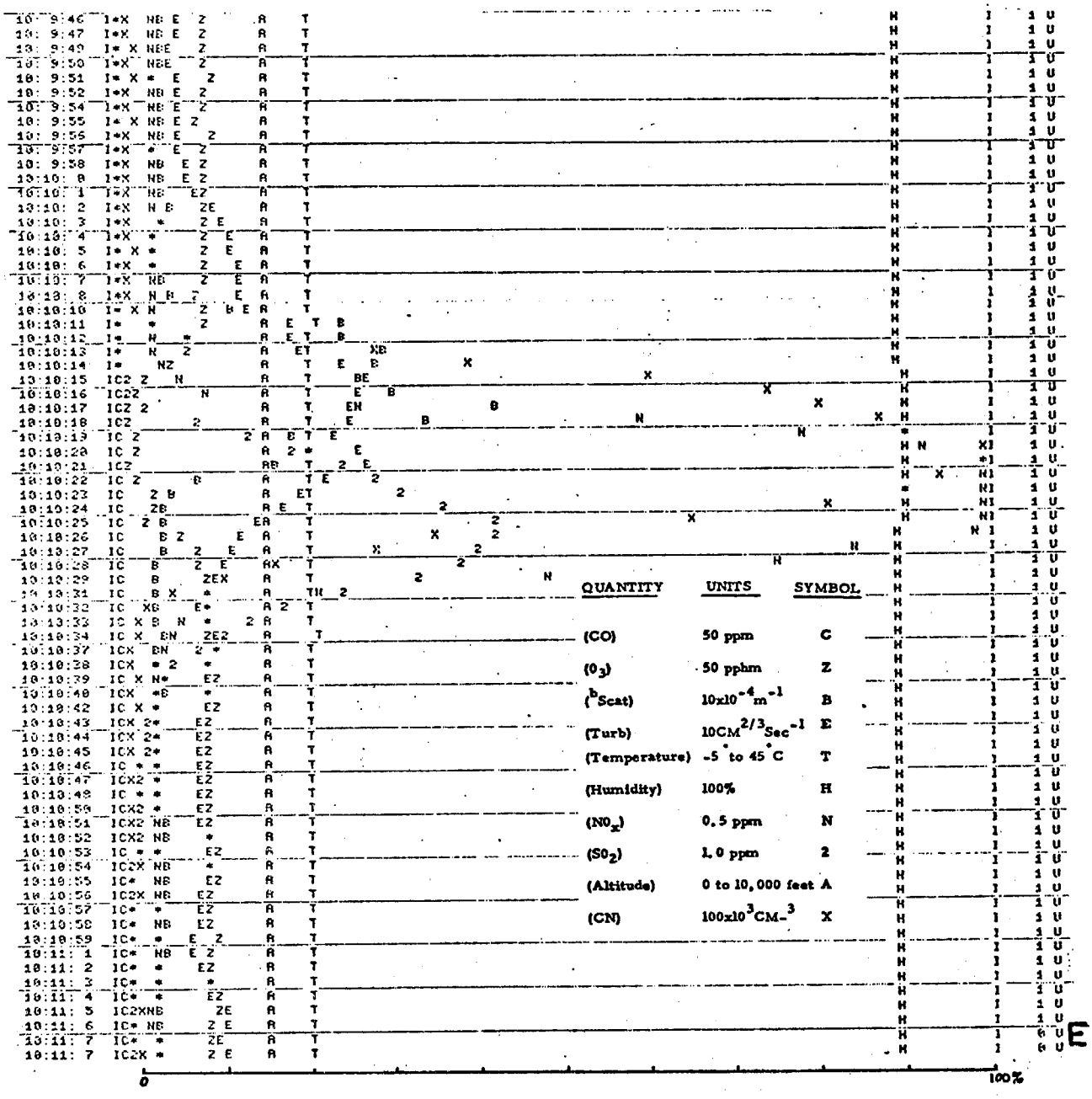

Fig. III-6. EXAMPLE OF CLEANED OUTPUT FROM PLCMB PROGRAM

TABLE III-9

LOCATIONS OF HOURLY METEOROLOGICAL OBSERVATIONS - NATIONAL WEATHER SERVICE CIRCUITS

Los Angeles Basin

Los Angeles International Airport	(LAX)
Santa Monica Airport	(SMO)
Hollywood-Burbank Airport	(BUR)
Long Beach Airport	(LGB)
Torrance Airport	(TOA)
Hawthorne Airport	(HHR)
Orange County Airport	(SNA)
Van Nuys Airport	(VNY)
Ontario International Airport	(ONT)
Riverside (March AFB)	(RIV)
San Bernardino (Norton AFB)	(SBD)
El Toro Marine Station	(NZJ)
Fullerton Airport	(FUL)
Mount Wilson	(MWS)
El Monte Airport	(EMT)
La Verne College	(POC)
Chino Airport	(CNO)
Riverside-Arlington Airport	(RAL)

San Francisco Basin

San Francisco International Airport	(SFO)
San Jose Airport	(SJC)
Oakland International Airport	(OAK)
Alameda Naval Air Station	(NGZ)
Hamilton Air Force Base	(SRF)
Moffett Naval Air Station	(NOQ)
Concord Airport	(CCR)

TABLE III-9 (Continued)

San Joaquin Basin

Castle Air Force Base	(MER)
Stockton Airport	(SCK)
Fresno Air Terminal	(FAT)
Bakersfield Airport	(BFL)
Sacramento Municipal Airport	(SAC)
Sacramento City	(SMF)
Lemoore Naval Air Station	(NLC)

TABLE III-10

WIND MONITORING STATIONS

Los Angeles County Air Pollution Control District
Wind Monitoring Stations

Mission Hills	(MISH)
Alhambra	(ALM)
Vernon	(VER)
Pomona	(POMA)
Whittier	(WHTR)
Redondo Beach	(RB)
Venice	(VEN)
Azusa	(AZU)
Pico-Rivera	(RVA)
La Habra	(LAH)
Anaheim	(AN)
Costa Mesa	(COS)
Compton Airport	(COMA)
Downey	(RLA)
Hollywood	(HOC)
Walnut	(WNT)
Canoga Park	(CPK)
Pasadena	(PASA)
Los Angeles (Downtown)	(CAP)
La Canada	(LACA)

Bay Area Air Pollution Control District
Wind Monitoring Stations

Pittsburg	(PITT)
Vallejo	(VAL)
San Rafael	(SAN)
Richmond	(RICH)
Livermore	(LIV)
Fremont	(FREM)
Redwood City	(RED)
Burlingame	(BUR)
San Jose State College	(CSSJ)

There are a number of other Bay Area stations which record wind data, but because of their non-availability or their position outside the area of study, they were not employed in this study.

5. Pibal and tracer data, courtesy of Metronics, Inc.

All meteorological information was synthesized into a concise meteorological summary for each sampling day. Included in this summary were discussions of the prevailing synoptic situation, radiosondes, and the surface observations. These were designed, not for intensive analysis, but rather for a meteorological overview of each sampling day.

During the 1972 sampling program, wind data were used as input in the AIRPOL computer program, a wind trajectory program written at the Jet Propulsion Laboratory in Pasadena. It computes wind trajectories over the Los Angeles Basin using a grid designed by the Los Angeles County Air Pollution Control District. Our wind data were adapted to this grid and trajectories computed for most sampling days. These are shown in the 1972 data volume.

The 1972 wind data were also used to construct the afternoon transport speeds for each sampling day after Miller (1967). These were defined as the mean wind speed in the period 1200 to 1600 PST. This period represents the time of maximum mixing depth during the day. The mean wind speed during this period, therefore, gives an indication of the maximum transport wind within the mixing layer during this period of effective mixing. A high wind speed represents considerable mixing and reduced pollutant concentrations, whereas a low speed represents stagnation of the air, little mixing, and higher pollutant concentrations. A contour map of the afternoon transport wind speed for each sampling day is given in the data volume for 1972.

The trajectory and transport wind speed analyses were not done for the 1973 data due to the different scope of the sampling missions during the 1973 program.

F. Additional Data Processing

A number of techniques were employed in analyzing the data obtained from the vertical airplane soundings. These included integration of vertical data, construction of cross-sections, and others. Probably the most important to this study, however, is the definition of mixing heights from the soundings.

Mixing layers were determined from each of the aircraft soundings taken during the 3-D Gradient Study. The flights were generally spaced during the day so that soundings could be grouped into morning, midday, and afternoon periods. In general, morning encompassed the period 0800-1100 PDT, midday 1200-1400 PDT, and afternoon 1500-1800 PDT. Contour maps of mixing layer heights were prepared for each of these periods.

Turbulence, b_{scat}, etc., were used to define the top of the mixing layer with emphasis on as much physical consistency as possible among the various parameters. McCaldin and Sholtes (1970) have reported that, for turbulence, the top of the mixing layer is attained when the amplitude of the turbulence trace decreases to 50 percent of the mean amplitude within the mixing zone. Without sufficient turbulence, adequate mixing cannot take place. For particulates, the same authors reported that the mixing height was the altitude at which the particle count dropped to 5 percent of full scale. These generalized rules, along with a thorough knowledge of the meteorological processes at work at that time, provided an adequate knowledge base from which to choose the tops of the mixing layers.

Discrepancies between the various parametric definitions were reconciled as they appeared. In most situations, the definition of the mixing layer height was simple and unequivocal. In others, the most consistent definition was used.

An example of a well defined mixing layer height is seen in Fig. III-7. All parameters in this sounding point to a definite top to the mixing layer around 900 feet (msl). Perhaps 90 percent of all soundings exhibited well defined mixing layer heights. The other 10 percent were selected using the most consistent definition.

Once the mixing layer heights were determined from each sounding, a number of other analyses could be carried out. Charlson et al. (1968) have shown that integration of the b_{scat} trace gives an indication of the mass of particulates in a given column. In the present analysis, integrations were carried out only to the top of the mixed layer, resulting in a value for the mass of particulates trapped within this layer. This integration was performed by hand on data collected during the 1972 program. The result takes the form

$$\int_{\text{surface}}^{\text{mixing height}} b_{scat}\, dz$$

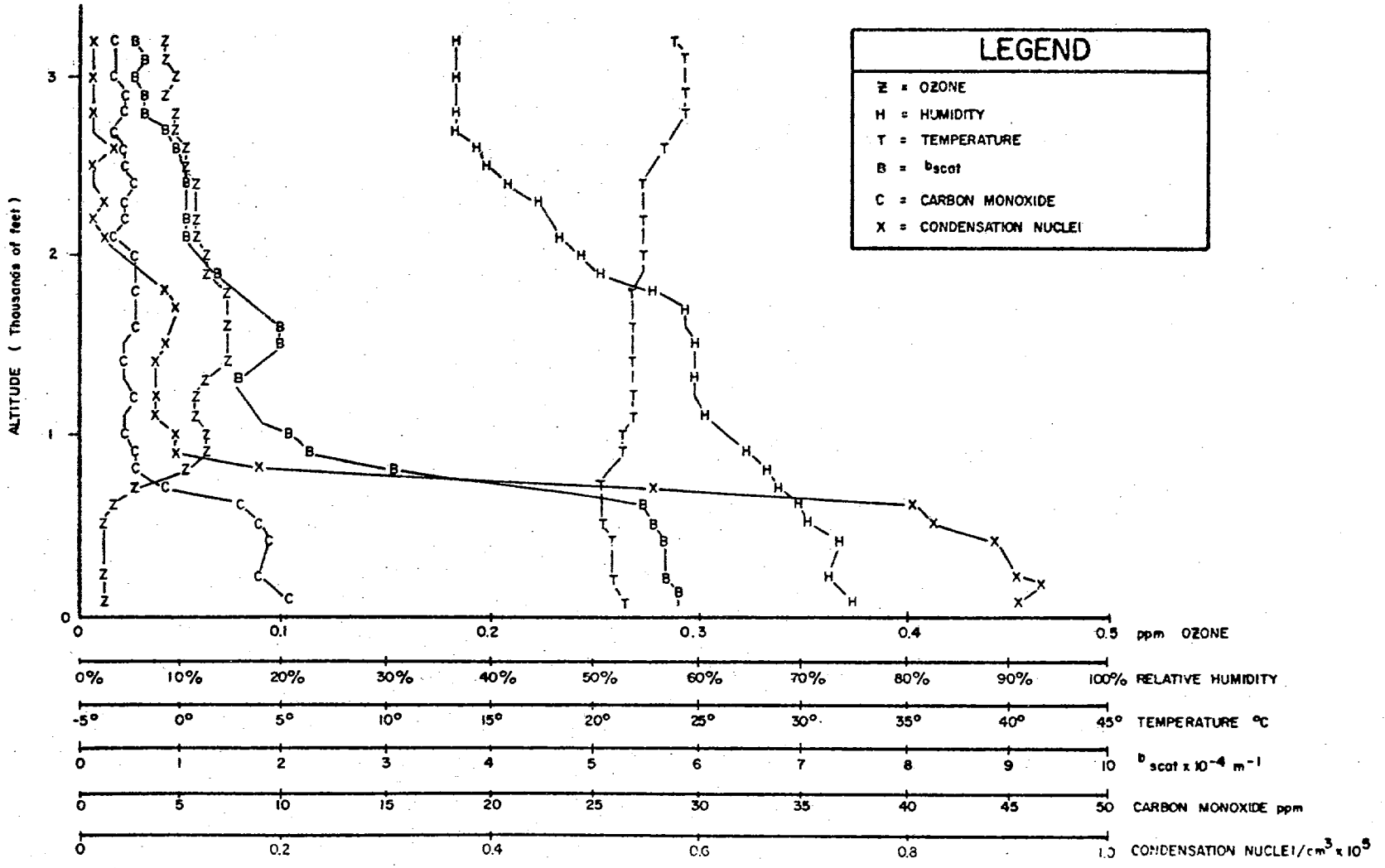

Fig. III-7. VERTICAL SOUNDINGS OVER HAWTHORNE AIRPORT (HHR) at 9:15 A.M. PDT SEPTEMBER 20, 1972

with units (1/m) m. This task was alleviated during the 1973 program by use of a computer program designed to integrate all pollutant parameters including b_{scat}, condensation nuclei, CO, ozone, and NO_x, through intervals from the surface to each 100-foot level up to 5000 feet (msl). Values of $\int b_{scat}$ up to the mixing layer were plotted and analyzed in contour form for the same periods as the mixing heights.

Vertical cross-sections of the b_{scat} trace were done for most sampling days along a line parallel to the movement of air. These diagrams served to show the effects of topography, convergences, inversions, shears, and related phenomenon on the particulate concentrations.

G. Summary of Sampling Days

Table III-11 lists those days during the 1972 and 1973 programs which were selected for special study. (A complete list of all sampling flights undertaken during both the 1972 and 1973 programs is given in Appendix D.) The data for these days have been "cleaned" and comprise the data base for this report. Volume II-1972 and II-1973 are collections of the data for these special days.

TABLE III-11

DAYS CHOSEN AS SPECIAL STUDY DAYS

1972 Program

8-25-72	San Francisco Bay Area
8-29-72	Los Angeles Basin, Metronics release
9-07-72	San Joaquin Valley
9-13-72	San Joaquin Valley
9-20-72	Los Angeles Basin, Metronics release
9-21-72	Los Angeles Basin, Metronics release
9-26-72	Los Angeles Basin
9-27-72	Los Angeles Basin
9-28-72	Special experiment with R. Husar, Los Angeles Basin
9-29-72	Special experiment with R. Husar, Los Angeles Basin
10-05-72	Los Angeles Basin
10-06-72	Los Angeles Basin
10-18-72	Los Angeles Basin, cloudy conditions
10-19-72	Los Angeles Basin, cloudy conditions
10-24-72	Los Angeles Basin, Metronics release
10-25-72	Los Angeles Basin, Metronics release
11-02-72	Los Angeles Basin, special night flights

1973 Program

7-11-73	Los Angeles Basin
7-12-73	Los Angeles Basin
7-18-73	Los Angeles Basin
7-19-73	Los Angeles Basin
7-25-73	Los Angeles Basin
7-26/27-73	Los Angeles Basin, 24 hour study - Riverside Route
8-02-73	Los Angeles Basin
8-03-73	Los Angeles Basin, Metronics release
8-04-73	Los Angeles Basin, Metronics release
8-09-73	Los Angeles Basin
8-10-73	Los Angeles Basin
8-16-73	Los Angeles Basin and Mountain-Desert Route
8-17-73	Los Angeles Basin
8-23-73	Los Angeles Basin
8-24-73	Los Angeles Basin and Mountain-Desert Route
8-28-73	Los Angeles Basin
9-06-73	Los Angeles Basin, N. A. S. C. Blimp Flights

TABLE III-11 (Continued)

1973 Program (Continued)

9-13-73	Los Angeles Basin, Metronics release
9-14-73	Los Angeles Basin, Metronics release
9-28-73	Los Angeles Basin
9-29-73	Los Angeles Basin, Metronics release
10-04-73	Los Angeles Basin, Upland Freeway Study
10-05-73	Los Angeles Basin

IV. REPRESENTATIVENESS OF THE DATA

A. Meteorological Conditions During the Sampling Period

The temperature aloft, e.g., 850 mb (5000 feet msl), can be used as an excellent indicator of the strength of the semi-permanent low-level temperature inversion over the South Coast Basin of California. In order to break through the low-level temperature inversion and permit vertical dispersion of pollutants, the afternoon maximum surface temperature must equal or exceed the temperature aloft with due regard for the adiabatic decrease in temperature with height. If one assumes a critical value for the temperature at 850 mb (T_{850}) of 20°C for the warm months of July, August, and September, surface temperatures of 32°C (90°F) would be necessary to break any low-level inversions present. A typical situation on such days might be for the inversion to break inland but not in the coastal sections where lower surface temperatures prevail. A similar critical value of 15°C is selected for use in October. A surface temperature of 28°C (80°F) would then be necessary to break any low-level inversions under these conditions.

To obtain an estimate of the pollution potential and representativeness of the sampling days, 850 mb temperatures were recorded from daily radiosondes taken at Los Angeles International Airport (LAX) and Vandenberg Air Force Base (VBG). Figure IV-1 is a graph of the 850 mb temperatures (T_{850}) in °C from the 0000 GMT (1600 PST) radiosonde at VBG for the months of July, August, September, and October, 1972 and 1973. Days selected for sampling by the RISC instrumented van are labeled, as are aircraft sampling and Metronics tracer study days. Peaks in the data signify warmer air aloft resulting in stronger temperature inversions and an increased pollutant potential while valleys imply cooler air aloft and weaker inversions.

During the 1973 season, periods of warm air aloft included 24 July through 2 August and 12 August through 20 August 1973. Secondary peaks were centered around 4 July, 10 July, and 28 September 1973. The plot shows generally warm temperatures through 20 August and then occasionally thereafter.

Table IV-1 gives the frequency of occurrence of 850 mb temperature above the critical value for each month along with the absolute maximum (in parentheses) for that month and year. The table indicates that September 1972 and 1973 were unusually low in frequency of warm temperatures aloft indicating reduced pollutant potentials. The months of July and August for both years, however, tend to be more representative of previous years with frequencies as well as peak values near normal.

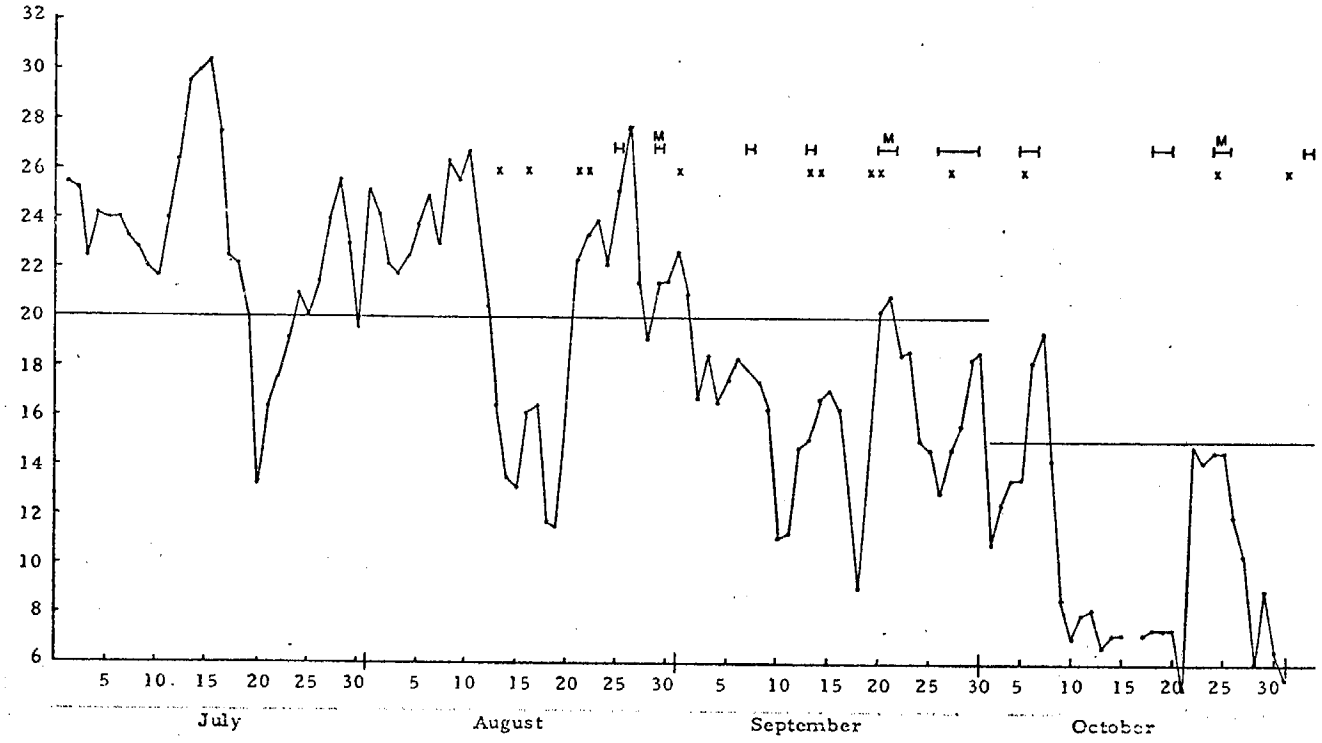

T_{850} at 1600 PST (0000Z) 1972

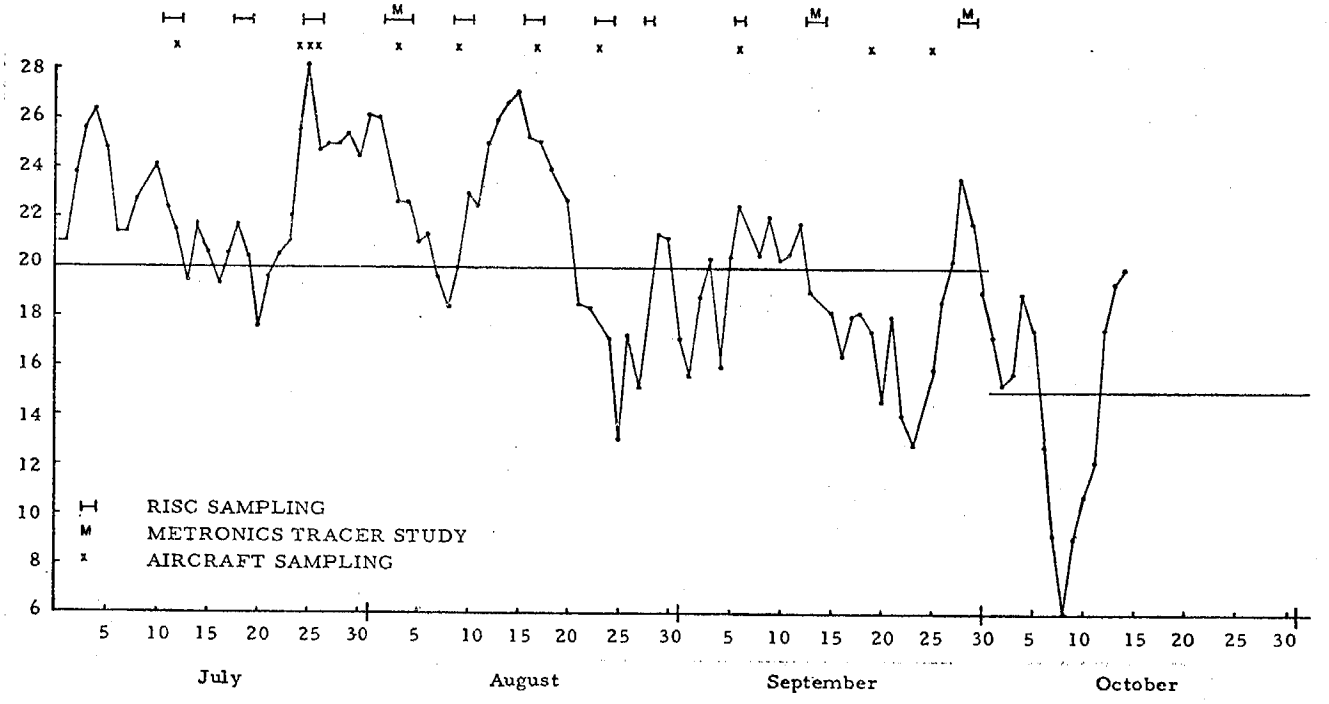

T_{850} at 1600 PST (0000Z) 1973

Fig. IV-1. T_{850} AT 1600 PST (0000Z) 1972 AND 1973

TABLE IV-1

FREQUENCY OF OCCURRENCE OF 850 mb
TEMPERATURES ABOVE REFERENCE LEVELS

	July (>20°C)	August (>20°C)	September (>20°C)	October (>20°C)
1972	26(30.4)*	16(27.5)	2(22.5)	4(18.0)
1973	~22(26.0)	25(25.6)	~ 9(25.8)	~19(20.0)
1959		23(26.2)	13(26.4)	22(24.7)
60	25(30.6)	23(26.3)	22(25.6)	19(19.6)
61	26(30.3)	22(26.3)	9(24.1)	17(24.0)
62	24(25.7)	27(28.0)	23(25.7)	18(21.6)
63	24(25.9)	25(25.5)	20(27.8)	17(24.6)
64	26(28.4)	25(26.0)	13(23.6)	24(24.5)
66*		27(28.3)	11(22.2)	16(21.1)
67*		30(26.4)	11(23.5)	26(22.9)
68*	23(24.7)	13(25.2)	19(25.0)	20(21.9)
69*	18(24.5)	26(27.7)	15(24.6)	8(21.7)
70*	29(26.4)	29(28.3)	15(22.7)	15(24.1)

All Data From Santa Monica Unless Otherwise Noted.

*Data from Vandenberg Air Force Base.
**Data from Los Angeles International Airport.

Note: Numbers in parentheses are the maximum 5000 ft temperature (°C) during month.

Since much of the 1972 experimental program was performed during late August and September, it is clear from Fig. IV-1 and Table IV-1 that few high pollution days were available for sampling. The program was continued into 1973 because of the lack of good sampling days in 1972. Sampling was started earlier to take advantage of the likelihood of a higher frequency of potential pollution days in the early summer. Many days with high pollution potential were indeed sampled in 1973, and from Fig. IV-1, it is clear that maximum advantage was taken of the few potential days that existed in late 1972.

B. Aircraft Data vs. Ground Data

In order to check the relationship of aircraft-obtained data to surface concentrations and to test the representativeness of the aircraft (and ground) data, two types of comparisons were made. For both 1972 and 1973 data, surface concentration contour maps of O_3, CO, and NO_x were drawn for selected days, both using low-level aircraft data and then using surface data provided by the ARB and local agencies. In addition, for 1973, aircraft data for intensive study days were correlated with surface data. The data were compared for those areas in which one of the airplanes spiraled over a location "near" an APCD reporting station. These data were grouped by parameter (NO_x, CO, O_3) and correlation coefficients determined. In neither case, however, was the difference in ozone calibration procedures between the LA APCD and the surrounding agencies taken into account. The aircraft instruments were calibrated in accordance with the method used by the ARB, not the LA APCD.

In comparing the contour maps, the density of the sampling network in each data set was approximately the same, and quite similar spatial patterns of CO and oxidant could be drawn from both sets of data. In the case of the 1972 NO_x data, however, the agreement between aircraft and ground data was not as satisfactory and, in some instances, quite different spatial patterns of NO_x would have resulted from the ground vs. aircraft data. The reasons for this disagreement are quite possibly instrumental. Different instrumental techniques and possible interference from other pollutants may be responsible for the discrepancies. In view of the disagreement, 1972 NO_x data have not been used in the analysis portions of the present report although the data appear in the data volume. After the 1972 program, the NO_x instruments were modified as described in Chapter III, and the 1973 aircraft and ground NO_x contours agreed quite well.

In describing the correlation coefficients between aircraft and ground data, the constants m and b from the slope intercept form of the linear regression line ($y = mx+b$) were determined. The values of m and b, and the correlation coefficient r are given in Table IV-2 with the number, n, of point-pairs considered.

TABLE IV-2

CORRELATION BETWEEN AIRCRAFT AND GROUND DATA

Parameter	r	m	b[1]	n
CO	0.63	0.66	1.13	23
O_3	0.85	1.11	1.72	37
NO_x	0.70	0.96	3.47	34

APCD hourly average vs airplane lowest altitude data. Correlation coefficient, r; slope, m, and intercept b; of regression line; and number of point-pairs, n, considered.

[1] Positive b indicates aircraft data greater than APCD data.

The table shows that the correlations and slopes for O_3 and NO_x are quite reasonable, especially in light of the variations in calibration procedures and the fact that the instantaneous aircraft data were compared with ground-level hourly averages. The CO data, however, were more poorly correlated, and the slope of the regression line was only 0.66. This is possibly due to the fact that the aircraft rarely sampled high levels of CO, and the instruments were generally operating in the lower five percent of the scale. Small variations in absolute CO concentration were thus large compared to the sensitivity of the instruments. The slope of only 0.66 also indicates that the ground stations may be more susceptible to local sources than the aircraft. The aircraft operated from airports and were generally removed by one-half mile or more from high automobile traffic areas. The general agreement between the contour maps, on the other hand, indicates that the aircraft data are adequate for determining the relative spatial distribution of CO across the basin.

For comparison purposes, CO and ozone were examined for the same times and days at Riverside-Rubidoux and Riverside-UCR monitoring stations. Results are given in Table IV-3.

Here, the CO data are also poorly correlated, with O_3 data about the same as in Table IV-2. This points out that short term spatial variations may be of significance over even a short geographical extent so that care must be exercised when interpolating between data points.

TABLE IV-3

CORRELATION BETWEEN RIVERSIDE-RUBIDOUX AND RIVERSIDE-UCR AIR QUALITY STATIONS

Parameter	r	m	b^1	n
CO	0.26	0.67	5.67	8
O_3	0.91	1.03	2.20	13

Correlation coefficient, r, slope, m and intercept, b, of regression line; and number of data pairs considered, n.

V DESCRIPTION OF METEOROLOGY AND 3-D DISTRIBUTION OF POLLUTANTS IN THE L. A. BASIN

A. Background

Air pollution meteorology in the Los Angeles Basin is dominated by subsidence resulting from large-scale high pressure areas to the northwest or northeast of the Los Angeles region. This subsidence generates warm temperatures aloft and generally stable temperature lapse rates above the lowest few thousand feet. The entrapment of pollutants in the low layers is further enhanced by the relatively constant ocean surface temperatures which produce a reservoir of cool surface air. This underlying marine air, together with the warm temperatures aloft, result in the low-level temperature inversions so characteristic of the Southern California area. Although this condition is characteristic of most of the summer and early fall, variations occur, depending on the strength of the high pressure (influencing the temperatures aloft) and as a result of changes in the offshore water temperatures (influencing the surface air temperatures). The remaining air stability characteristic of interest is the diurnal change in air temperatures in the Basin due to surface heating and cooling. Vertical mixing of pollutants upwind is enhanced during the day time and restricted during the night as a result of these surface temperature changes. As a result of the temperature inversions in the area, vertical mixing in the Basin is characteristically restricted to the lowest two thousand feet on most pollution days.

In the frequent absence of large-scale pressure gradients, the wind flow patterns in the Los Angeles Basin during pollution periods are dominated by local heating and cooling influences. During the early morning hours, the flow is frequently weak and poorly organized. An illustration is shown in Fig. V-1 which represents the streamline pattern for 1000 PDT on September 20, 1972. This pattern contributes strongly to the accumulation of pollutant material in the major source regions near metropolitan Los Angeles. By 1200 PDT, the characteristic seabreeze flow has usually become established, continuing through the early evening. This pattern is illustrated by the 1600 PDT streamline flow for September 20, 1972, as shown in Fig. V-2. This west-to-southwest flow brings in cleaner, marine air along the coast and, at the same time, moves the accumulated pollution to the east and northeast of the metropolitan area. After sunset, the land-sea temperature difference which caused the seabreeze diminishes, and the wind pattern becomes weaker and less well organized. Near the mountains, cool drainage flows frequently develop which may clear out the surface pollution in the foothill areas.

Pollution carried eastward from the Los Angeles area has several possible mechanisms for escaping from the Basin. Several of these are illustrated in the following section, together with a more detailed description of the mixing layer structure.

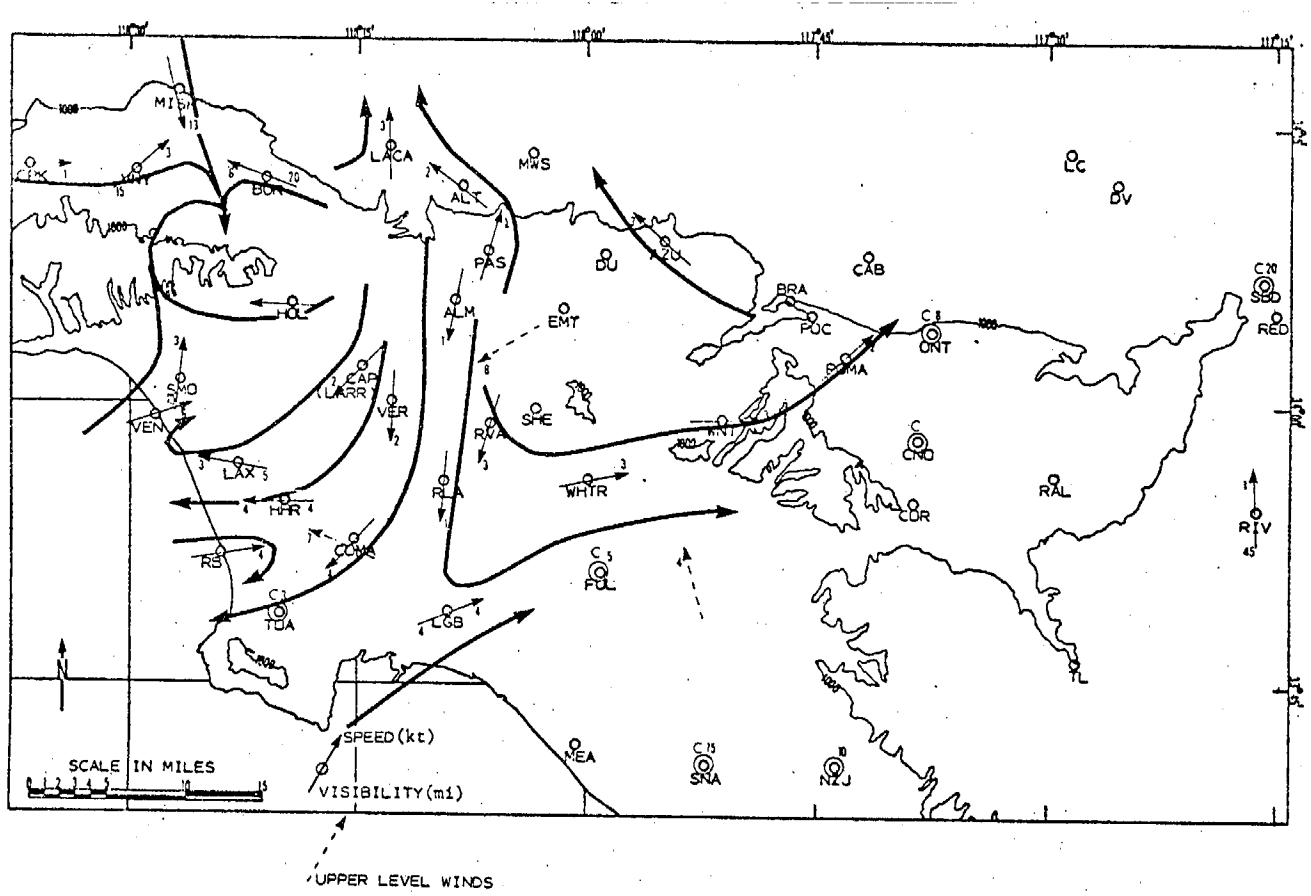

Fig. V-1. STREAMLINE ANALYSIS - 1000 PDT, SEPTEMBER 20, 1972

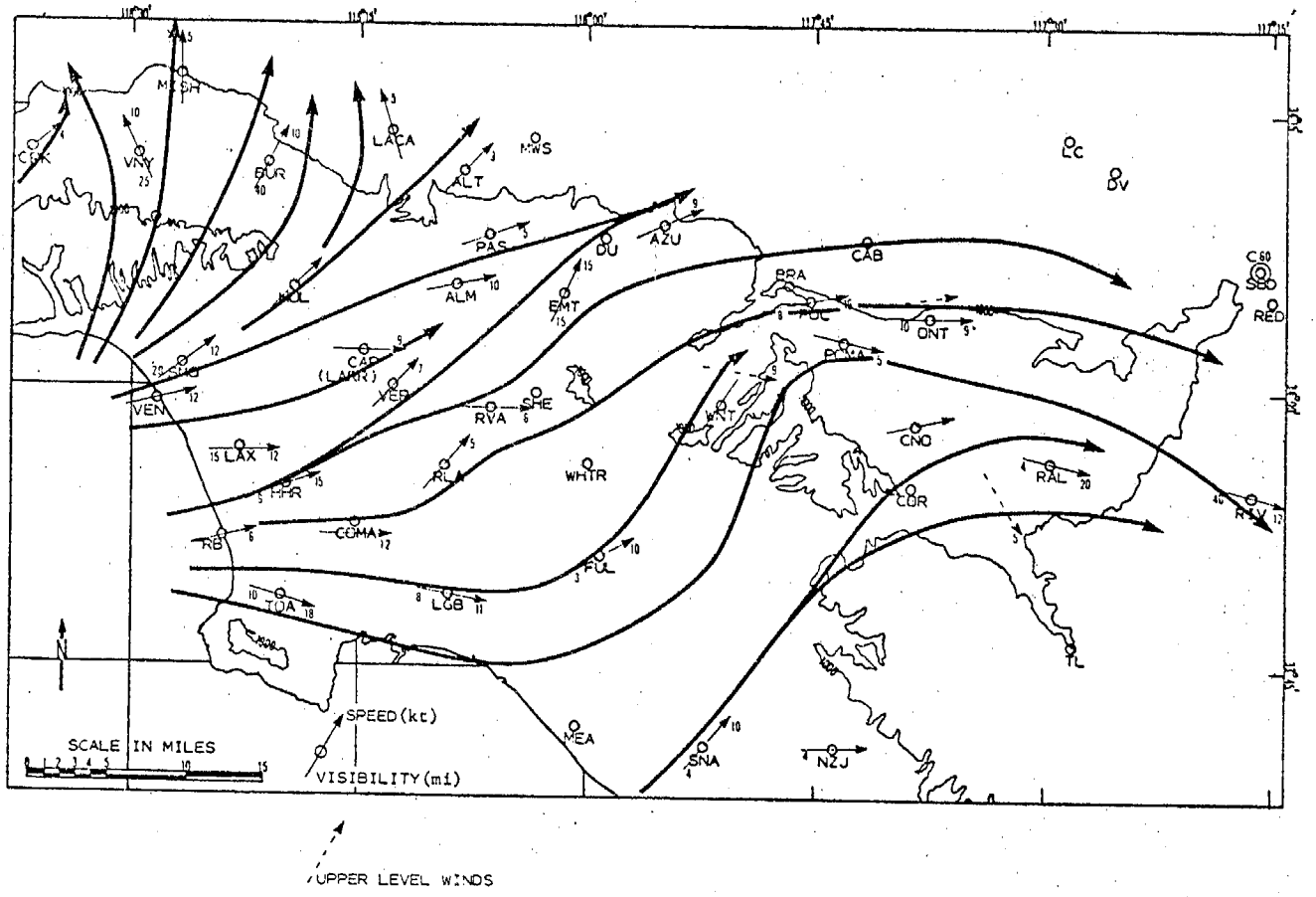

Fig. V-2. STREAMLINE ANALYSIS - 1600 PDT, SEPTEMBER 20, 1972

B. Structure of the Mixing Layer

Diurnal variations in the height of the mixing layer over the Los Angeles Basin can be illustrated by the sequence of contour maps shown in Figs. V-3 through V-5. Individual aircraft soundings for September 20, 1972, were examined to determine mixing layer height. Although the temperature structure (inversion location) was one of the most common indicators of mixing height used, other parameters such as turbulence and pollutant profiles also were used to obtain the most meaningful value for the height at the time of the sounding. These values were plotted in the form of isopleth maps of the mixing layer height (above sea level) for three periods of the day corresponding to the three aircraft flights per day. Individual values for the heights are shown near each sounding location.

During the morning flight (Fig. V-3) the top of the mixing layer was relatively flat with the lowest value (650 ft) at Fullerton (FUL). By midday (Fig. V-4), the mixing layer heights had increased markedly at all inland locations due to surface heating. Changes along the coast (e.g., HHR), however, were minimal. By the afternoon flight (Fig. V-5), the depth of the mixing layer exceeded 4000 ft msl in the inland areas due to surface heating but decreased from the midday soundings at areas as far inland as Fullerton and El Monte (EMT). This produced the marked gradient in the contours shown in Fig. V-5.

The decrease in mixing layer height near the coast is shown in greater detail in Figs. V-6 and V-7. These data give aircraft soundings at Fullerton on September 20 at 1240 and 1628 PDT, respectively. Depths of the mixing layer are indicated on the figures. The principal change shown in the meteorology is a temperature increase in the layer from 1000 to 2000 ft, resulting in lower effective mixing heights. This change is presumably a compensating subsidence near the coast associated with the upward flow inland near the mountain slopes. This subsidence, along with the onset of the sea breeze, results in a shallow afternoon mixing layer extending a considerable distance inland from the coast. Changes in the mixing layer structure on September 20 are shown in vertical cross section in Fig. V-8. Cross sections of b_{scat} are drawn from Torrance (TOA) to Corona (COR) from morning, midday, and afternoon flight data. Shallow mixing layer heights are shown in the morning followed by a deeper layer by midday and the accumulation of pollution in the Fullerton area. By afternoon, the effects of surface heating have contributed to a deep mixing layer in the east while the mixing layer to the west of Fullerton (toward Torrance) has become shallower due to subsidence and the sea breeze.

Another example of diurnal changes in mixing layer height is shown in Fig. V-9 which gives the aircraft sounding at El Monte for 1656 PDT on July 25, 1973. Two general layers of pollutants are shown. An earlier pollutant layer had extended to about 2500 ft depth (msl). By 1656, the shallower sea breeze had arrived with a depth of approximately 1300 feet.

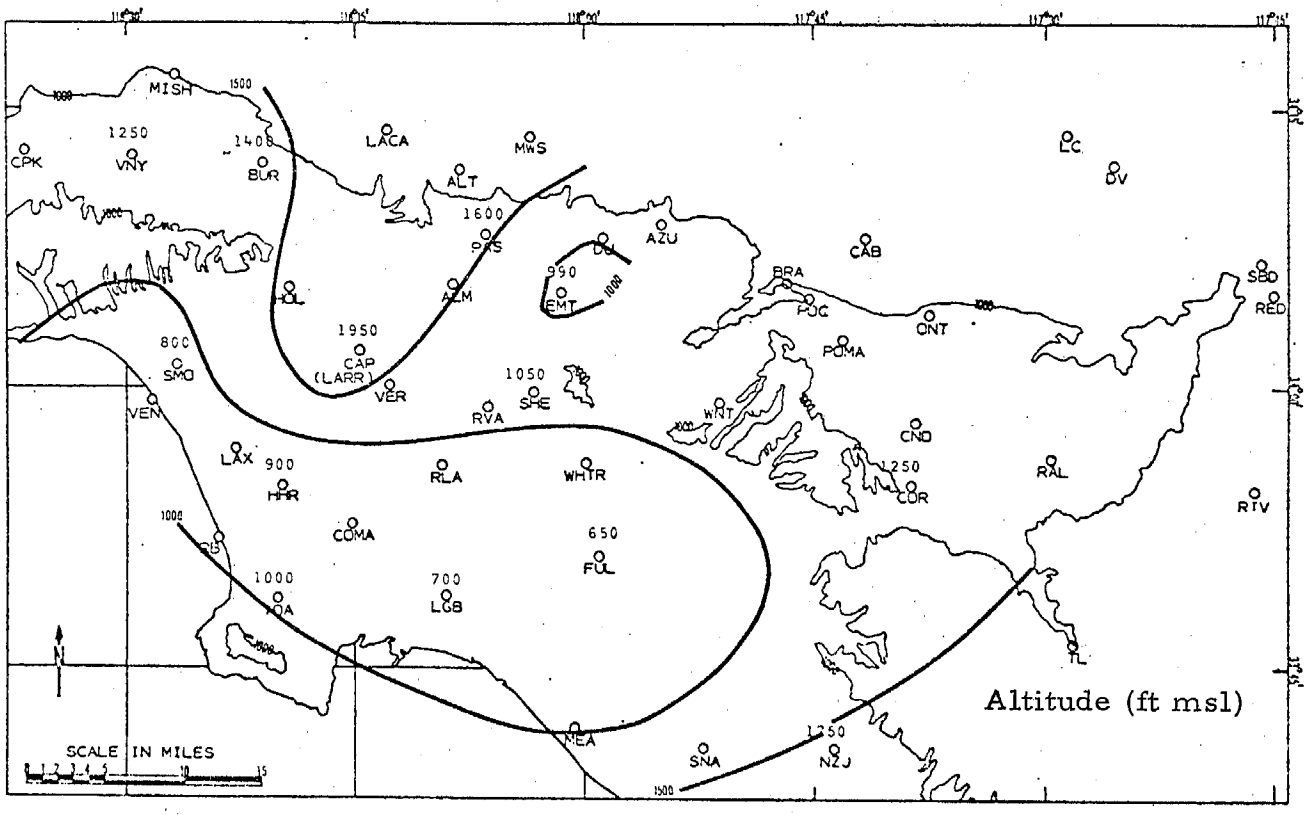

Fig. V-3. MIXING LAYER HEIGHTS - MORNING, SEPTEMBER 20, 1972

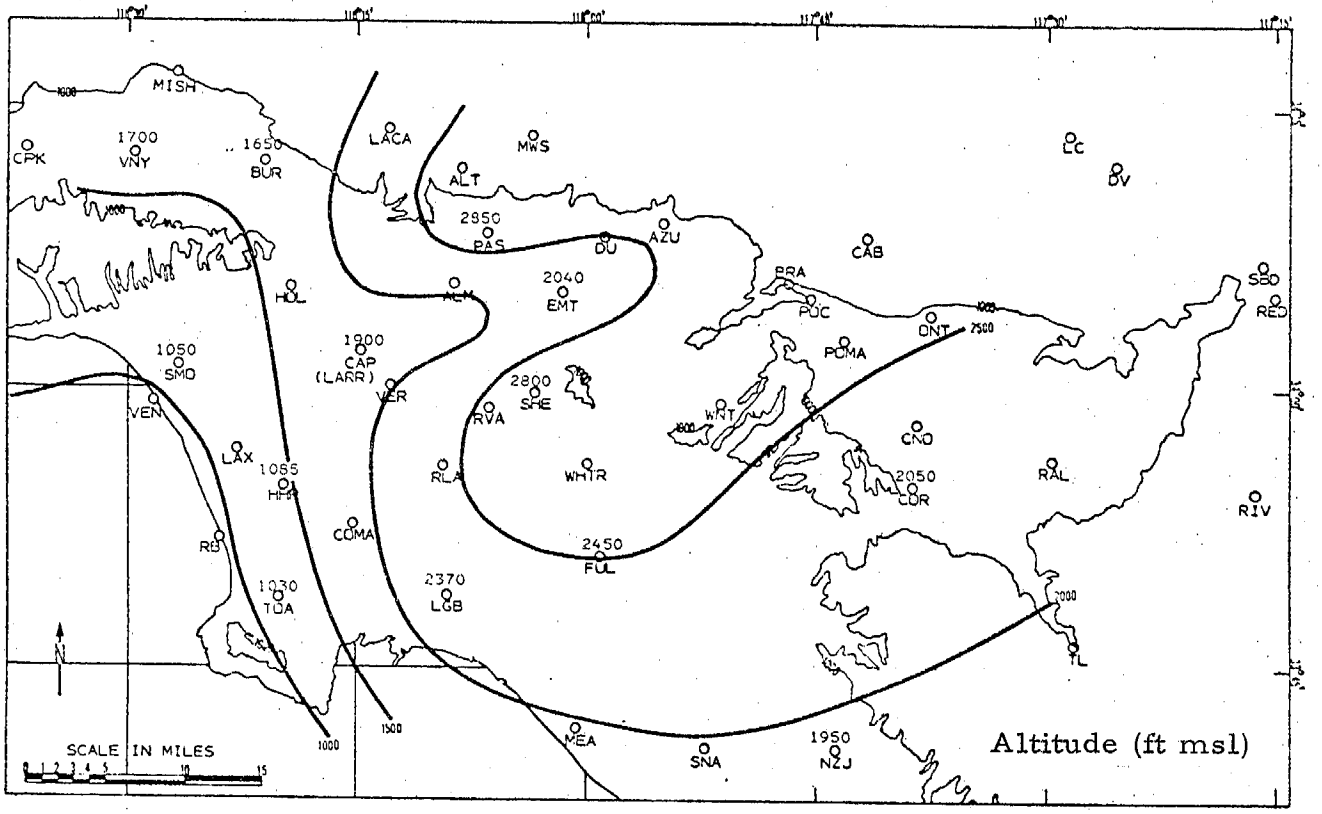

Fig. V-4. MIXING LAYER HEIGHTS - MIDDAY, SEPTEMBER 20, 1972

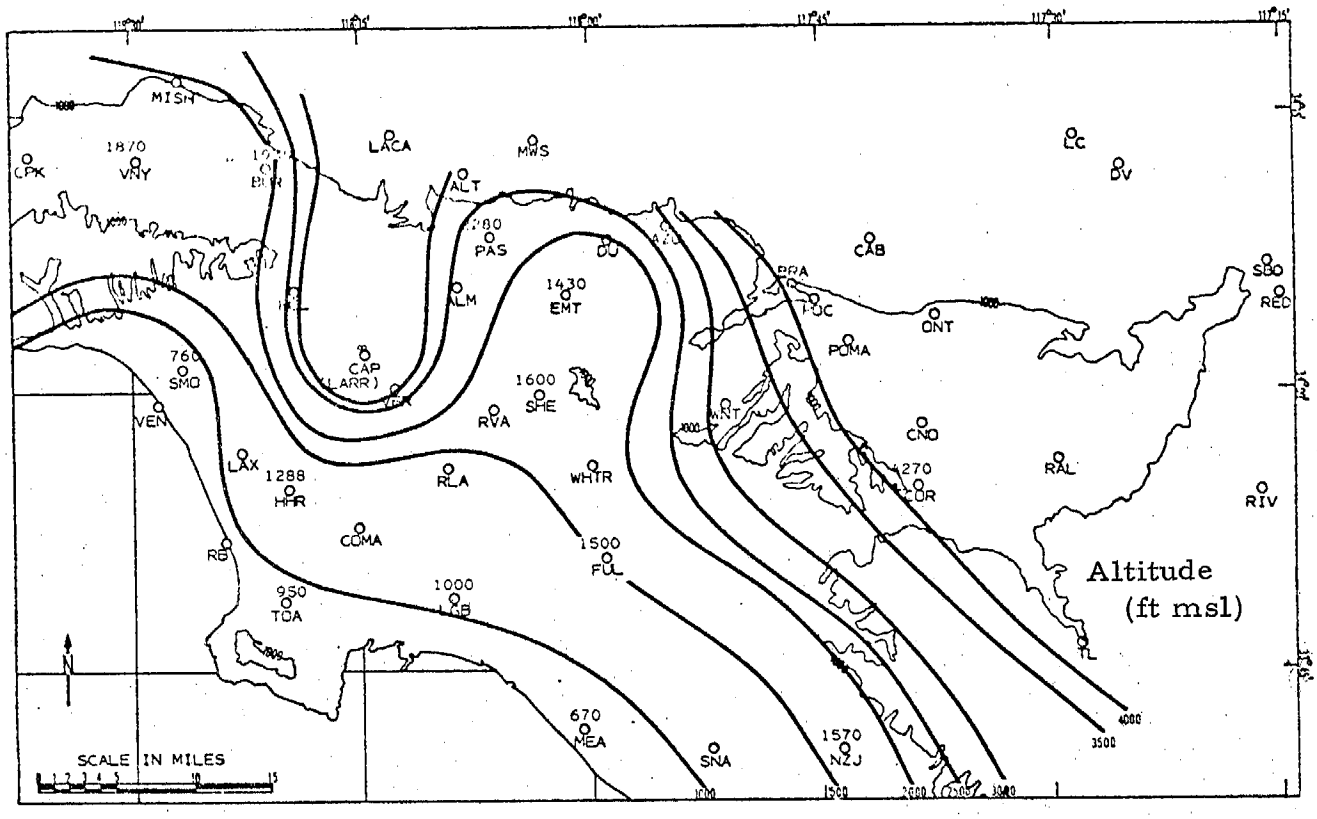

Fig. V-5. MIXING LAYER HEIGHTS, AFTERNOON, SEPTEMBER 20, 1972

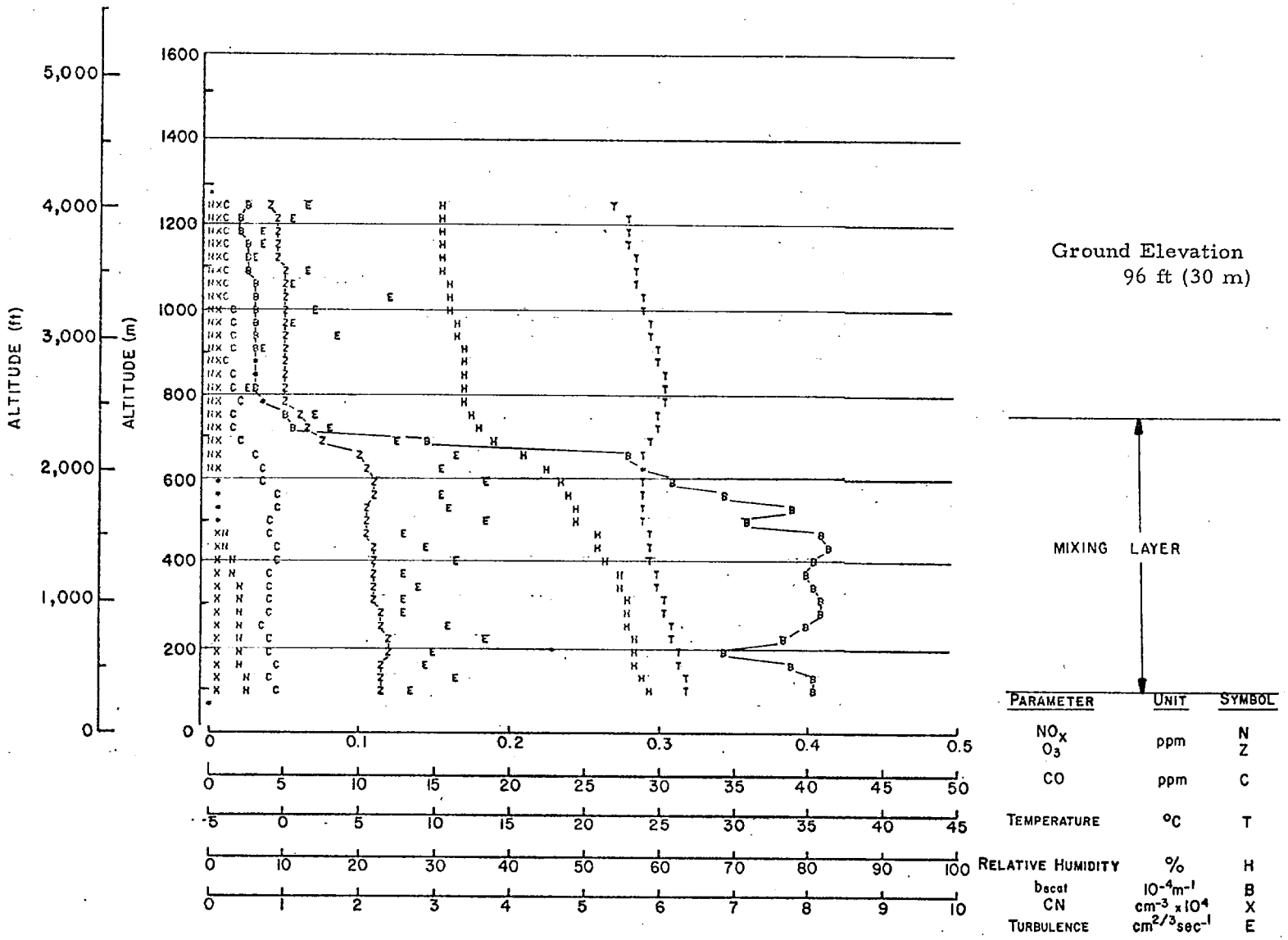

Fig. V-6. VERTICAL PROFILE OVER FULLERTON (FUL)
SEPTEMBER 20, 1972, 1240 PDT

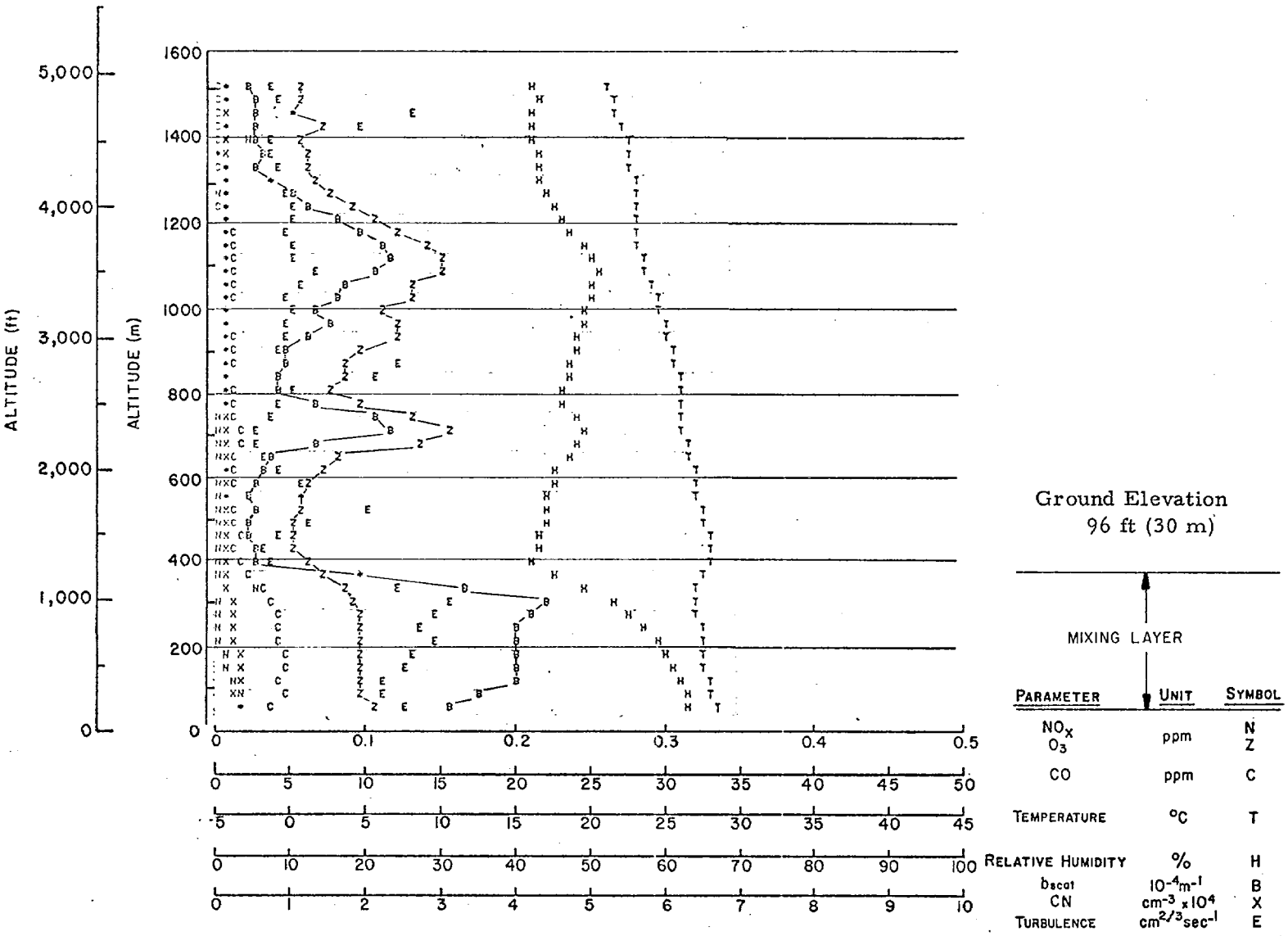

Fig. V-7. VERTICAL PROFILE OVER FULLERTON (FUL) 1628 PDT, SEPTEMBER 20, 1972

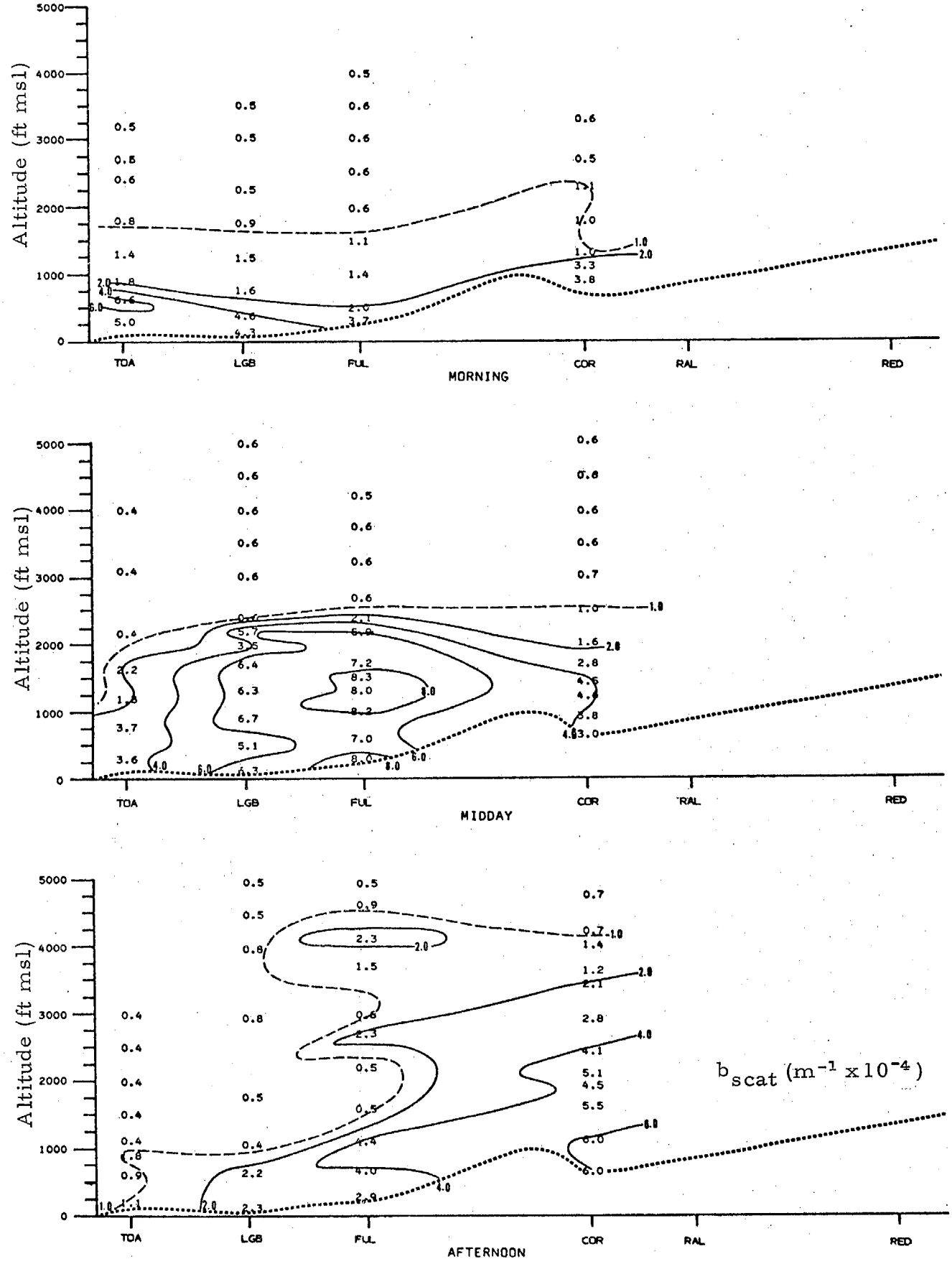

Fig. V-8. VERTICAL CROSS-SECTION OF b_{scat} - MORNING, MIDDAY, AFTERNOON, SEPTEMBER 20, 1972

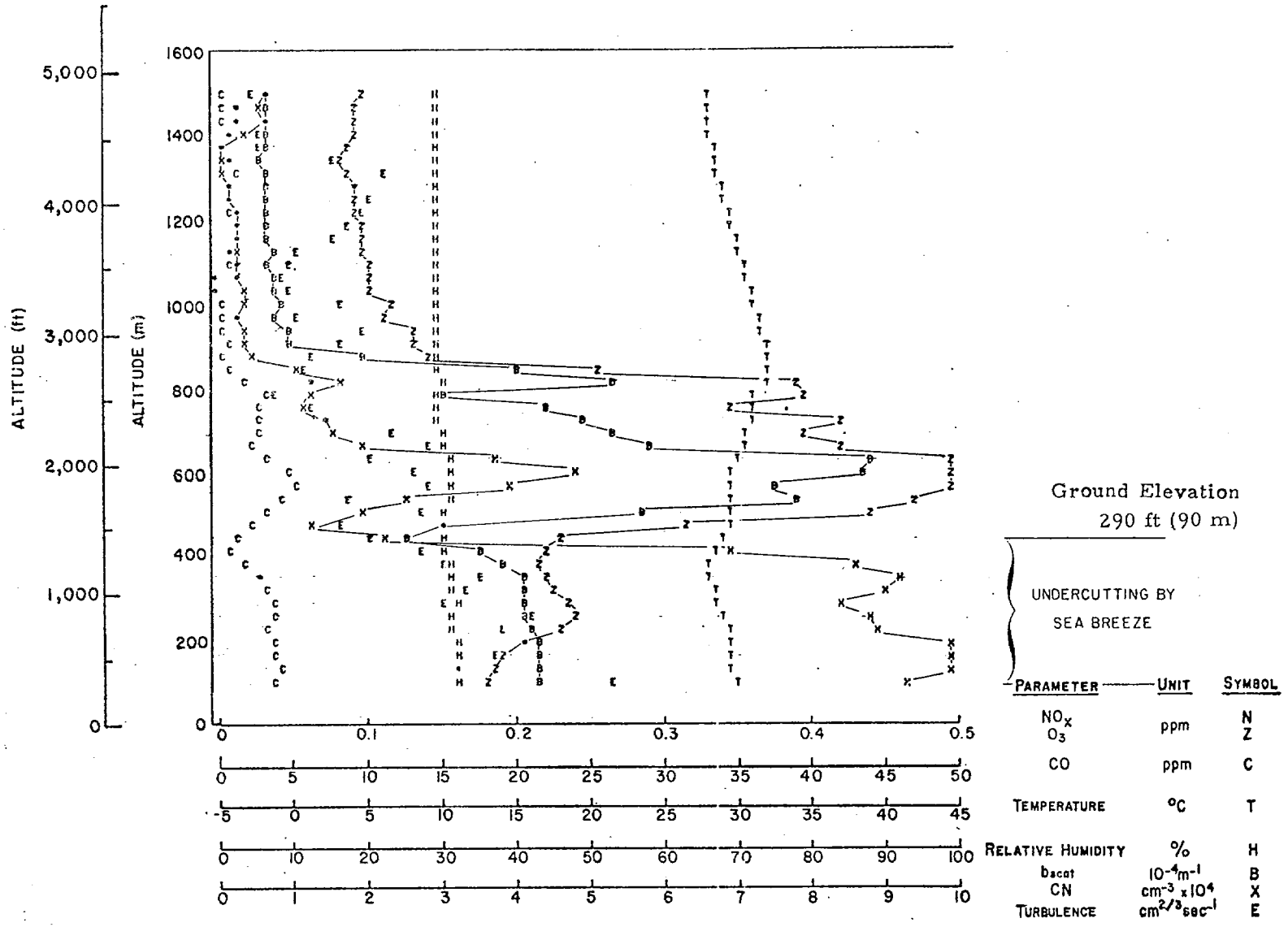

Fig. V-9. VERTICAL PROFILE AT EL MONTE (EMT) JULY 25, 1973, 1656 PDT, SHOWING UNDERCUTTING BY THE SEA BREEZE

Heating in the inland areas, and particularly along the slopes of the foothills, is an effective mechanism for removing pollutant material from the Basin. Figure V-10 shows the contours of mixing layer heights (above sea level) for the afternoon flight of July 19, 1973. The foothill areas (CAB, RIA, SBD) show high values of mixing layer heights due to surface heating. The effect of this on the vertical pollutant profile is shown in Fig. V-11 which gives the aircraft sounding at Rialto for 1738 PDT. A mixing layer height of 3200 ft is shown with an additional layer above. This top layer appears to be the result of air moving up the slope between Rialto and the foothils and being injected into the air above Rialto. The upper layer is clearly separated from the lower mixing layer, and its trajectory is dependent upon the winds at that level.

Another mechanism for removing pollutants from the lower mixing layer is convergent wind flow. In the case of October 24, 1972 (Fig. V-12), a mild Santa Ana condition existed in the eastern portion of the Basin. The convergence between this flow and the normal sea breeze flow resulted in the convergence line shown near Redlands at midday and near Riverside (RAL) in the afternoon. In both cases, pollutant material is carried aloft where it can be dispersed by upper level winds. Such a process is occurring in Fig. V-12 at the 4000-5000 ft level in the afternoon.

Finally, Fig. V-13 illustrates the mixing layer conditions in the early morning after nocturnal cooling has reduced the effective mixing layer to a very small depth. Remnants of previous pollution exist aloft in stratified layers during this period but are not connected to the surface layers by any effective mixing process. This is readily apparent from the vertical inhomogeneities shown in the figure for various parameters. As the ground surface heats during the day, the depth of the mixing layer increases, incorporating some of these layers aloft in the process.

The illustrations shown in this section are intended to show some of the complexities of the mixing layer structure in the Los Angeles Basin. These variations and complexities are bound to be of considerable importance in the treatment and understanding of the area's pollution problems.

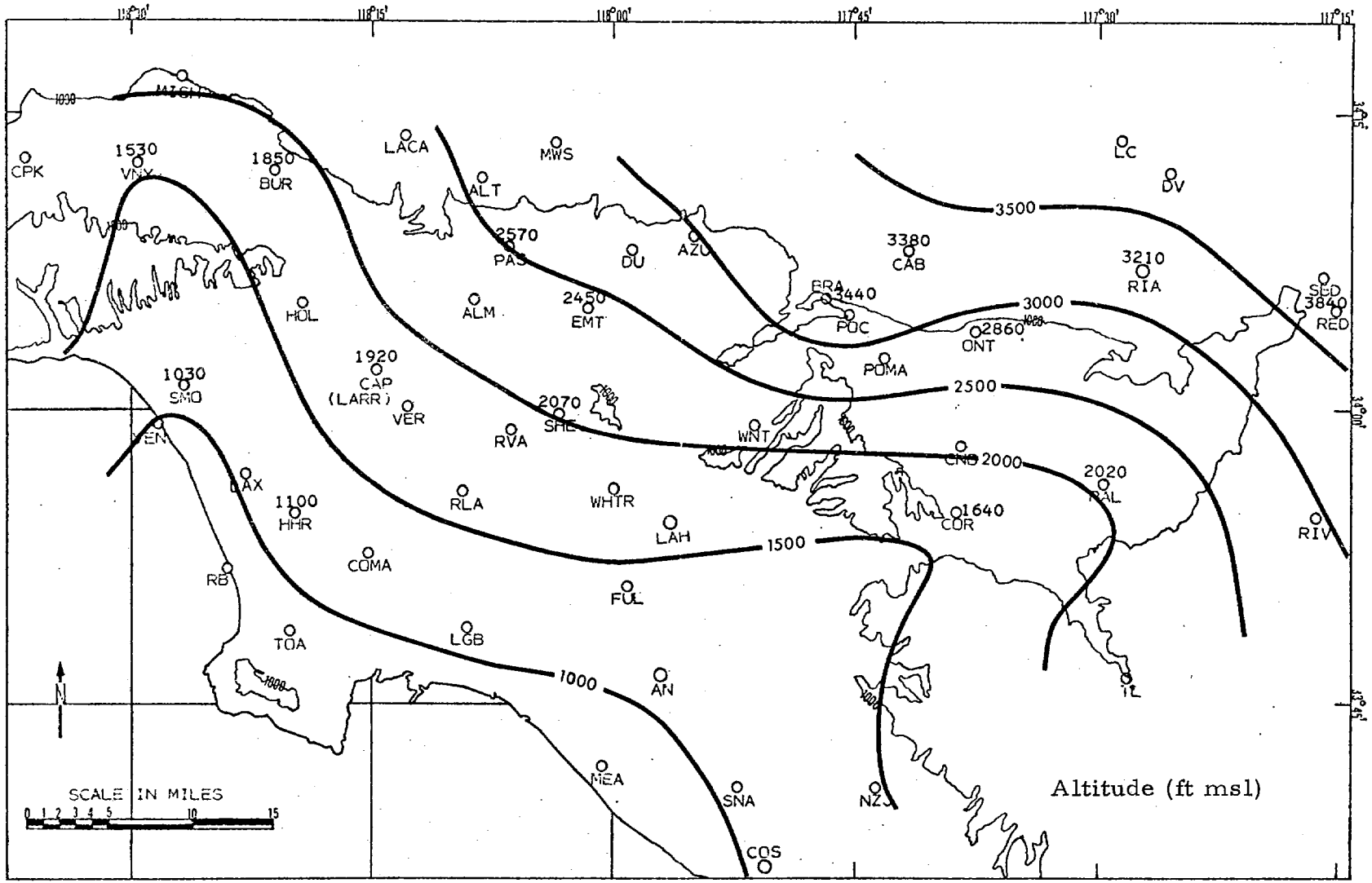

Fig. V-10. MIXING LAYER HEIGHTS, AFTERNOON, JULY 19, 1973

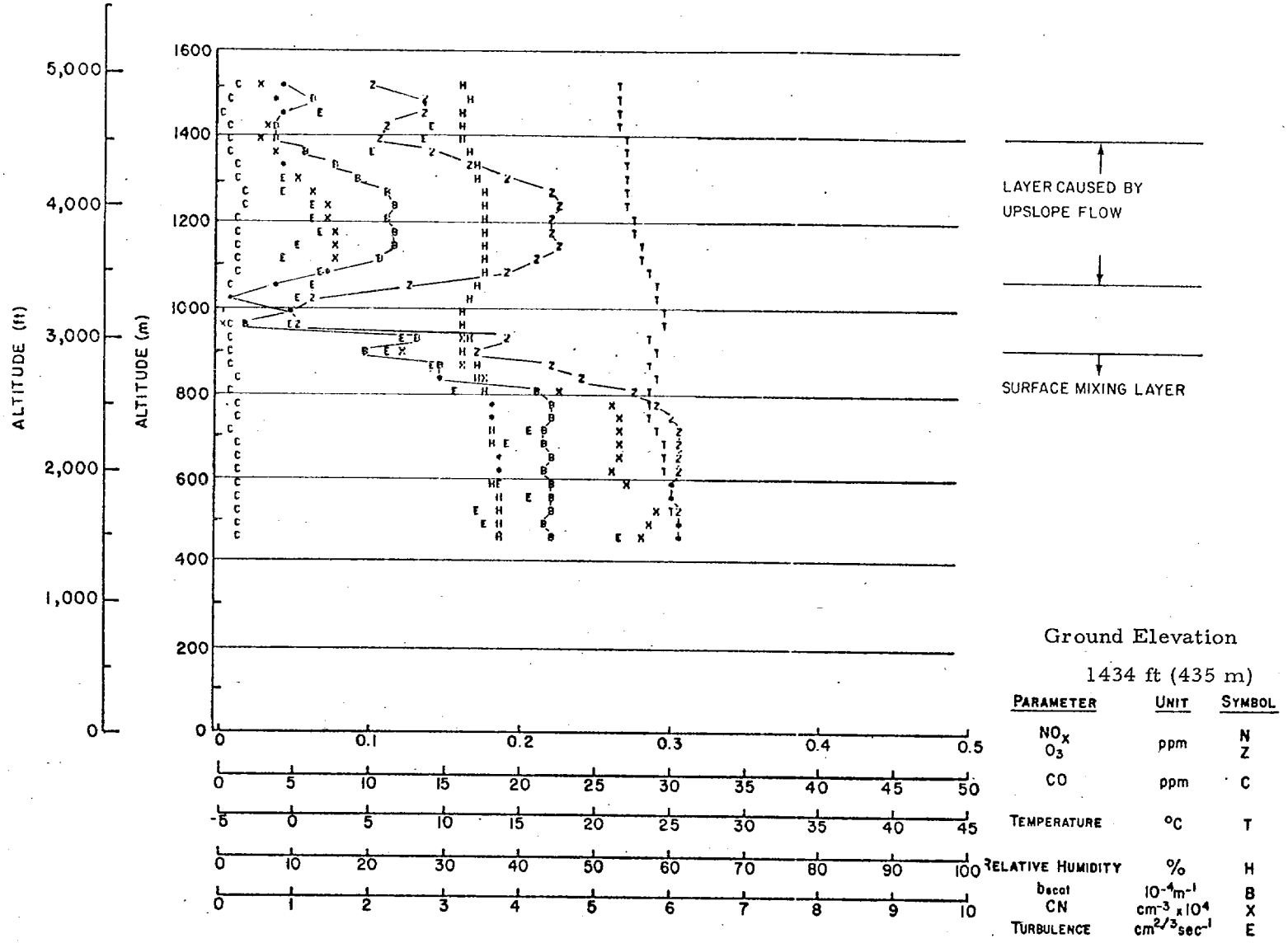

Fig. V-11. VERTICAL PROFILE AT RIALTO (RIA) JULY 19, 1973, 1738 PDT, SHOWING LAYER CAUSED BY UPSLOPE FLOW

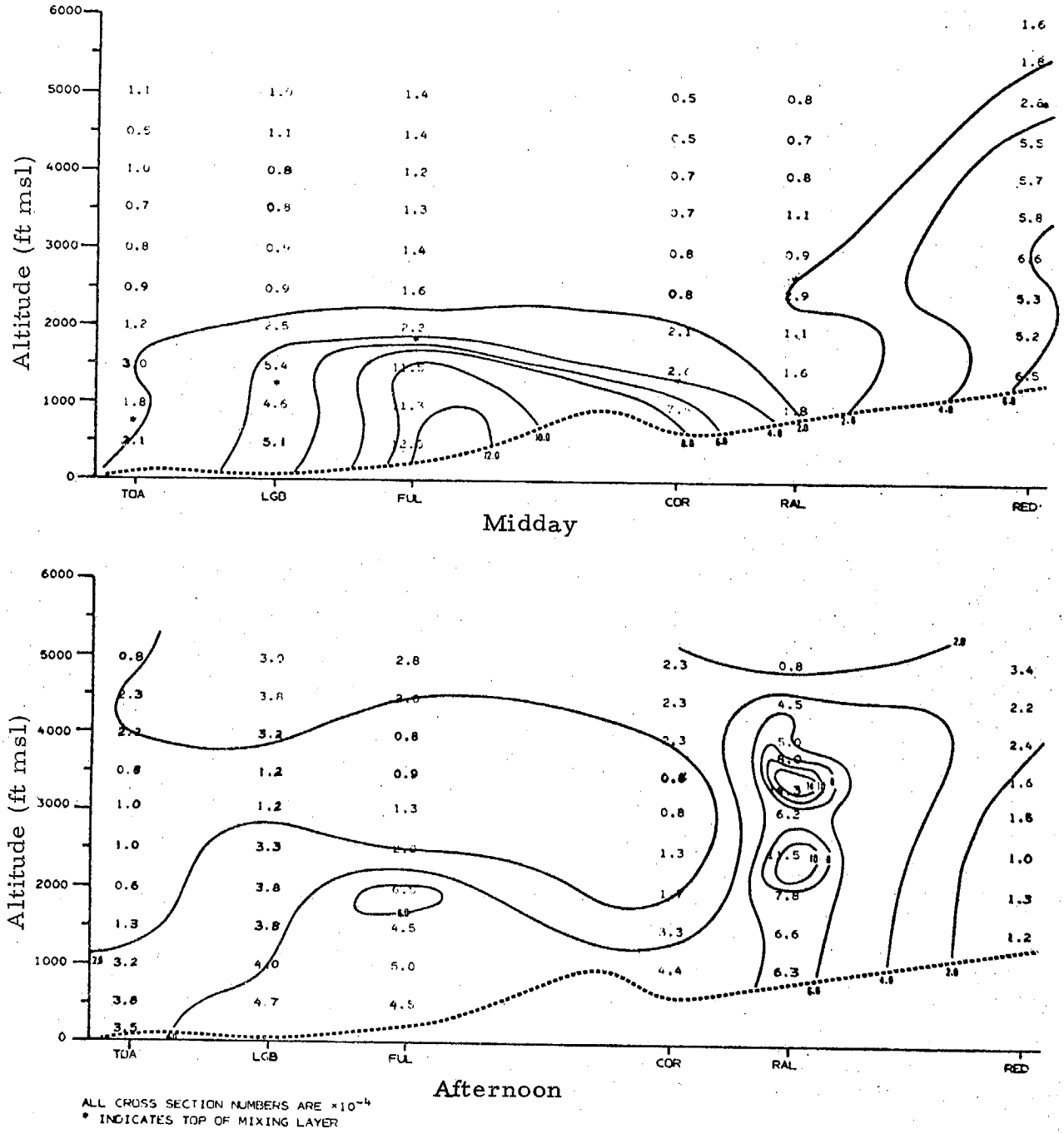

Fig. V-12. VERTICAL CROSS-SECTION OF b_{scat} MIDDAY AND AFTERNOON, OCTOBER 24, 1972

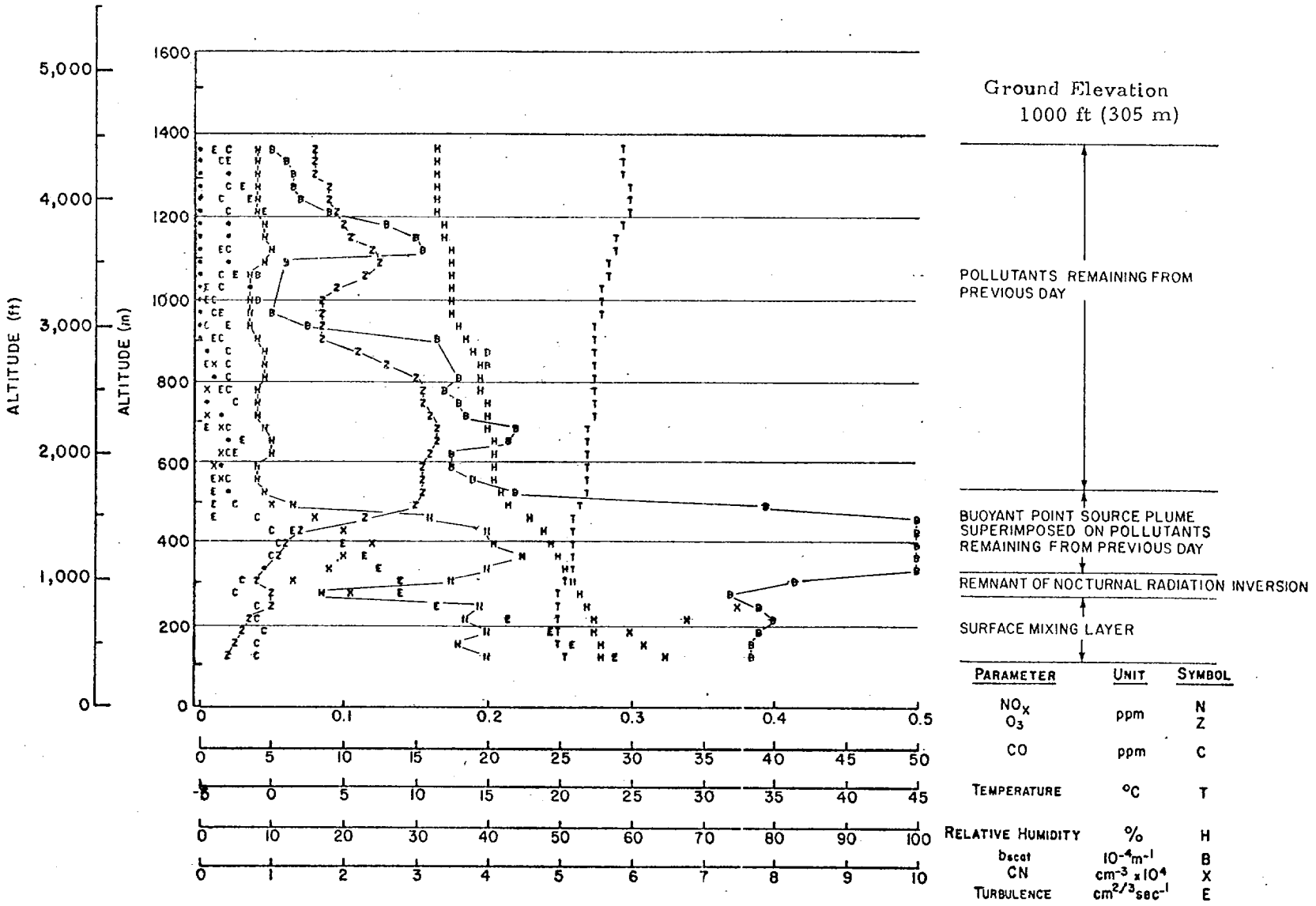

Fig. V-13. VERTICAL PROFILE OVER BRACKETT (BRA) JULY 26, 1973, 0825 PDT SHOWING BUOYANT PLUME AND UNDERCUTTING BY RADIATION INVERSION

C. Average 3-D Pollutant Distributions in the L. A. Basin

1. Introduction

The pollutant mapping program described in this report has revealed complex and varied patterns of pollutant formation and transport in the Los Angeles air basin. Nevertheless, certain phenomena are so characteristic that they survive extensive averaging of the data. In this chapter, we describe these "grand average" features of the data as a background for subsequent discussion of specific case histories.

Our discussion is based on "grand average" vertical profiles for Hawthorne, El Monte, Ontario, and Riverside (Fig. V-14). All 1973 soundings at these locations were used to calculate the mean and standard deviation of all measured parameters for each location, time period (a.m. or p.m.), and hundred-foot altitude increment. A typical computer printout for a mean profile is given in Table V-1 indicating the number of data points, the mean, and the standard deviation (sigma) as a function of altitude.

The average profiles presented in this section are calculated from a sample population which was biased toward photochemical smog conditions as mapping was intentionally restricted to days with above average smog potential. Although they cannot be taken as representative on an overall basis, the mean profiles should be fairly typical of conditions during smoggy summer and early fall days since they are drawn from data on 24 days of this type.

2. Meteorological Parameters

a. Temperature

A primary factor in the production of high pollutant concentrations in Los Angeles air is the frequent occurrence of temperature inversions which restrict the vertical dispersion of pollutants. This phenomenon is evident in Fig. V-15, which shows the mean morning and afternoon temperature profiles at Hawthorne, El Monte, Ontario, and Riverside. In the mean morning profiles at all four locations, the temperature of the air at 3000 feet msl is higher than the temperature of the air near the surface, with a non-negative lapse rate from 3000 feet down almost to the surface. As the day progresses, the surfaces of inland areas of the basin are heated by the sun, warming the air near the ground and eroding the inversion from below. By afternoon, the mean profiles for all three inland locations show a well-defined layer at the surface in which the lapse rate is adiabatic.

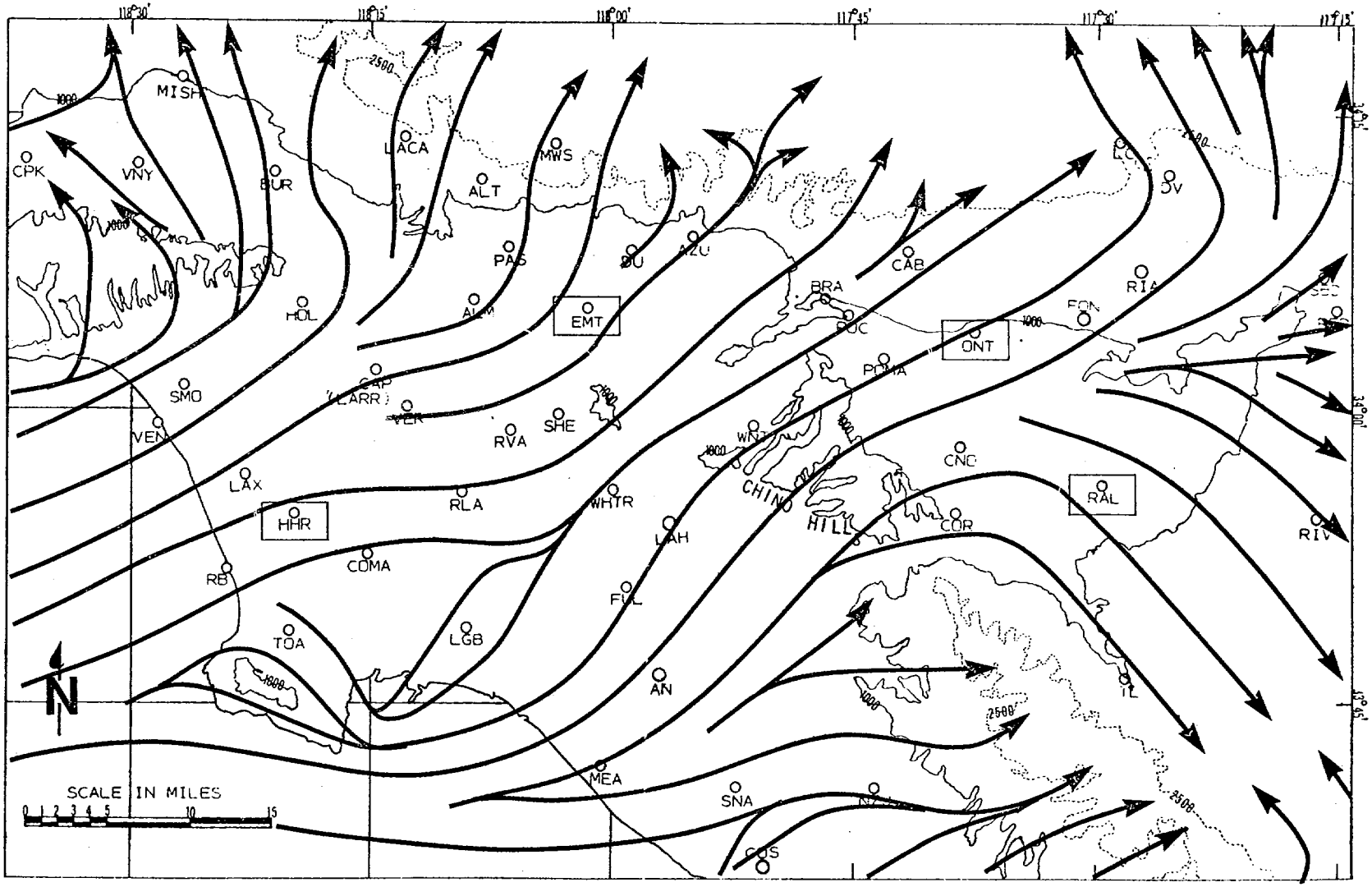

Fig. V-14. MAP OF THE LOS ANGELES AIR BASIN. STREAMLINES SHOW MOST FREQUENT AFTERNOON SURFACE WINDS DURING JULY (DE MORRAIS ET AL., 1965)

TABLE V-1

TYPICAL COMPUTER PRINTOUT FOR THE AVERAGE POLLUTANT PROFILE

PARAMETER- SCAT PM RIVERSIDE

ALT MAX	NUMBER	SUM X	MEAN	SIGMA	SUMSQR
100	C	0.CCCCCE+00	0.00000E+00	0.0C000E+00	0.C0CCCE+C0
200	C	0.CCCCCE+00	0.00000E+00	0.0C000E+00	0.C0CCCE+C0
300	C	0.CCCCCE+00	0.00000E+00	0.0C000E+00	0.C0CCCE+C0
400	C	0.CCCCCE+00	0.00000E+00	0.0C000E+00	0.C0CCCE+C0
500	C	0.CCCCCE+00	0.00000E+00	0.0CCC0E+00	0.C0CCCE+C0
600	C	0.CCCCCE+00	0.00000E+00	0.0C000E+00	0.C0CCCE+C0
700	4	2.8C959E+01	7.02499E+00	2.6C585E+00	2.17773E+C2
800	25	1.13420E+02	4.53679E+00	2.29973E+00	6.41491E+C2
900	709	3.99592E+03	5.63599E+00	3.08123E+00	2.92427E+C4
1000	475	3.53392E+03	7.43983E+00	3.42274E+00	3.18447E+C4
1100	524	3.5784CE+03	6.82900E+00	3.48264E+00	3.07EC2E+C4
1200	631	4.27122E+03	6.76897E+00	3.86246E+00	3.831C4E+C4
1300	734	4.45535E+03	6.06996E+00	3.75654E+00	3.73876E+C4
1400	645	4.56817E+03	7.08244E+00	3.78180E+C0	4.15643E+C4
1500	820	5.52381E+03	6.73635E+00	3.67689E+00	4.82828E+C4
1600	653	5.65141E+03	6.62534E+00	3.76916E+00	4.95465E+C4
1700	782	4.86643E+03	6.22306E+00	3.51370E+00	3.59264E+C4
1800	869	5.56051E+03	6.39874E+00	3.73741E+00	4.77C47E+C4
1900	774	4.63225E+03	5.98892E+00	3.69461E+00	3.82748E+C4
2000	802	5.28159E+03	6.58553E+00	3.93167E+00	4.71C4CE+C4
2100	774	4.1C741E+03	5.30674E+00	3.74495E+00	3.26380E+C4
2200	796	4.93647E+03	6.19937E+00	3.92943E+00	4.28671E+C4
2300	918	4.94533E+03	5.38707E+00	3.86892E+00	4.C3C7CE+C4
2400	890	4.01570E+03	4.51202E+00	3.25215E+00	2.75214E+C4
2500	835	3.7C196E+03	4.43348E+00	3.43595E+C0	2.62585E+C4
2600	651	2.23012E+03	3.22738E+00	2.79206E+00	1.25764E+04
2700	696	1.85296E+03	2.66229E+00	2.02432E+00	7.78114E+C3
2800	813	1.98575E+03	2.44250E+00	2.01599E+00	8.15C33E+C3
2900	838	1.69589E+03	2.02374E+00	1.63947E+00	5.68180E+C3
3000	911	1.564C1E+03	1.71681E+00	1.49305E+00	4.71368E+C3
3100	1C18	1.56787E+03	1.54015E+00	1.25983E+00	4.02695E+C3
3200	767	1.3763CE+03	1.79439E+00	1.25506E+00	3.67620E+C3
3300	819	1.28139E+03	1.56458E+00	1.04872E+00	2.90448E+C3
3400	836	1.55679E+03	1.66324E+00	1.1C346E+00	3.72778E+C3
3500	802	1.371C0E+03	1.70947E+00	1.14267E+00	3.38953E+C3
3600	678	1.11295E+03	1.64152E+00	1.11215E+00	2.66430E+C3
3700	766	1.13575E+03	1.48271E+00	8.8C850E-01	2.27155E+C3
3800	736	1.19198E+03	1.61953E+00	1.1C213E+00	2.82324E+C3
3900	733	1.10303E+03	1.50482E+00	1.06186E+00	2.48523E+C3
4000	752	1.0C747E+03	1.33972E+00	9.31615E-01	2.00153E+C3
4100	784	1.C7988E+03	1.37739E+00	1.02980E+00	2.31178E+C3
4200	770	1.07055E+03	1.39033E+00	1.05336E+00	2.34167E+C3
4300	763	8.52537E+02	1.11735E+00	7.79384E-01	1.41545E+C3
4400	683	8.41095E+02	1.23147E+00	8.86822E-01	1.57214E+C3
4500	763	8.41134E+02	1.10240E+00	7.26696E-01	1.33189E+C3
4600	735	7.45535E+02	1.01433E+00	7.07767E-01	1.12391E+C3
4700	741	7.12736E+02	9.61857E-01	5.77886E-01	9.32675E+C2
4800	781	6.96254E+02	8.91542E-01	5.98841E-01	9.00492E+02
4900	688	5.66955E+02	8.24062E-01	5.87484E-01	7.04315E+C2
5000	577	5.22636E+02	9.05781E-01	6.69913E-01	7.31893E+C2
5100	342	3.05477E+02	8.93208E-01	6.64890E-01	4.23604E+C2
5200	292	2.71198E+02	9.28759E-01	7.97546E-01	4.37162E+C2
5300	298	2.43398E+02	8.16771E-01	6.98838E-01	3.43648E+C2
5400	310	2.29958E+02	7.41928E-01	6.37254E-01	2.96124E+02
5500	348	2.47258E+02	7.10510E-01	6.11534E-01	3.05618E+C2
5600	185	1.33979E+02	7.24209E-01	4.22430E-01	1.29863E+C2
5700	152	1.25279E+02	8.24202E-01	5.35266E-01	1.46518E+C2
5800	132	1.07339E+02	8.13174E-01	5.76548E-01	1.30831E+02
5900	176	1.47079E+02	8.35674E-01	5.9C772E-01	1.83987E+C2
6000	135	1.36359E+02	1.01007E+00	8.3C604E-01	2.30179E+C2
6100	19	7.45986E+00	3.92624E-01	1.66207E-02	2.93389E+C0
6200	20	7.75982E+00	3.87991E-01	1.86219E-02	3.C1747E+C0
6300	40	1.49797E+01	3.74492E-01	3.07181E-02	5.64657E+C0
6400	41	1.7C396E+01	4.15601E-01	2.96411E-02	7.1173CE+C0
6500	19	8.29986E+00	4.36835E-01	2.76980E-02	3.63548E+C0
6600	11	4.41994E+00	4.01813E-01	1.4CC61E-02	1.77195E+C0
6700	16	5.87981E+00	3.67488E-01	1.23861E-02	2.163C6E+C0
6800	24	8.91982E+00	3.71659E-01	2.88411E-02	3.33426E+C0
6900	22	7.79984E+00	3.54538E-01	4.28465E-02	2.803E9E+C0
7000	14	4.73991E+00	3.38565E-01	1.65772E-02	1.60E34E+C0
7100	17	4.91988E+00	2.89405E-01	3.35952E-02	1.44233E+C0
7200	27	7.85978E+00	2.91103E-01	2.24258E-02	2.301C8E+C0
7300	5C	1.56396E+01	3.12793E-01	2.38185E-02	4.91577E+C0
7400	24	6.71983E+00	2.79993E-01	2.28462E-02	1.89351E+C0
7500	22	5.63981E+00	2.56355E-01	2.8C448E-02	1.46221E+C0
7600	4	1.13998E+00	2.84996E-01	1.0C098E-02	3.25191E-C1
7700	0	0.CCCCCE+00	0.00000E+00	C.0C000E+00	C.C0CC0E+C0
7800	C	0.CCCCCE+00	0.00000E+00	0.0C000E+00	C.C0CC0E+C0
7900	C	0.CCCCCE+00	0.00000E+00	0.0C000E+00	C.C0CC0E+C0
8000	C	0.CCCCCE+00	0.00000E+00	C.C0000E+00	C.C0CCCE+C0

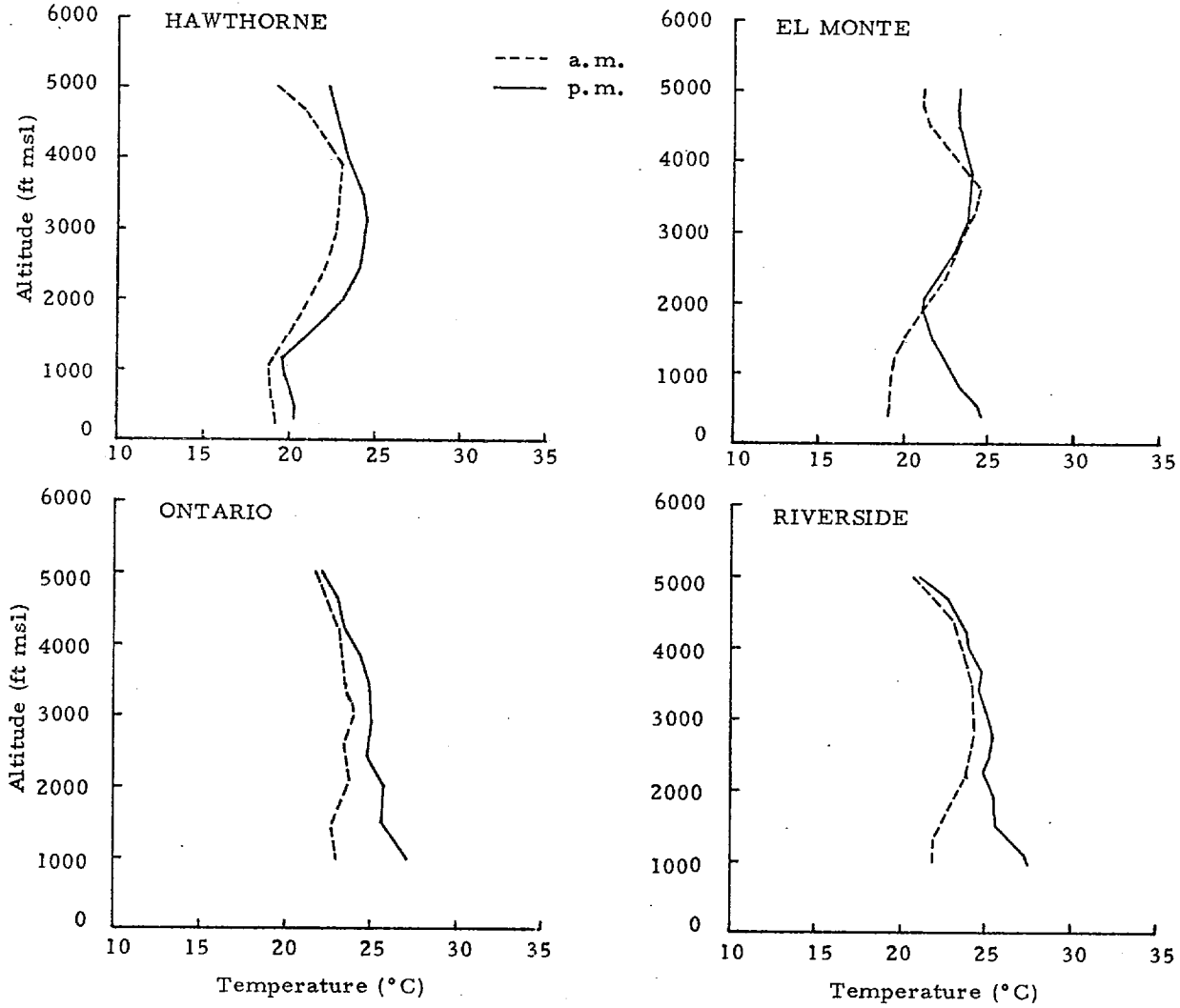

Fig. V-15. MEAN MORNING AND AFTERNOON TEMPERATURE PROFILES

The effect of surface heating is seen from another perspective in Fig. V-16, which displays the four mean afternoon temperature profiles on one graph. At Hawthorne, the afternoon profile is little changed from the morning profile due to the stabilizing influence of the nearby ocean. As air moves inland with the usual afternoon flow, however, temperatures near the surface increase, eroding the inversion. The unstable layer at the surface deepens until, at Ontario and Riverside, it may "break through" the inversion.

b. Turbulence

The mean profiles of small-scale turbulence intensity (Fig. V-17) are compatible with the mean thermal structure. In the morning, when air is stable, turbulence is confined to a shallow layer at the surface, where it is generated by mechanical effects and local heat sources. In the afternoon, turbulence extends about 1000 feet above the unstable surface layer. In all profiles, the intensity of the turbulence decreases with height until it reaches a "background" value of about 0.5 $cm^{2/3}$ sec^{-1}, reflecting the dissipation of energy introduced at the surface.

c. Relative Humidity

Mean afternoon profiles of relative humidity are shown in Fig. V-18. Mean morning and afternoon relative humidities are generally in the range 30-50 percent, except in the surface layers at Hawthorne and Riverside.

3. Reactive Gas Concentrations

a. Nitrogen Oxides

The first two oxides of nitrogen are important participants in the photochemistry of the Los Angeles atmosphere. Photodissociation of NO_2 ($NO_2 + h\nu \rightarrow NO + O$) starts the chain of reactions leading to the buildup of ozone. Oxidation of NO ($NO + O_3 \rightarrow NO_2 + O_2$) limits the rate of this buildup in its early stages. Although these two reactions affect the relative concentrations of NO and NO_2 in the air, they leave invariant their sum, the concentration of NO_x. NO_x is formed almost exclusively by combustion sources such as motor vehicles and power plants and is lost through reactions with surfaces and by the formation of nitrates.

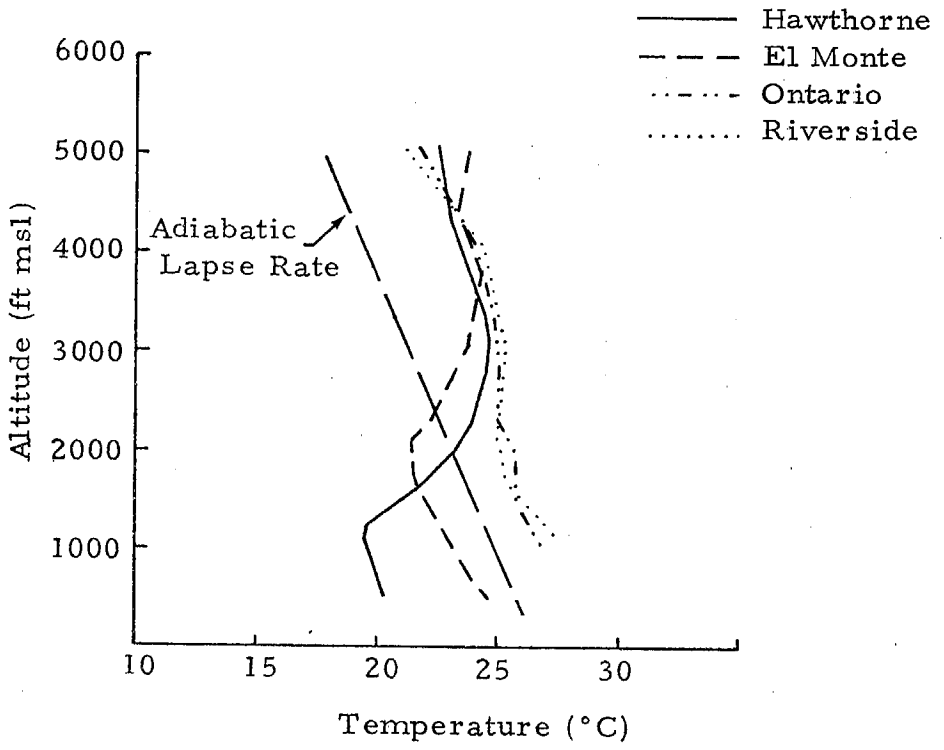

Fig. V-16. MEAN AFTERNOON TEMPERATURE PROFILES

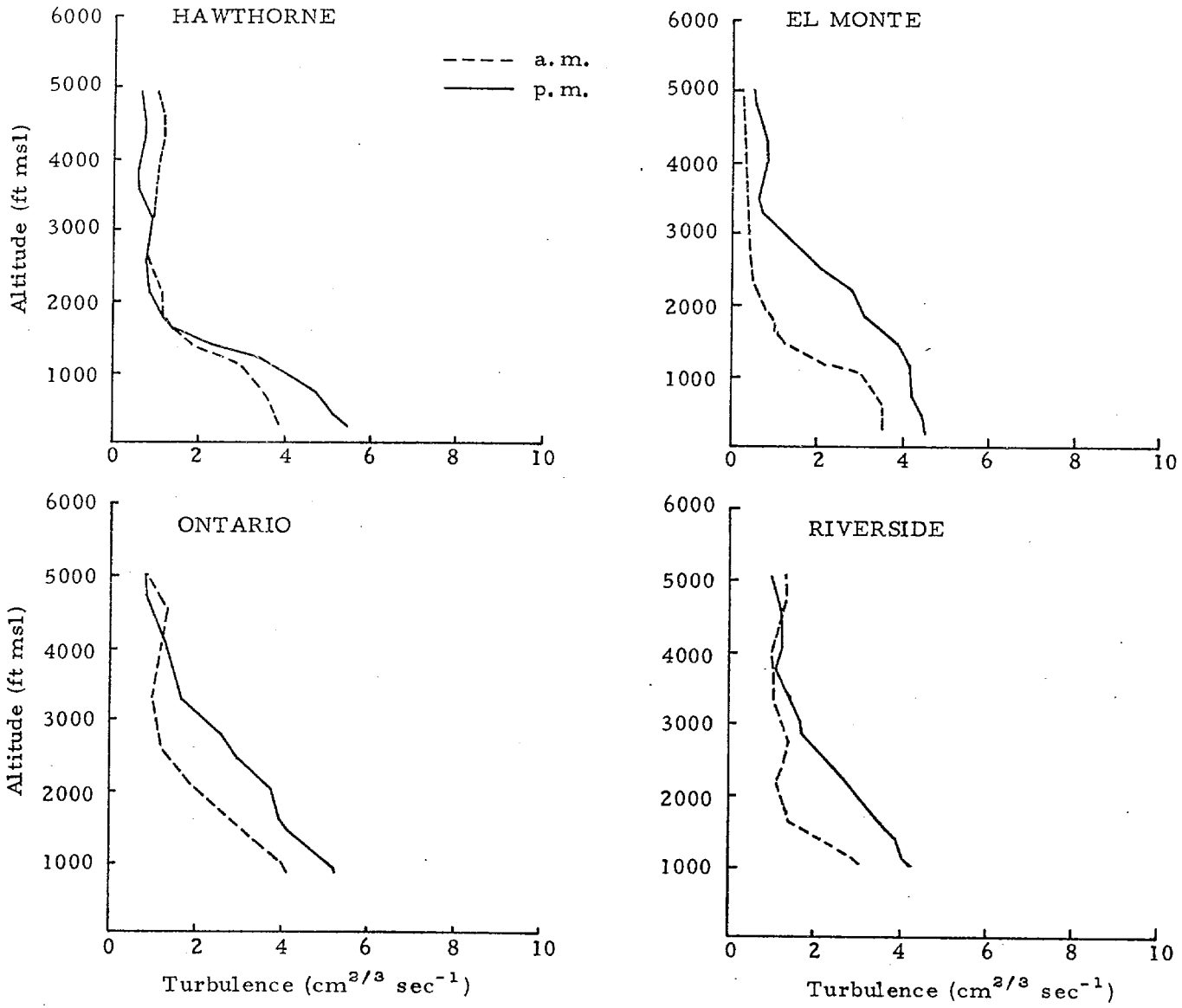

Fig. V-17. MEAN MORNING AND AFTERNOON TURBULENCE PROFILES

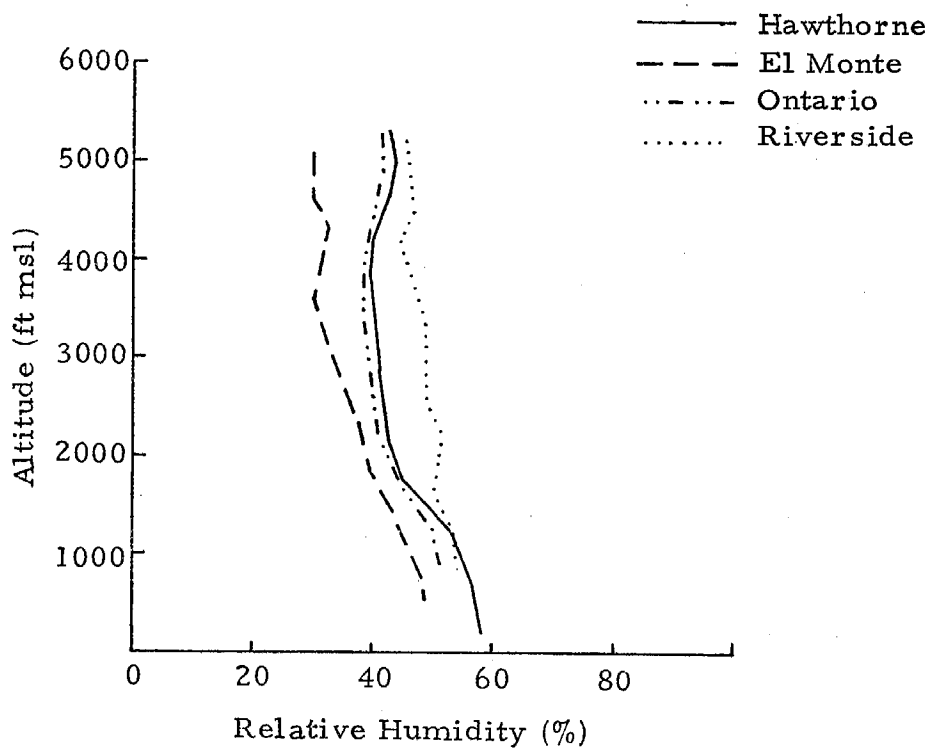

Fig. V-18. MEAN AFTERNOON RELATIVE HUMIDITY PROFILES

Mean profiles of NO_x concentration are shown in Figs. V-19 and V-20. Some substantial concentration gradients appear near the surface in the morning profiles due to the generally poor mixing prevailing at this time. By afternoon, concentrations become fairly uniform through the unstable surface layer. In both morning and afternoon profiles, mean concentrations drop to about 0.03 ppm above the turbulent surface layer.

The smallest values for mean NO_x concentrations and the integral of these concentrations with respect to height are seen in the afternoon profile for Riverside. The latter half of a typical afternoon trajectory to Riverside passes over a predominantly rural area, where emissions of NO_x are apparently not sufficient to balance losses. Peroxyacetyl nitrate concentrations at Riverside can reach 0.05 ppm on smoggy days (Lundgren, 1970). Particulate nitrate concentrations of over 100 $\mu g/m^3$, equivalent to over 0.04 ppm of NO_x, were measured there during the 1973 Aerosol Characterization Study for the California Air Resources Board (Hidy et al., 1974). These concentrations are comparable with the mean afternoon NO_x concentrations measured at Riverside, indicating that a substantial fraction of the NO_x emitted in the western portion of the air basin may be converted to nitrates en route to Riverside.

b. Ozone

Unlike NO_x, ozone is not emitted directly, but is formed in the atmosphere through the sequence of reactions initiated by the photodissociation of NO_2. It reacts very rapidly with NO, the principal constituent of NO_x emissions, so that fresh emissions of NO_x tend to lower, rather than raise, ozone concentrations. These characteristics are nicely demonstrated in the mean profiles of ozone (Fig. V-21).

Note that ozone concentrations do not drop to background levels (about 0.04 ppm) above the surface mixed layer. At Hawthorne, for example, the mean temperature, turbulence, and NO_x profiles all indicate a surface mixed layer strongly confined below 2000 feet msl, yet the mean ozone concentration at 3000 feet msl is 0.1 ppm, greater than the federal standard. Mechanisms by which polluted air occurs above the surface mixed layer are discussed elsewhere in this report. What is important in the present context is that the ozone at 3000 feet over Hawthorne is part of a polluted air mass which has aged above the surface mixed layer. In the absence of scavenging by fresh NO_x emissions, which are confined within the surface mixed layer, reactions have proceeded almost to

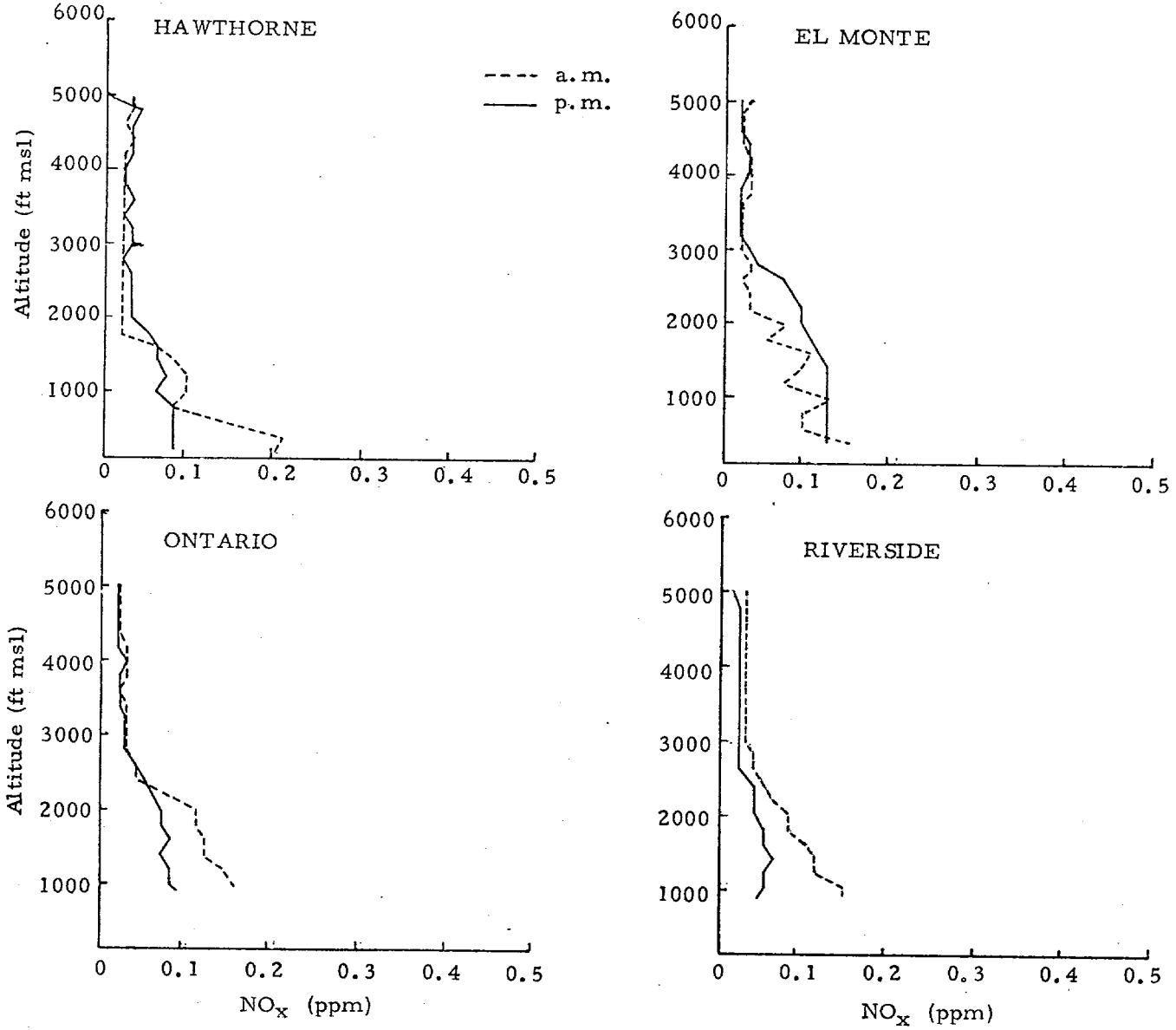

Fig. V-19. MEAN MORNING AND AFTERNOON NO_x PROFILES

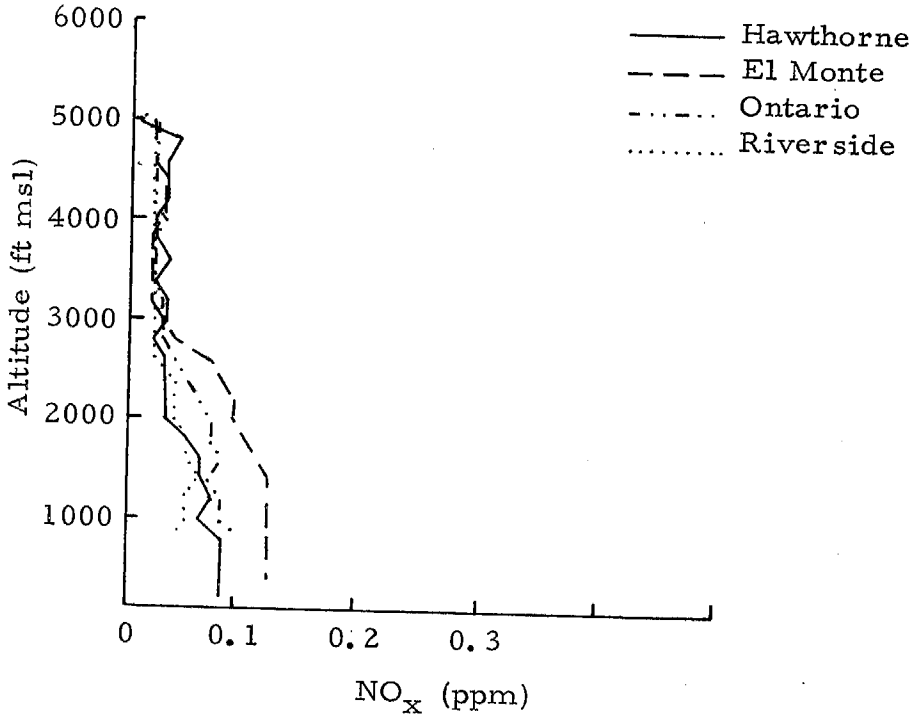

Fig. V-20. MEAN AFTERNOON NO_x PROFILES

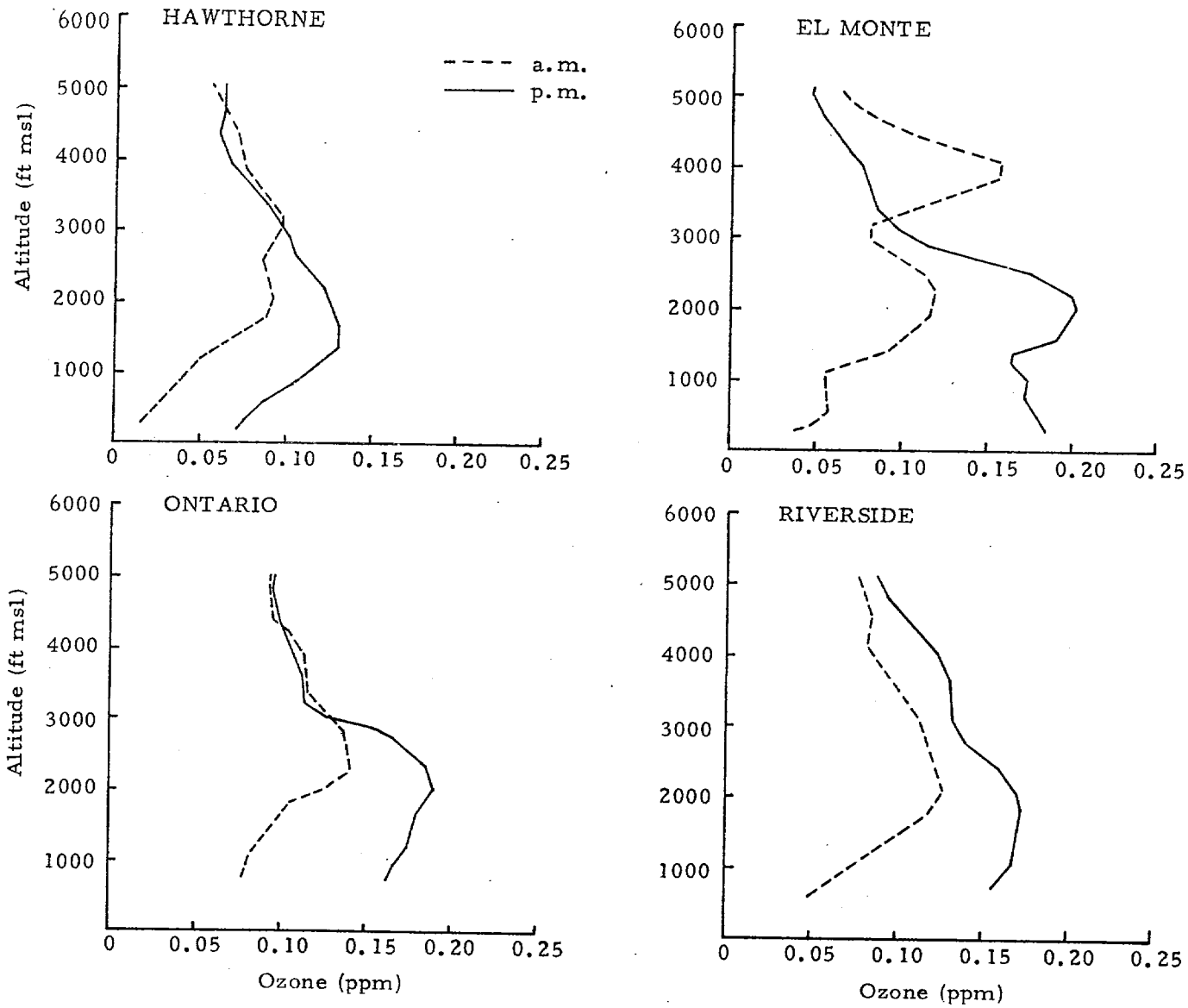

Fig. V-21. MEAN MORNING AND AFTERNOON OZONE PROFILES

completion, producing relatively large ozone concentrations from small concentrations of NO_x and hydrocarbons.

A second feature of the mean profiles which is unique to ozone is the occurrence of deficits near the surface. The most striking example of this is the morning profile at Hawthorne, where mean ozone concentrations near the surface are under 0.02 ppm, less than the 0.04 ppm background levels observed in clean air (Section VIII-C). In fact, all four morning profiles, as well as the afternoon profile at Hawthorne, show ozone concentrations which are lower within the turbulent surface layer than they are immediately above it. These ozone deficits are due principally to scavenging by fresh emissions of NO_x which are trapped within the shallow, well-defined surface mixed layers exhibited in these profiles.

4. Aerosol Parameters

a. Condensation Nuclei Count

Since small particles are much more numerous than large particles, the condensation nuclei count (CN) is primarily an index of the small particle fraction of the aerosol. Particle size distribution measurements by Whitby et al. (1972) have shown that particles under 0.1 μm in diameter account for nearly all of the CN (Fig. V-22). Particles in this size range are produced by combustion sources and (under conditions thought to be rare in ambient Los Angeles air) by homogeneous nucleation (Whitby et al., 1972, Husar and Whitby, 1973). These particles coagulate rapidly with larger particles and with each other, so that the half-life of CN under typical Los Angeles smog conditions is on the order of an hour (Husar et al., 1972, Davies, 1974).

Mean profiles of CN are shown in Figs. V-23 and V-24. Substantial CN gradients are observed near the surface in all four morning profiles and in the afternoon profile at Hawthorne. Above the surface mixed layer, CN counts drop to about 5×10^3 cc^{-1}, less than one tenth of the counts within the surface mixed layer. Counts within the surface mixed layer are lowest at Riverside. With the exception of the afternoon profile at Hawthorne, the mean profiles of CN are qualitatively similar to the mean profiles of NO_x, which also is produced chiefly by combustion sources and decays in the atmosphere.

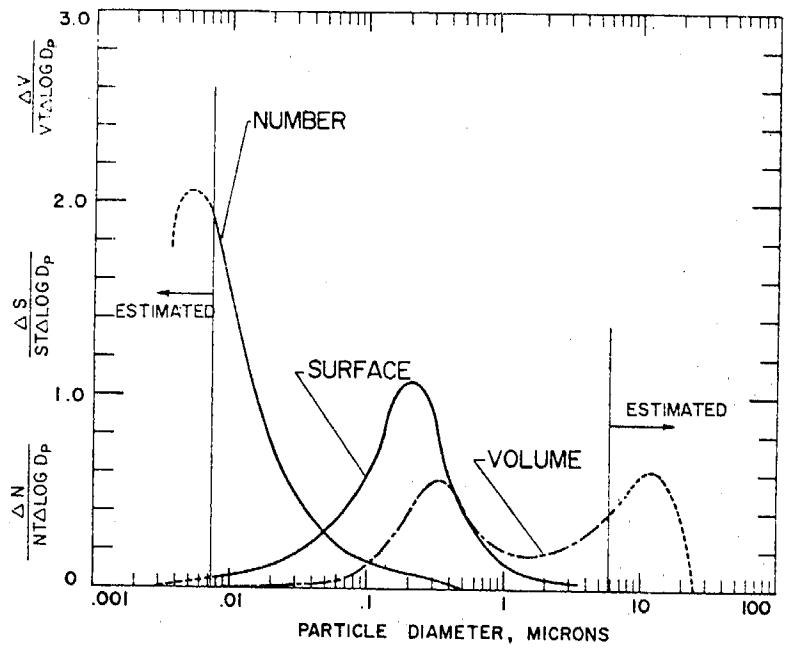

Fig. V-22. GRAND AVERAGE NUMBER, SURFACE AREA, AND VOLUME DISTRIBUTIONS OF SMOG AEROSOLS MEASURED DURING 1969 PASADENA AEROSOL CHARACTERIZATION STUDY (WHITBY ET AL., 1972). LINEAR ORDINATE IS NORMALIZED BY TOTAL NUMBER, AREA, OR VOLUME, AND AREA UNDER CURVES IS PROPORTIONAL TO QUANTITY IN SIZE RANGE.

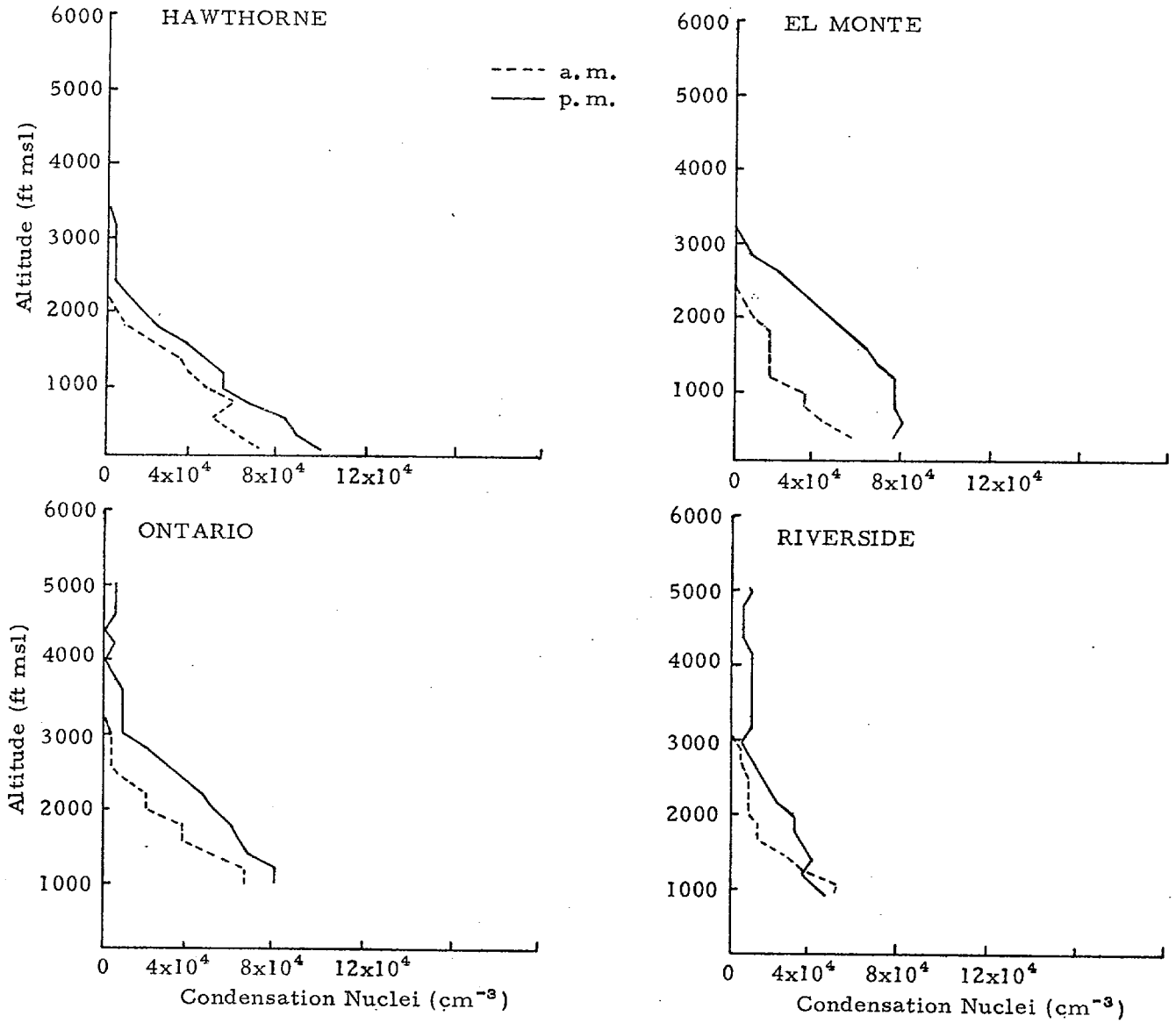

Fig. V-23. MEAN MORNING AND AFTERNOON CONDENSATION NUCLEI PROFILES

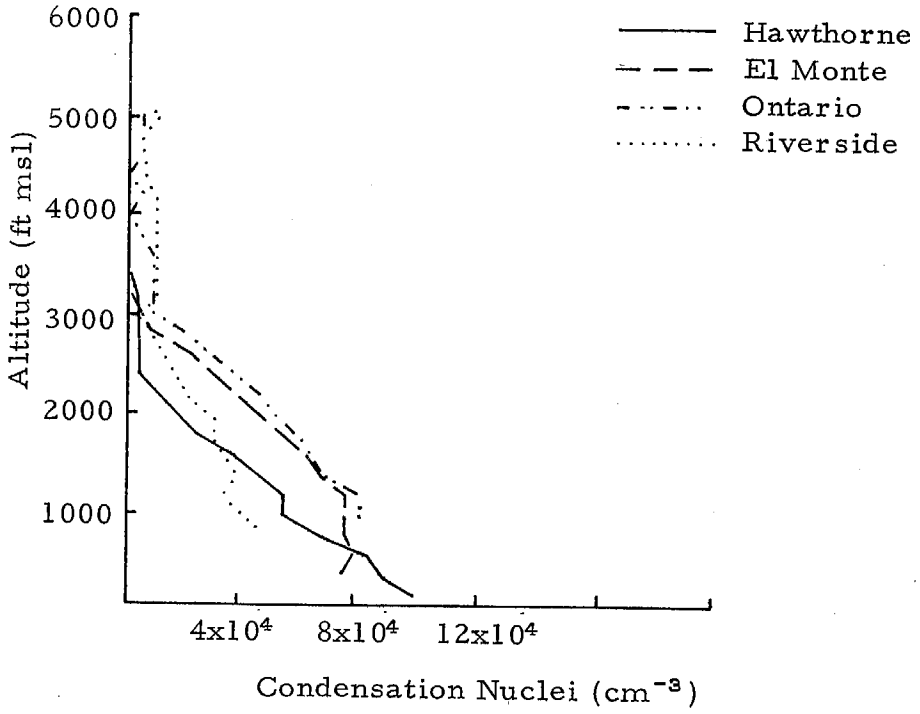

Fig. V-24. MEAN AFTERNOON CONDENSATION NUCLEI PROFILES

b. Light Scattering Coefficient

The light scattering coefficient (b_{scat}) of the atmosphere is determined largely by the concentration of particles with diameters in the range 0.1-1.0 μm (Fig. V-25), since these are the most efficient scatterers of visible radiation. Chemical analyses (Hidy et al., 1974) and electron micrographs (Section IX-C) indicate that, under photochemical smog conditions, many of the particles in this size range have grown from much smaller nuclei through the addition of nitrates, sulfates, and organics produced from the gas phase. Some of this material is hygroscopic and b_{scat} is affected by high ambient relative humidities (Fig. V-26). Once formed, the light scattering fraction of the aerosol is a fairly stable component of the atmosphere, with low surface loss rates (Chamberlain, 1967) and low coagulation efficiencies (Davies, 1974).

Of the four air quality parameters studied in this chapter, b_{scat} is the most stable and least sensitive to fresh emissions. These qualities are shown in the mean afternoon profiles of b_{scat} (Fig. V-27). In all four profiles, b_{scat} is fairly uniform through the surface unstable layer and drops to low levels above the surface turbulent layer. Afternoon b_{scat} is high at Riverside, indicating that the low CN observed there is due more to coagulation of small particles than to a net loss of aerosol.

5. Pollutant Aging

Figure V-14 shows that the characteristic air masses sampled over Hawthorne and Riverside in the afternoon have different histories. Hawthorne is only about 30 minutes downwind from the ocean. During those 30 minutes over land en route to Hawthorne, air passes over the San Diego Freeway and State Highways 1 and 107, as well as the heavily industrialized region around El Segundo. The afternoon soundings at Hawthorne thus sample predominantly fresh emissions, superimposed on the marine background (which itself may contain well aged anthropogenic contaminants).

Riverside, on the other hand, is from three to six hours downwind of the ocean. As marine air moves inland, it first passes over the urban and industrialized areas of Los Angeles and Orange counties, then over the relatively rural region from the Chino Hills and Santa Ana mountains eastward to Riverside. As a result, most of the contaminants sampled in the afternoon soundings at Riverside have had from two to four hours to age en route.

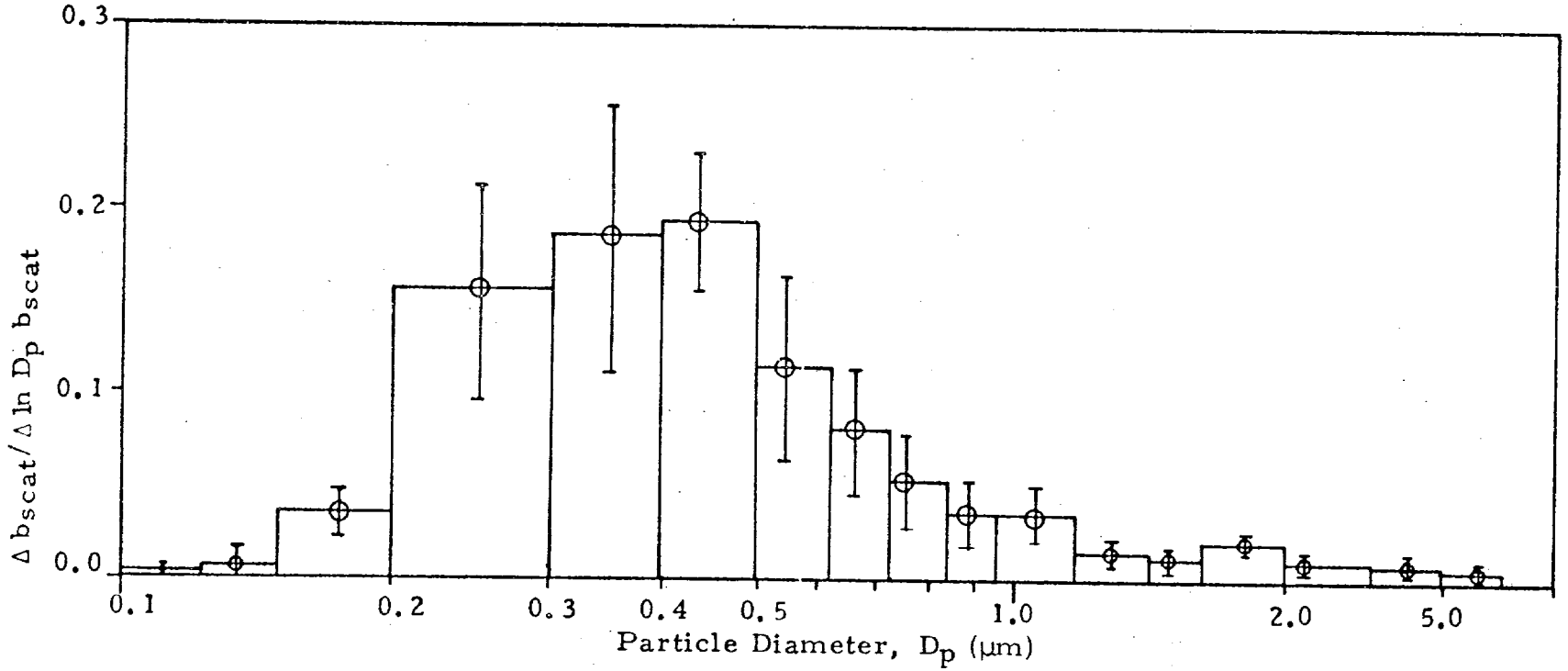

Fig. V-25. AVERAGE INCREMENTAL SCATTERING COEFFICIENT FOR SMOG AEROSOLS MEASURED DURING 1969 PASADENA AEROSOL CHARACTERIZATION STUDY, WITH 1 σ LIMITS (ENSOR, 1974). CALCULATED FROM MIE THEORY FOR AEROSOL REFRACTIVE INDEX 1.50 AND LIGHT WAVELENGTH 5460 Å.

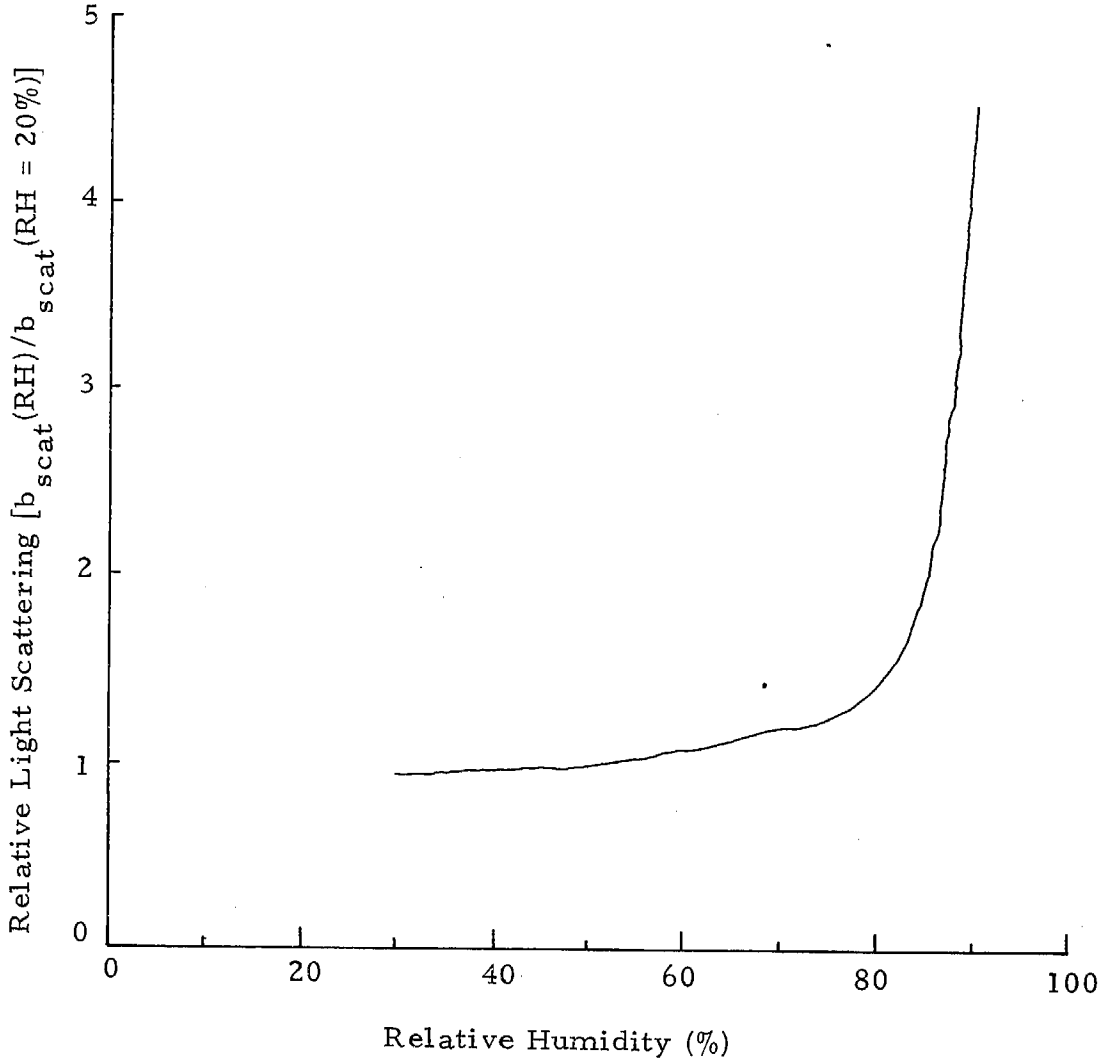

Fig. V-26. VARIATION OF b_{scat} WITH RELATIVE HUMIDITY FOR AEROSOL MEASURED AT ALTADENA, 1510 PDT, 9-21-71 (COVERT ET AL., 1972)

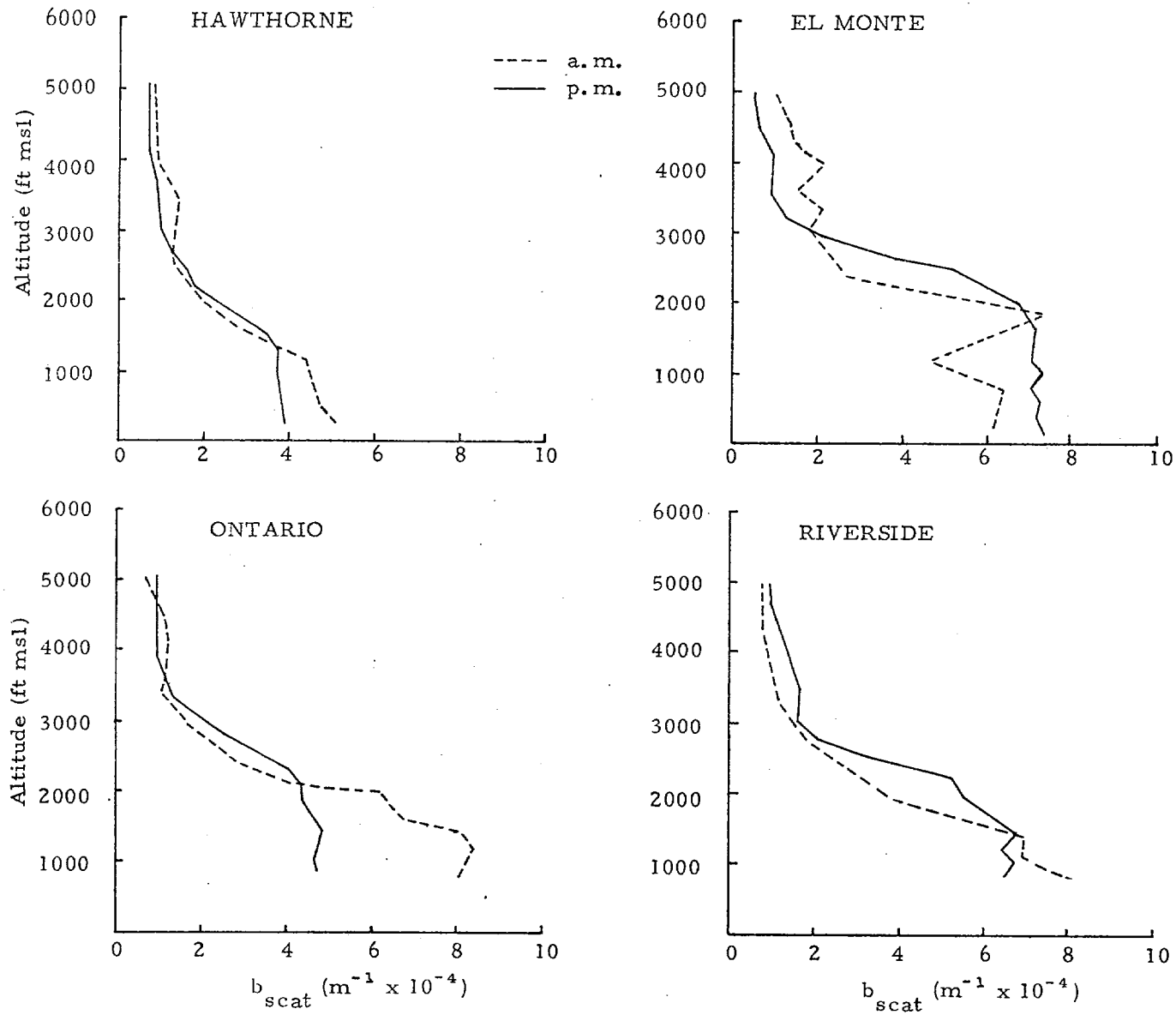

Fig. V-27. MEAN MORNING AND AFTERNOON b_{scat} PROFILES

The afternoon contaminant characteristics of the two locations are summarized and compared in Fig. V-28, which shows the afternoon means for NO_x, O_3, CN, and b_{scat} in the first 200 feet above ground level. It is apparent from Fig. V-28 that the afternoon contaminant mixes at Hawthorne and Riverside reflect the different histories of the air sampled, with significantly more NO_x and CN at Hawthorne and significantly more O_3 and b_{scat} at Riverside. Direct emissions account for most NO_x and CN, which decay in the atmosphere. High values of these parameters are thus generally indices of fresh emissions. Ozone, and a large fraction of the light scattering aerosol, are not emitted directly, but are produced in the atmosphere. High values of these parameters are generally indices of pollutant aging.

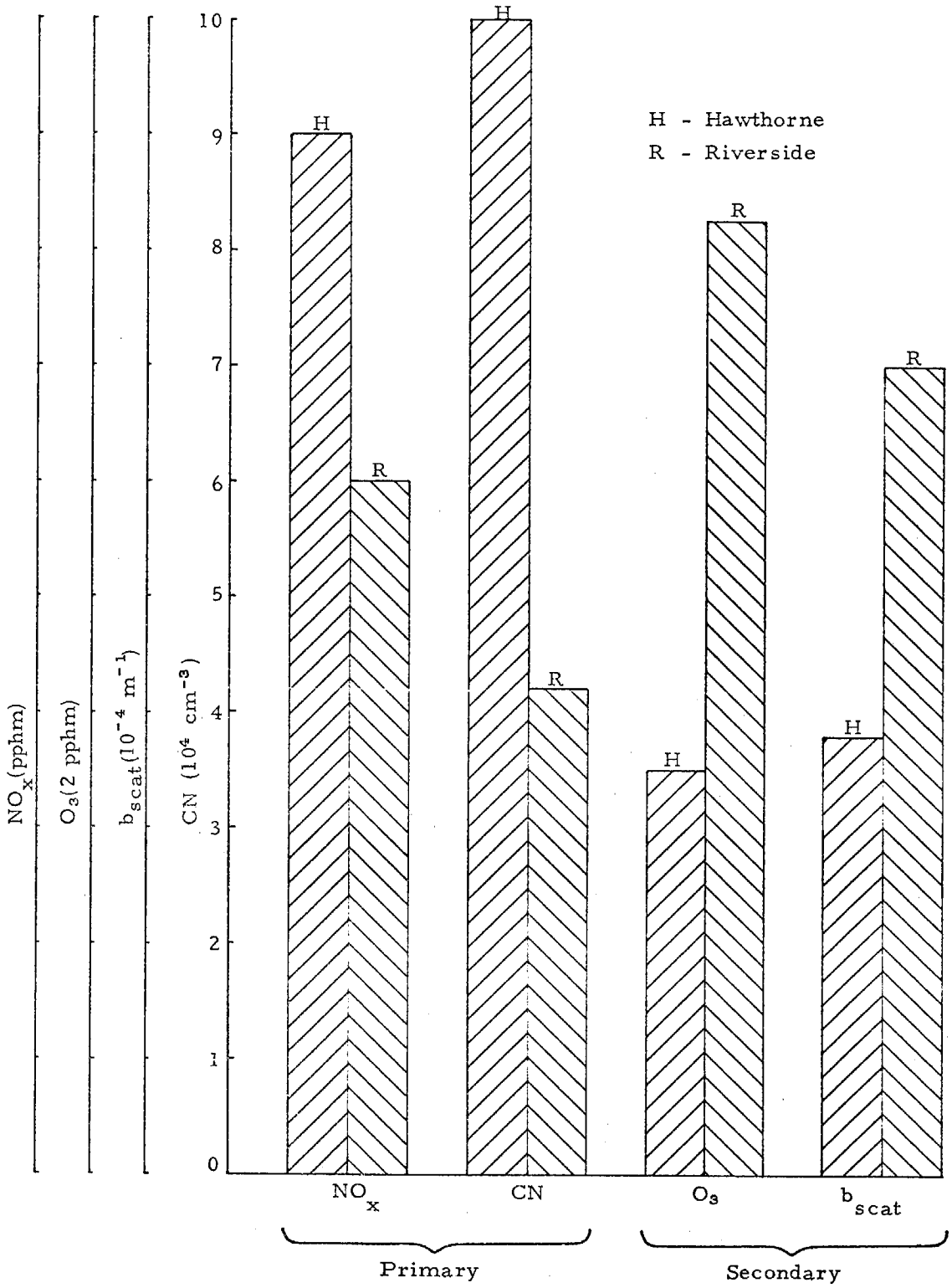

Fig. V-28. MEAN AFTERNOON CONTAMINANT CHARACTERISTICS IN FIRST 200 FEET ABOVE GROUND AT HAWTHORNE AND RIVERSIDE